Some Aspects of the Co-ordination Chemistry of Mercury.

by

Paul A. Lampe

A thesis submitted to the University of Warwick in partial fulfilment of the requirements for the degree of Doctor of Philosophy.

Department of Chemistry and Molecular Sciences

September 1980.

C O N T E N T S

List of Tables.

List of Figures.

List of abreviations.

d or D	Deuterium
δ	Chemical shift
dmso	Dimethyl sulphoxide
$\Delta H^{\ddagger}$	Enthalpy of activation
ΔS^{*}	Entropy of activation
ϵ	Extinction coefficient
J	n.m.r. coupling constant
k	Reaction rate constant
K	Equilibrium constant for complex formation
λ	Wavelength
m/e	Mass/charge
n.m.r.	Nuclear magnetic resonance
p.p.m.	Parts per million
σ	Standard deviation
Σ	Sum of
TMS	Tetramethylsilane

ACKNOWLEDGEMENTS

I would particularily like to thank my supervisor Dr. P. Moore for his advice and encouragement throughout the course of this research. I would also like to thank Dr. N. W. Alcock for his guidance through many crystallographic problems, Dr. G.R. Quick for his assistance in the stopped-flow experiments and all the other members of the Department of Chemistry and Molecular Sciences who made this work possible.

Financial support from the Medical Research Council is gratefully acknowledged.

Parts of the work reported in this thesis have been published in the scientific literature with the following references:

N.W. Alcock, P.A. Lampe and P.Moore,
J.C.S. Dalton, 1978, 1324.

P.A. Lampe and P. Moore,
Inorg. Chim. Acta, 1979, 36, 27.

N.W. Alcock, P.A. Lampe and P. Moore,
J.C.S. Dalton, 1980, 1471.

To my wife.

SUMMARY

The crystal structures of the 1:1 complexes formed by methylmercury(II) with L-tyrosine (1) and L-2-amino-4-phenylbutanoic acid (2) have been determined by X-ray diffraction studies. In both cases the ligand is bound principally via the the amino group with a weaker carboxylate bond. Complex (2) has an additional weak intermolecular bond with a neighbouring carboxylate group. Complex (1) shows further weak intramolecular contacts between mercury and the phenyl ring with Hg-C distances of 3.19(2) and 3.33(2)Å. In the case of (1) there is fairly good agreement between the crystal structure and that observed in solution as estimated from conformational analysis based on the backbone vicinal coupling constants and the ^{1}H n.m.r. anisotropic shift of the methyl group. Complexes of methylmercury(II) have been prepared with several homologous series of ligands which contain phenyl rings: $C_6H_5(CH_2)_nX$ ($X=NH_2, S^-, n=1,2,3$; and $X=CO_2^-$, $n=0,1,2$). The observation of a high field shift of the [$MeHg^+$] ^{1}H n.m.r. resonance is interpreted as an anisotropic shielding effect due to an intramolecular interaction between the mercury(II) ion and the phenyl ring. Such an interaction is only observed when $X=NH_2$ or S^- and n=1 or 2. Bis(methylmercury(II)) complexes have been prepared with three dithiolate ligands which each have a rigid carbon backbone structure holding the two sulphur atoms in a favourable position for chelation. The crystal structure of trans-(1,2-dimercapto)cyclohexanebis(methylmercury(II)) shows that one of the mercury atoms is bonded to a single sulphur (Hg(2)-S(2) 2.363(4)Å) while the other mercury atom has a weaker chelate bond (Hg(1)-S(2) 2.857(3)Å) in addition to the primary mercury-sulphur bond (Hg(1)-S(1) 2.367(4)Å). There is good evidence (from n.m.r. spectra) that a similar structure exists in solution for all three complexes. The reaction of 2-methyl-2-(2-pyridyl)thiazolidine (A) has been studied with methylmercury(II), mercury(II) and zinc(II). The thiazolidine ring of the ligand was opened to form the corresponding Schiff base in the presence of the metal ions. Methylmercury(II) only caused complete ring opening of (A) when acetate counterion was used to absorb the proton released on thiol co-ordination. In the reaction of mercury(II) with (A) there was a very fast rearrangment of the coordinated ligand. The product Hg(A)ClO_4 was characterised by ^{13}C n.m.r. as containing the ligand in a ring opened form. The reaction of zinc(II) perchlorate with (A) was seen to have two stages- an initial binding of (A) which was largely first order and a non-first order ligand rearrangement stage. In the analogous reaction with zinc(II) acetate the first stage could not be detected, while the second stage had become first order due to acetate buffering. The activation parameters for the second stage (i.e. co-ordinated ligand rearrangment) are reported together with characterisation of the complex by ^{13}C n.m.r. . The reaction of methylmercury(II) with four tetra-aza macrocyclic ligands was investigated by n.m.r. spectroscopy. The reaction with the secondary amine ligands caused partial decomposition of methylmercury(II) to produce varying quantities of $HgMe_2$ and Hg° . In the reaction with the tetramethylated ligands decomposition of the methylmercury(II) complex produced Hg^{2+} and $HgMe_2$. Electrophilic attack by free methylmercury(II) on complexed methylmercury(II) is proposed to account for the observed decomposition. The demethylation of methylmercury(II) under mild conditions in its reaction with thiolate ligands is reported. Equimolar quantities of mercaptan and methylmercury(II) produced varying quantities of $Hg(SR)_2$, $HgCl_2$ and CH_4 as additional reaction products to the methylmercury(II) thiolate complex. The thiolate proton which is released upon complexation is proposed to cause the demethylation reaction.

Chapter 1

Introduction.

The work described in this thesis is concerned with investigating the co-ordination chemistry of methylmercury (II) and to a lesser extent mercury(II). The long-term aim of the work is to improve upon the current chomotherapeutic treatment of heavy metal poisoning by gaining a greater understanding of the chemistry involved.

1.1 Mercury in the Environment.

Man has greatly increased the amount of mercury in the environment over and above the background level that is present due to the natural mercury cycle. It has been shown that concentrations of organomercurials of as low as 0.1μg/kg can inhibit photosynthesis in phytoplankton whereas the estimated natural background level of mercury in the sea is only 0.03 μg/kg (1). The major sources of mercury pollution are the release of mercury used as an electrode or catalyst in the manufacture of chlorine, caustic soda, vinyl chloride and acetaldehyde. Organomercurials are used as bacteriocides and fungicides in agriculture and in the manufacture of paints and paper because of their high toxicity to all living species. A considerable quantity of mercury is released into the atomosphere by the burning of fossil fuels which contain trace amounts of mercury. Obsolete electrical, laboratory and industrial equipment (in which mercury has many applications) also contribute a significant quantity of mercury into the environment. Mercury enters the environment in three

different forms as elemental mercury, bivalent mercury and organomercury compounds. All three forms eventually find their way into an aquatic environment and tend to accumulate in the sediment of rivers lakes and seas. Elemental mercury is oxidised to bivalent mercury and the alkoxymercury compounds normally used as biocides and fungicides are readily dealkoxylated to bivalent mercury (2-4).

There had been several isolated cases of organomercury poisoning prior to the first epidemic of methylmercury poisoning which occured in Minimata Bay, Japan in the 1950's [organomercury poisoning is often referred to as Minimata disease] (5,6). In 1956 the first victims of the Minimata Bay disaster were admitted to hospital suffering from numbness of the limbs, severe loss of co-ordination, partial blindness and loss of hearing. The cause of the symptoms was thought to be a heavy metal but the principal contaminant, mercury(II), did not produce the symptoms which were being found. Large quantities of mercuric sulphate were being discharged into Minimata Bay from a chemical plant where mercuric sulphate was used as a catalyst in the synthesis of acetaldehyde [an intermediate in the manufacture of octanol and diacetylphthalate]. It was not until 1959 that organomercury compounds were suspected of causing the poisoning and in 1961 methyl(methylmercapto) mercury(II) was actually isolated from shellfish caught in Minimata Bay (7).

Closer examination of the factory effluent showed that it

did indeed contain small quantities of methylmercury(II) chloride which the shellfish in the bay accumulated as the methyl mercaptide complex (8). Low yields of methylmercury (II) species have been produced in the laboratory from a mixture of reagents used in the synthesis of both acetaldehye and vinyl chloride (9). At about this time the first example of methylation of inorganic mercury by a microorganism was reported (10). Both mono- and di-methylmercury(II) were produced when $HgCl_2$ was incubated with lake bottom sediment and rotten fish. It was also shown that under strictly anaerobic conditions methyl cobalamin could transfer a methyl group to inorganic mercury (11). Under anaerobic conditions there is normally a high concentration of hydrogen sulphide which binds inorganic mercury to form mercury sulphide and hence the mercury available for methylation is drastically decreased. For this reason it is probable that methylation of mercury under aerobic conditions is the principal source of methylmercury species in the environment. Another route to methylation of mercuric ion by mutants of **Neurospora** has been described as an "incorrect synthesis" of methionine (12).

The most serious epidemic of methylmercury poisoning which occured in 1972 in Iraq was caused by the eating of methylmercury treated grain. The grain had been treated with fungicide prior to distribution for sowing but instead was used to make bread and resulted in several thousand cases of methylmercury poisoning and over 600 deaths within one year

(13).

1.2 Solution chemistry of methylmercury(II).

The most widely used technique for studying methylmercury (II) species in solution is nuclear magnetic resonance spectroscopy. The ^{1}H and ^{13}C n.m.r. spectra of the methyl group of MeHgX consist of a singlet flanked symmetrically by two less intense satellite lines. The satellites are due to the methyl groups bonded to ^{199}Hg (16.9% natural abundance, I=½) while the central line is due to the methyl groups bonded to the other mercury isotopes. The value of $^{2}J(^{199}Hg-^{1}H)$ is negative (14) and typically in the range 100-260 Hz while $^{1}J(^{13}C-^{199}Hg)$ is typically in the range 600-2000Hz for MeHgX species. The ^{2}J coupling is due to Fermi contact interaction and thus the magnitude of ^{2}J depends on the contribution of the Hg 6s orbital to the Hg-C bond (15,16). In MeHgX species the value of ^{2}J decreases with the increasing strength of the Hg-X bond. For example in the series MeHgX, with X=CH_3, RS^-, RNH_2 and NO_3^- (ranging from covalent to virtually ionic species) the ^{2}J values are typically 100,160,210 and 250 Hz respectively (17). The values of ^{2}J for a series of MeHgX species have a linear relationship with the logarithm of the formation constants, and for a series of structurally similar ligands possessing the same ligating atom, with the proton-basicity of X (18-27).

The model used to describe the nature of methylmercury(II)

species in aqueous solution was developed from pH titrations of $MeHg^+$ ion and it is proposed that the major species are $MeHgOH_2^+$, MeHgOH, $(MeHg)_2OH^+$ and $(MeHg)_3O^+$ (28-32). The nature of the ligating species in complexes of methylmercury(II) with many ambidentate and monodentate inorganic ligands has been determined by a combination of Raman and nuclear magnetic resonance spectroscopy (33). In the Raman spectra there is a dependence of the symmetrical CH deformation and the Hg-C stretch vibrations on the nature of the co-ordinating atom.

The mercury of methylmercury(II) has a very strong tendency towards linear two-coordination although it does possess some residual Lewis acidity. The first evidence of a higher co-ordination number than two was the formation of $MeHgI_2^{2-}$, which was proposed to account for the increased solubility of methyliodomercury(II) in aqueous KI solution (27). The formation constant of this was estimated to be 2 which is much smaller than that of MeHgI ($K = 4 \times 10^6$). This residual Lewis acidity in MeHgX is much smaller than that of HgX_2 which readily forms complex ions of the form HgX_4^{2-}. The formation of complex anions has subsequently been observed for $(MeHgX_3)^{2-}$ when X= SCN^-, Cl^-, Br^- and I^-. The presence of these anions were detected by a combination of infra-red/Raman spectroscopy and nuclear magnetic resonance spectroscopy (34,35).

The most fully characterised chelate complex of methylmercury(II) is that with 2,2'bipyridine (bipy). The ^2J

coupling constant increases from 229.6 Hz for the unidentate pyridine complex to 238.8 Hz for the complex with bipy, and the log(Kf) values from 4.8 to 5.9. A deviation from the linear correlation of ^{2}J with the proton basicity is often interpreted as a change in the nature of the bonding in the species being studied. For example the complex with 3,3'-dimethyl-2,2'-bipyridine (in which chelation is prevented by steric interaction between the methyl groups) fits the correlation for unidentate pyridine complexes rather than that for chelating bipyridine complexes (36-38).

The fact that methylmercury(II) is a "soft" Lewis acid is demonstrated by the stability constants of methylmercury(II) halide complexes which increase in the order F<Cl<Br<I (39,40). Complexes of methylmercury(II) have been prepared with a wide variety of organic ligands in an attempt to gain more understanding of the mode of action of methylmercury poisoning. Since methylmercury(II) forms its most stable complexes with mercaptans it has been suggested that the blocking of enzyme and protein sulphydryl sites can explain some of its properties in biological systems.

The methylmercury(II) complexes of glutathione and cysteine have log(Kf) values of 15.9 and 15.7 respectively (41). n.m.r. studies have shown that there is complete complex formation of methylmercury(II) with the sulphydryl groups of glutathione, cysteine and penicillamine over the pH range 1-13 (42,43). The formation constant of the methylmercury(II)

complex with a cysteine containing enzyme, papain (log Kf=18.1), is significantly larger than that for cysteine itself (44). A possible explanation for this large difference will be discussed later. With complexes which have a smaller formation constant, competition from other species in solution becomes significant. At very low pH protons compete with $MeHg^+$ for those ligating groups which are Brönsted bases while at high pH hydroxide ions compete with the ligand for $MeHg^+$.

In methylmercury(II) complexes with multidentate ligands the binding site can often show a pronounced pH dependence. For example in simple amino acids methylmercury(II) binds at the amino group at high pH, the carboxylate group at low pH and at intermediate pH values the solution contains a mixture of both species in a dynamic equilibrium. At the low and high extremes of pH the complex dissociates due to competition with the species outlined above. Formation constants of the individual species can be derived from the n.m.r. data of a pH titration (45). In the case of methionine (an amino acid which contains a thioether group) it has been shown that binding through sulphur only occurs at pH<2 i.e. when the amino group is protonated (46).

A further example of the extent to which the nature of methylmercury(II) complexes are dependant on pH is the methylmercury(II)-imidazole system (Fig 1.2.1). As the pH of an equimolar mixture of imidazole and methylmercury(II) is

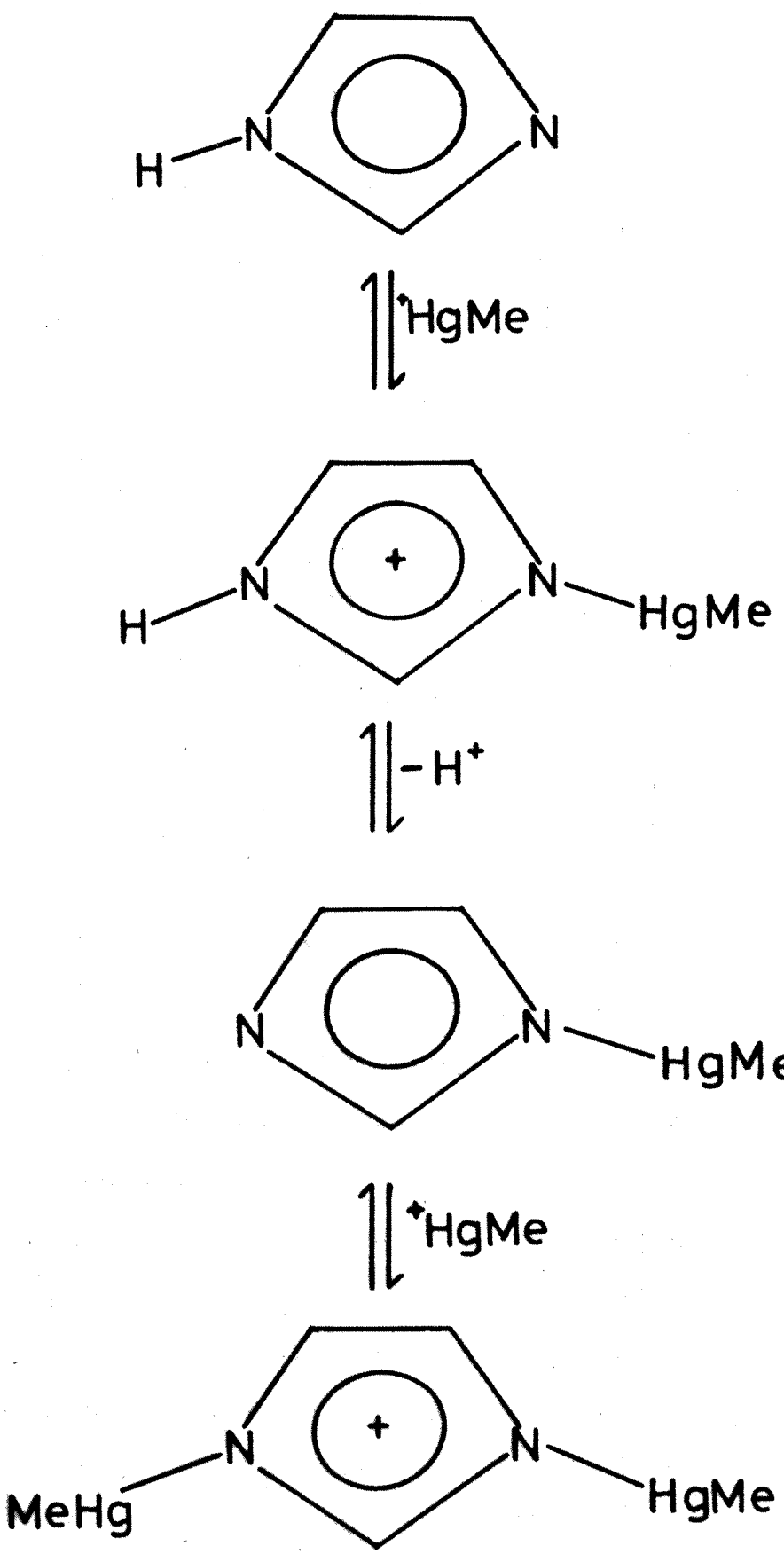

Figure 1.2.1

increased $MeHg^+$ first binds at the pyridine nitrogen. This causes an increase in the acidity of the proton on the pyrrole nitrogen which dissociates to form a neutral complex. The stability of methylmercury(II) complexes increases with increasing basicity of donor group and the result of this is a rearrangment to produce free imidazole and an imidazolebis(methylmercury(II)) species (47).

Since it was reported that methylmercury(II) causes chromosome damage (48) there have been several studies of the bonding of methylmercury(II) with nucleosides, nucleotides and polynucleotides which show binding at several sites of the bases to form both mono- and polynuclear complexes depending on both pH and the bases present (49-53).

1.3 Solid state structures of methylmercury(II) complexes.

Methylmercury(II) forms complexes with a wide range of organic and inorganic ligands with a formal co-ordination number of one. Methyl(cyano)mercury(II) exists as a linear molecule with mercury co-ordinated via the carbon atom of the cyanide (54). Tris(methylmercuri)oxonium nitrate has a near linear O-Hg-C bond angle (175°) (55) as does methyl(azido)mercury(II) with N-Hg-C (173°) (56). The mercury atoms in both these structures have additional weak interactions which probably account for the non-linearity observed. The structure of $B_{10}H_{10}C(HgCH_3)C(CH_2Cl)$ (A) shows a C-Hg-C bond angle of 174° with the methyl carbon bent away

from a weakly co-ordinating chlorine atom (57). The selenourea complex of methylmercury(II) again shows a linear C-Hg-Se bond angle with no significant weak interactions(58).

Methyl(2,2'-bipyridyl)mercury(II) nitrate (B) was the first observed example of a truly three co-ordinate chelated methylmercury(II) complex (59). The 2,2'bipyridyl ligand is unsymmetrically chelated with Hg-N and Hg-N' distances of 2.24 and 2.42 Å respectively. The methyl group is bent away from the more weakly bonding nitrogen, N', with an N-Hg-C bond angle of 164° and N, N', Hg and C are co-planar. In the case of methyl(3,3'dimethylbipyridyl)mercury(II) (60) where the methyl groups prevent chelation by the second pyridyl ring the N-Hg-C bond angle increases to 173° with bond lengths very similar to those observed for methyl(pyridyl) mercury(II) (61). The chelation has increased the Hg-C bond lengths from 2.01 to 2.07 Å and the principal Hg-N bond length from 2.11 to 2.24 Å.

In methyl(N,N-diethyldithiocarbamato)mercury(II) (C) the mercury ion is chelated with Hg-S and Hg-S' bond lengths of 2.42 and 2.96 Å respectively and the methyl group is again bent away from the chelating atom S' with a S-Hg-C bond angle of 171° (62). In methyl(2-mercaptopyrimidinato)mercury(II) (D) the mercury is principally bonded through sulphur but also has a weak interaction with a pyrimidine nitrogen (Hg-N 2.83 Å) and a S-Hg-C bond angle of 174° (63).

Fig 1.3.1

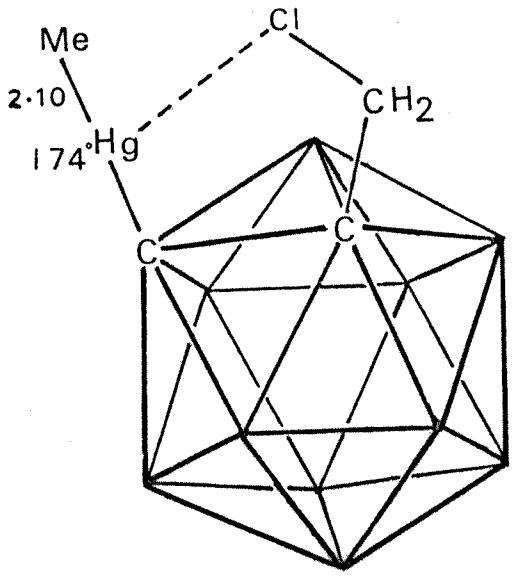

A

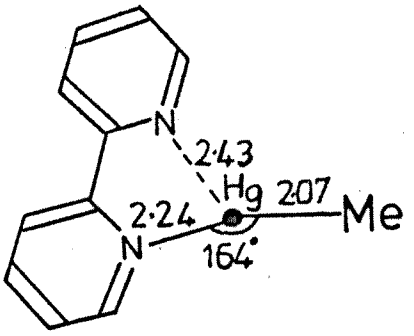

B

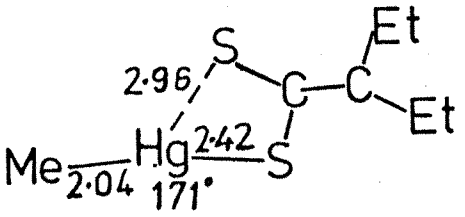

C

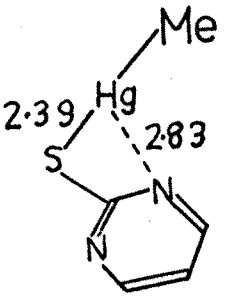

D

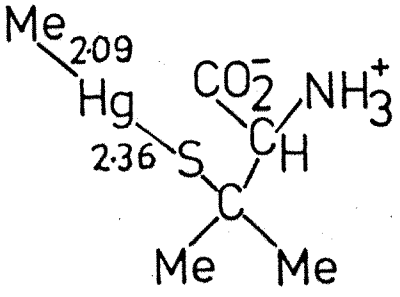

E

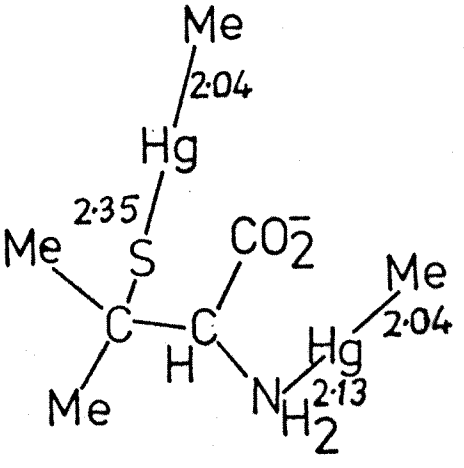

F

The structures of methylmercury(II) amino acid complexes have been determined and used as models for the interaction of methylmercury(II) with proteins and enzymes. Methylmercury(II) being a classic soft acid forms its most stable complexes with soft bases so the complexes studied have all been with sulphur containing amino acids

In methyl(DL-penicillaminato)mercury (II) monohydrate **(E)** the mercury(II) ion binds **via** a deprotonated sulphydryl group as might be expected, and in u-DL-penicillaminato-bis (methylmercury(II)) **(F)** the second mercury atom binds **via** the amino group(64-66). The C-Hg-S bond angles are 175° in both cases with very similar bond lengths around mercury whilst the C-Hg-N bond angle is 170° due to additional weak interactions.

Methyl(L-cysteinato)mercury(II) **(G)** has the mercury bound **via** the deprotonated sulphydryl group whilst in methyl(DL-methionine)mercury(II) **(H)** [a thioether amino acid] the mercury is co-ordinated through the amino group and has an additional weak carboxylate interaction which causes a N-Hg-C angle of 173° (67-69).

Bis(methylmercury(II)) complexes of adenine **(J)** and 9-methyladenine **(K)** have been studied as model compounds for methylmercury(II)-nucleic acid interactions (70). In the adenine complex the mercury atoms bind at the nitrogen atoms in the 7 and 9 positions while in the 9-methyladenine

Fig. 1.3.2

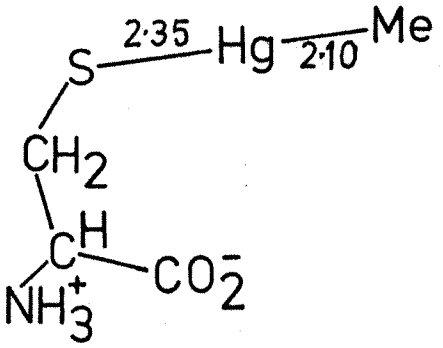
2·35
Hg
2·10
Me
S
CH2
CH
NH3+
CO2−

G

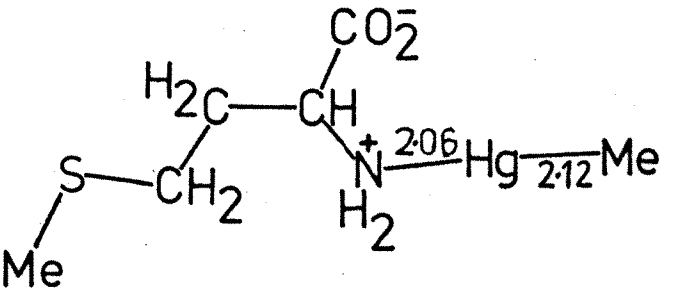
CO2−
H2C
CH
2·06
Hg
2·12
Me
S
CH2
N+
H2
Me

H

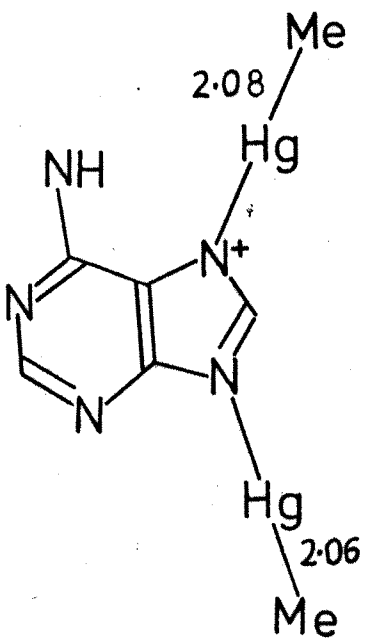
Me
2·08
Hg
NH
N+
N
N
N
Hg
2·06
Me

J

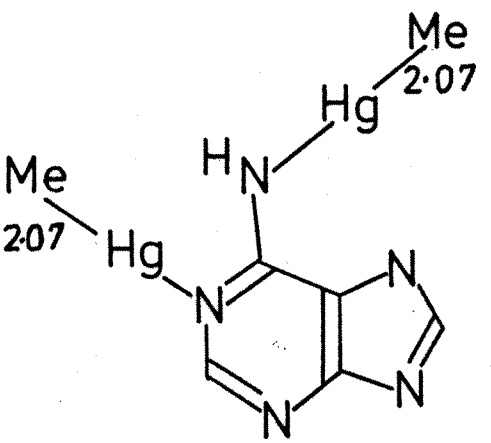
Me
2·07
Hg
HN
Me
2·07
Hg
N
N
N
N
N

K

complex, co-ordination is with N1 and the deprotonated amine group.

1.4 The Toxicology and Treatment of Methylmercury(II) Poisoning.

Methylmercury(II) behaves quite differently to other forms of mercury in biological systems. Inorganic mercury tends to accumulate in the kidney and is unable to cross the blood-brain barrier whereas methylmercury(II) is lipid soluble and readily crosses the blood-brain barrier to accumulate in the brain. Elemental mercury behaves similarly to inorganic mercury except that some Hg^{0} in the blood does diffuse across the blood-brain barrier where it damages the cells after it is oxidised to mercury(II) (71).

Methylmercury(II) normally enters the body in the form of a complex with cysteine-containing peptides and proteins of foodstuffs. The mode of absorption from the gastrointestinal tract into the bloodstream is not known although the formation of methylmercury(II) chloride is one possible route (72). In the low pH and high chloride concentration of the stomach, a significant fraction of the total methylmercury (II) will be present as MeHgCl which is lipid soluble and can therefore readily enter the bloodstream. Once absorbed into the bloodstream methylmercury(II) exchanges rapidly between the various sulphydryl species that it encounters. 90% of the sulphydryl sites in blood are in the haemoglobin and this is where methylmercury(II) is predominantly bound (73). As the

blood flows through the brain, methylmercury(II) which is complexed to low molecular weight sulphydryl ligands is able to transfer across the blood-brain barrier and cause cell lysis. The reasons for the high selectivity of methylmercury(II) towards various target molecules in the brain and the means by which cell lysis occurs are both still unknown. Any damage occurring to brain cells will tend to be amplified because the functions of damaged cells are partly taken over by existing nerve cells rather than new replacement cells produced by cell division.

Methylmercury(II) is extracted from the bloodstream as it passes through the liver and is returned to the gastrointestinal tract in the liver bile although a small fraction is demethylated into Hg(II) in the liver (74). The mercury(II) and a fraction of the protein bound methylmercury(II) in the liver bile are excreted in the faeces at a rate of approximately 2% of total body burden per day while a much smaller amount is excreted in the urine. The remainder of the methylmercury(II) complexes in the bile are re-absorbed into the bloodstream hence completing a cycle which provides numerous opportunities for methylmercury(II) to pass through the brain. The biological half-life of methylmercury(II) in humans is about 70 days although the half-life of methylmercury(II) in the brain is somewhat greater. For comparison some fish have half-lives for methylmercury(II) removal of as long as 1000 days (75).

The symptoms observed in methylmercury(II) poisoning are all caused by damage to the central nervous system. Loss of sensation at the extremities of hands and feet are the first symptoms which appear with a methylmercury(II) total body burden of 25mg. These symptoms are followed by loss of co-ordination, slurred speech, loss of hearing and blindness as the body burden increases until death occurs at a body burden of around 200mg (71).

The only method of treating methylmercury(II) poisoning is to increase its rate of elimination from the body since there are not yet any treatments available which can repair damaged brain cells. British anti-Lewisite (BAL) was used as the treatment for both organic and inorganic mercury poisoning until it was shown to increase the amount of methylmercury(II) in the brain (76).

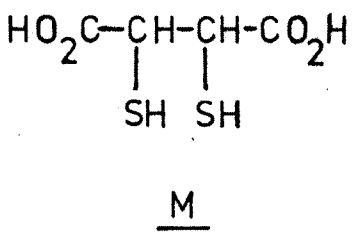

M

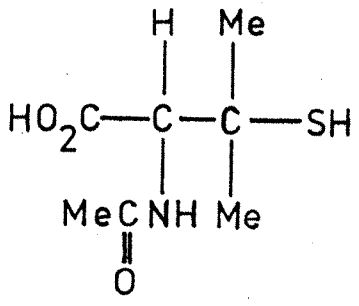

N

Dimercaptosuccinic acid (M) and N-acetyl-D,L-penicillamine (N) have been shown to be useful chemotherapeutic agents for methylmercury(II) poisoning, the latter having reduced the biological half-life of methylmercury(II) in mice from 10.4 to 1.7 days (77,78). The most succesful treatment in the

Iraq epidemic involved administration of a polystyrene resin containing free thiol groups (13). This treatment had the advantages that there was no re-distribution of methylmercury(II), the insoluble resin formed highly stable complexes that were readily excreted and there were not the usual side effects produced by other sulphydryl chemotherapeutic agents which enter the bloodstream.

1.5 Scope of this work

The work described in this thesis approaches the problem of methylmercury(II) poisoning from several angles. The interaction of methylmercury(II) with ligands which possess a range of potentially desirable properties have been studied. Factors which enhance the stability of methylmercury(II) complexes containing aromatic residues are reported in Chapter 2. A study of methylmercury(II) complexes formed with chelating dithiolate ligands is reported in Chapter 3. A method of protecting the thiol group from oxidation and its subsequent re-activation by heavy metal ions is reported in Chapter 4. Demethylation of methylmercury(II) under mild conditions and the reactions of some novel ligands with methylmercury(II) are reported in Chapter 5.

Chapter 2

Methylmercury(II)-Arene Interactions.

2.1 Introduction.

An interaction of methylmercury(II) with a phenyl ring was noted by Rabenstein (19) in a study of the formation constants of amino acid complexes of methylmercury(II). In the ^1H n.m.r. spectrum of the amine-bound phenylalanine (A) complex he noted a pronounced upfield shift of the methyl resonance from its expected position and attributed this to aromatic ring current anisotropy effects caused by a hydrophobic interaction of the phenyl ring with the methyl group of *MeHg*. The formation constant of the phenylalanine complex (log Kf =8.29) was considerably higher than that observed for other amino acid and peptide complexes (typically log Kf =7.5), suggesting that the aromatic interaction enhanced the stability of the complex.

In methyl(benzylmercapto)mercury(II) an upfield shift of the ^1H methyl resonance from its expected value was again attributed to an intramolecular methylmercury-arene interaction (25).

An early example of a mercury-arene interaction is that of $[CoHg_2(SCN)_6 \cdot C_6H_6]$ where the mercury has a very distorted tetrahedral arrangement of S-bonded thiocyanates and a weakly co-ordinated benzene ring with Hg-C distances of 3.66 and 3.52Å (79).An unpublished crystal structure quoted by Kiefer et al of 3-(p-methoxyphenyl)- 2-methyl-2methoxypropylmercuric

chloride (B) shows a mercury atom located 3.05Å above the Cl-C6 bond of the phenyl ring (80). The structure of benzyltriphenylmethylthiomercury(II) reveals an interaction between mercury and one of the phenyl rings of the thiol (with a mercury-carbon bond distance of 3.30Å) (81).

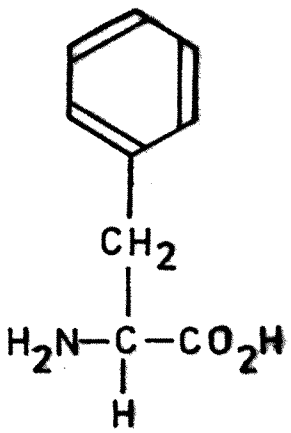

A

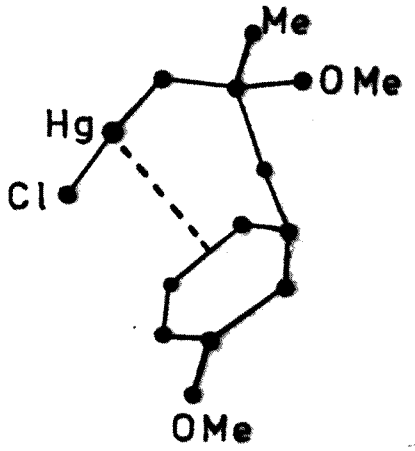

B

2.2 Solid State Crystallographic Studies

2.2.1 Methyl(L-tyrosinato)mercury(II). (1)

The nature of the mercury-phenyl ring interaction could only be satisfactorily characterised by a crystallographic structure determination. Attempts were made to prepare suitable crystals of the (phenylalanine) methylmercury(II) complex but these were unsuccessful. Suitable crystals were obtained with an analogous amino acid, tyrosine (p-hydroxyphenylalanine), which was known to have a similar ring interaction (82).

The preparation of complex (1) and the structure solution are described in Section 4. Crystal data, atomic co-ordinates, bond lengths and bond angles are given in Tables 2.2.1., 2.2.2., 2.2.3. and 2.2.4. respectively. A perspective view of (1) is shown in Figure 2.2.1. . The mercury is principally co-ordinated through the amino group with further weak intramolecular interactions with a carboxylate oxygen and with the phenyl ring. The Hg-N bond length [2.17(2)Å] is approximately equal to the sum of the covalent radii of mercury (1.48Å) and nitrogen (0.70Å) (83). The Hg-C(1) bond length [2.12(5)Å] is also in the expected range for methylmercury(II) complexes (54-70). The N-Hg-C(1) angle [169(1)°] is significantly distorted from linearity - bent away from the chelating carboxylate oxygen O(2) in a manner also observed in previous structures . The Hg-O(1) distance [2.62(2)Å] is greater than the sum of the covalent radii but significantly shorter than the sum of the van der Waals radii (2.90-3.13Å) (83).

The previously postulated "hydrophobic interaction" is seen to be due to a mercury-ring interaction rather than a methyl group-ring interaction. The mercury atom is located over the C(5)-C(10) bond with distances Hg-C(5) [3.33(2)Å] and Hg-C(10) [3.19(2)Å].

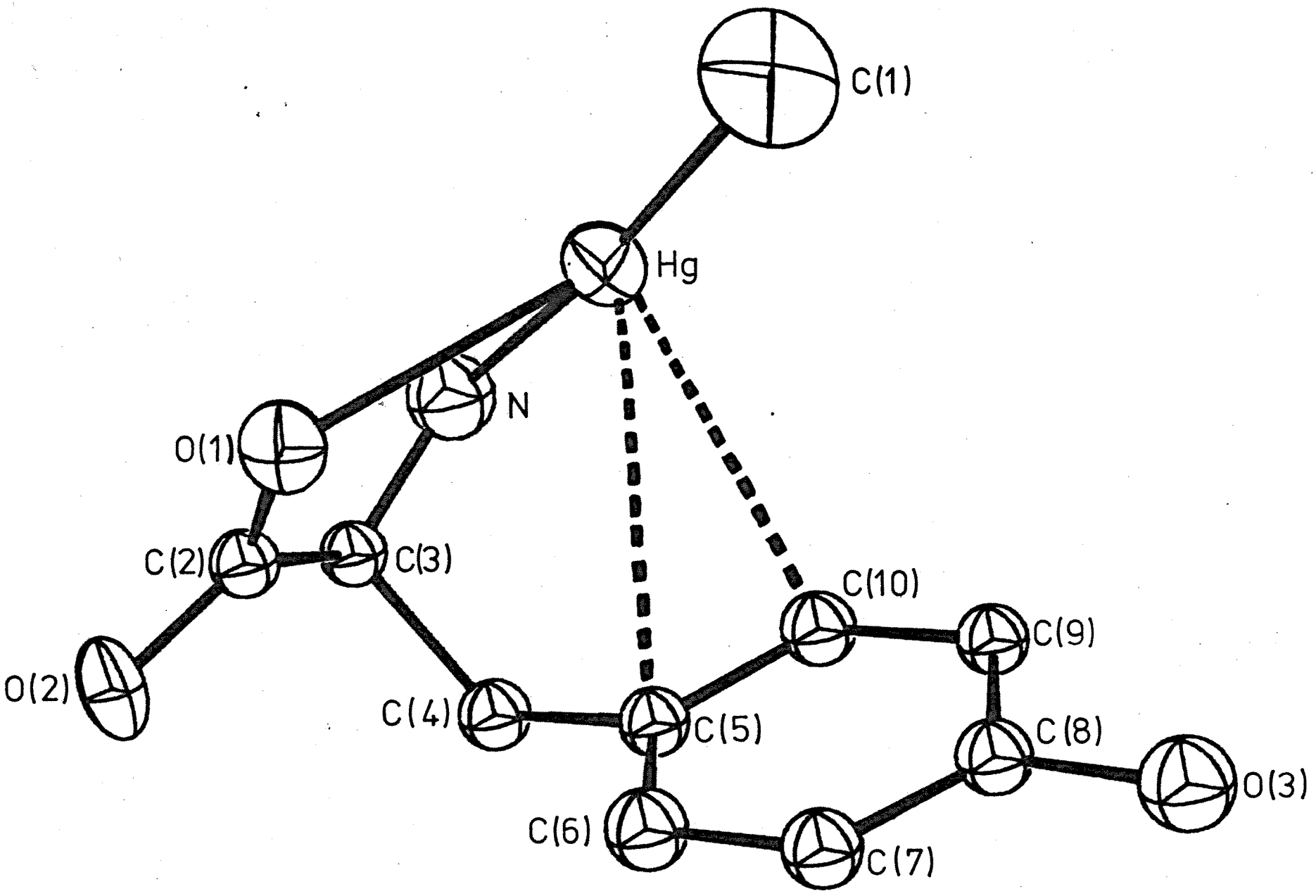

Fig. 2.2.1. Molecular Structure of (1)

Table 2.2.1.

Crystal data.

	Complex(1)	Complex(2)
Molecular formula	$C_{10}H_{13}HgNO_3.H_2O$	$C_{11}H_{15}HgNO_2$
Colour	White	White
Habit	Needle	Needle
Crystal System	Monoclinic	Orthorhombic
a/Å	9.0843(19)	14.853(4)
b/Å	6.1506(15)	9.438(3)
c/Å	11.6548(20)	8.755(2)
β/°	110.516(14)	
U/Å^3	605.18(22)	1227.25(58)
T/K	173	173
Space group	$P2_1$	$Pca2_1$
μ/cm^{-1}	126.7	125.4
Relative molecular mass	413.6	383.6
D_m/g cm^{-1}	2.16	2.20
D_c/g cm^{-1}	2.27	2.13
Z	2	4
N(3σ)	1078	674
λ(Mo-K$_\alpha$)/Å	0.71069	0.71069

Table 2.2.2.

Atomic co-ordinates ($X10^4$) with standard deviations in parentheses for complex (1).

Atom	X	Y	Z
Hg	2427.6(9)	2500.0	431.9(7)
O(1)	1697(18)	6439(26)	0901(14)
O(2)	0910(17)	8032(27)	2299(15)
O(3)	8399(14)	2459(60)	3626(11)
O(4)	9462(17)	8436(27)	3945(13)
N(1)	0788(16)	2361(54)	1404(14)
C(1)	3727(36)	2120(46)	-738(25)
C(2)	1197(23)	6374(36)	1786(18)
C(3)	0868(22)	4192(35)	2243(17)
C(4)	2125(22)	3573(36)	3521(17)
C(5)	3792(22)	3280(32)	3473(17)
C(6)	4810(23)	5054(37)	3685(19)
C(7)	6376(27)	4712(38)	3725(21)
C(8)	6839(18)	2785(50)	3525(14)
C(9)	5843(24)	0903(36)	3278(19)
C(10)	4260(25)	1279(38)	3253(19)

Table 2.2.3.

Bond lengths (Å) with standard deviations in parentheses for complex (1).

Hg-C(1)	2.12(5)
Hg-N	2.17(2)
Hg-O(1)	2.62(2)
Hg-C(10)	3.19(2)
Hg-C(5)	3.33(2)
Hg-ring plane	3.11(2)
C(2)-O(1)	1.26(3)
C(2)-O(2)	1.25(3)
C(2)-C(3)	1.51(3)
C(3)-N	1.42(4)
C(3)-C(4)	1.57(3)
C(4)-C(5)	1.55(3)
C(5)-C(6)	1.40(3)
C(5)-C(10)	1.36(3)
C(6)-C(7)	1.42(3)
C(7)-C(8)	1.30(4)
C(8)-C(9)	1.43(3)
C(8)-O(3)	1.39(2)
C(9)-C(10)	1.45(3)

Table 2.2.4.

Bond angles (°) with standard deviations in parentheses for complex (1).

C(1)-Hg-N	169(1)
C(1)-Hg-O(1)	118.8(9)
N-Hg-O(1)	68(1)
Hg-N-C(3)	117(2)
Hg-O(1)-C(2)	109(1)
O(1)-C(2)-O(2)	123(2)
O(1)-C(2)-C(3)	119(2)
O(2)-C(2)-C(3)	117(2)
C(2)-C(3)-N	113(2)
C(2)-C(3)-C(4)	112(2)
N-C(3)-C(4)	108(2)
C(3)-C(4)-C(5)	113(2)
C(4)-C(5)-C(6)	120(2)
C(4)-C(5)-C(10)	120(2)
C(6)-C(5)-C(10)	121(2)
C(5)-C(6)-C(7)	119(2)
C(6)-C(7)-C(8)	121(2)
C(7)-C(8)-C(9)	123(2)
C(7)-C(8)-O(3)	120(3)
C(9)-C(8)-O(3)	117(3)
C(8)-C(9)-C(10)	115(2)
C(9)-C(10)-C(5)	121(2)

Table 2.2.5.

Hydrogen bond lengths (Å) and angles(°) for complex (1) with standard deviations in parentheses.

Bond lengths.

O(4)...O(2)	2.68(3)
O(4)...O'(3)	2.64(4)
O(4)...O''(3)	2.86(3)
N...O'(2)	2.89(4)
N...O''(4)	2.90(3)

Bond angles.

O(2)..O(4)..O'(3)	103.6(8)
O(2)..O(4)..O''(3)	110.1(6)
O'(3)..O(4)..O''(3)	115.1(9)

The distance between the mercury atom and the ring plane is 3.11(2)Å while the C(1)-ring distance is 4.40(2)Å which is obviously too great a distance for any significant bonding to occur. The ring carbon atoms and O(3) are coplanar within experimental error although C(4) is 0.14Å out of the plane of the ring on the side away from the mercury atom. This non planarity of C(4) shows that the phenyl ring is so constrained that a closer mercury-ring interaction cannot occur.

A subsequent crystallographic study of

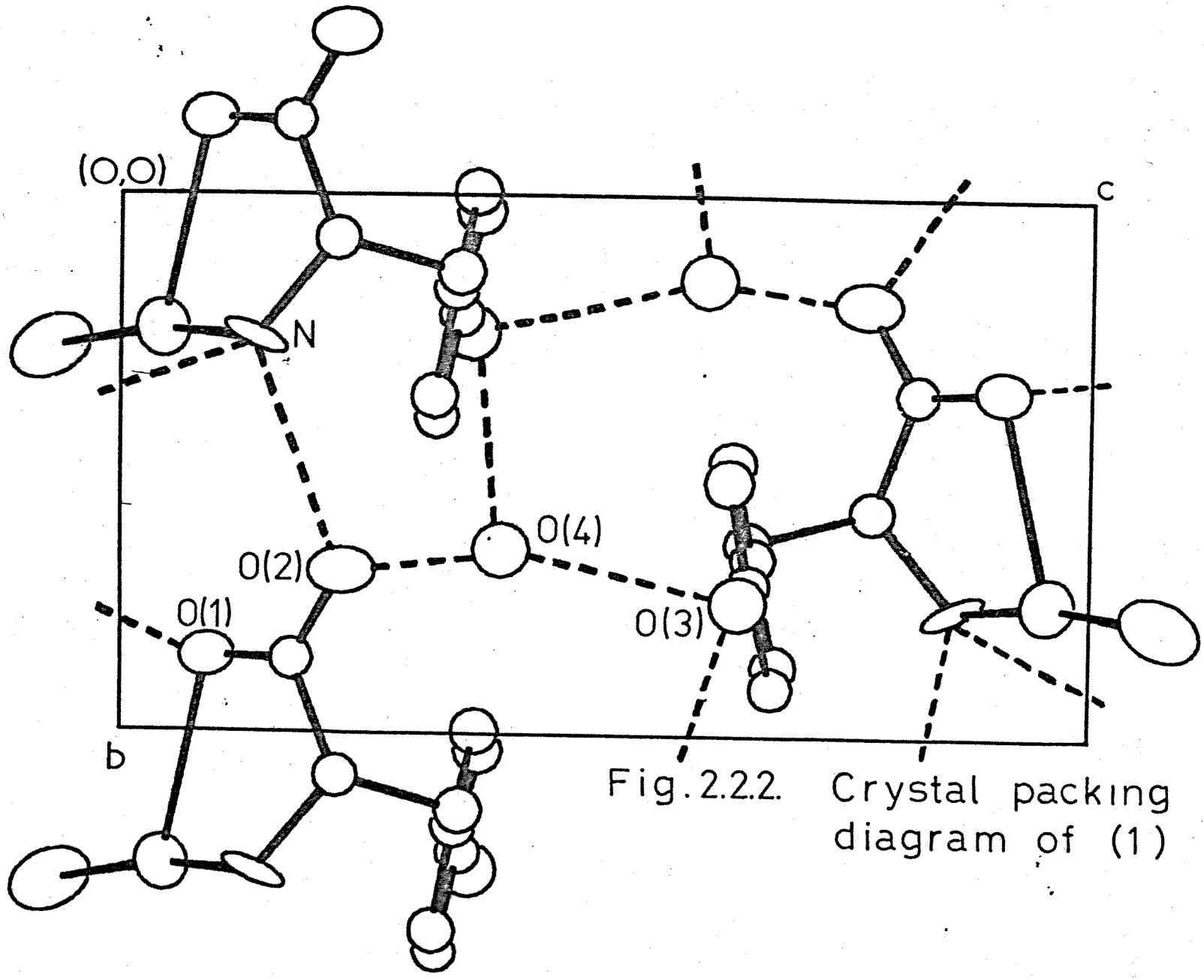

Fig. 2.2.2. Crystal packing diagram of (1)

methyl(2-benzylpyridine)mercury(II) shows the mercury to be located over the same two ring carbon atoms with similar bond lengths of 3.23(2) and 3.33(3)Å (84).

A subsequent crystallographic study of o-Methylbenzoin methylmercurio(p-tolylsulphonyl)hydrazone shows the mercury again located over the same ring carbon atoms with a mercury-ring distance of 3.09(Å) (85). The authors do not consider this to be significant although the interaction is identical to the cases discussed above.

A crystal packing diagram is shown in Figure 2.2.2. . Hydrogen bond lengths and angles are shown in Table 2.2.5. . Overall the molecules are linked into a hydrogen bonded three dimensional framework. Each oxygen atom O(4) of the water of crystallisation forms hydrogen bonds to three atoms arranged tetrahedrally; these are part of three separate molecules, the carboxylate oxygen O(2) and the phenolic oxygen atoms O'(3) of the molecule translated one unit cell along b and O''(3) of the molecule translated by the screw axis. The nitrogen atom is hydrogen bonded to the carboxylate oxygen O'(2) of the molecule translated one unit cell along b and the carboxylate oxygen O''(1) of the molecule translated by the screw axis.

2.2.2 Methyl(2-amino-4phenylbutanato) mercury(II). (2)

Complex (2) was prepared in an attempt to remove the constraint which prevents any closer interaction between

mercury and the aromatic ring. The preparation of the complex and its structure solution are described later. Crystal data, atomic co-ordinates, bond lengths and bond angles are given in Tables 2.2.1., 2.2.6., 2.2.7. and 2.2.8.. A perspective view of (2) is given in Figure 2.2.3..

Table 2.2.6.

Atomic co-ordinates ($X10^4$) with standard deviations in parentheses for complex (2).

Atom	X	Y	Z
Hg	541.0(12)	1212.3(7)	0.0
O(1)	2512(27)	0312(14)	1710(24)
O(2)	1785(29)	-805(17)	3103(30)
N(1)	0508(33)	-208(16)	-426(23)
C(1)	0530(48)	2610(21)	309(129)
C(2)	1745(35)	-358(21)	1954(34)
C(3)	0562(42)	-783(23)	0936(37)
C(4)	1036(35)	-1750(21)	0513(34)
C(5)	-176(50)	-2207(29)	-395(46)
C(6)	0317(45)	-3124(26)	-720(40)
C(7)	-169(40)	-3862(26)	-022(132)
C(8)	0371(52)	-4787(26)	-304(50)
C(9)	1335(56)	-4904(35)	-1227(51)
C(10)	1931(56)	-4173(31)	-2111(61)
C(11)	1484(51)	-3262(29)	-1812(51)

Table 2.2.7.

Bond lengths (Å) with standard deviations in parentheses for complex **(2)**.

Hg-C(1)	2.12(3)
Hg-N	2.15(3)
Hg-O(1)	2.72(2)
Hg-O'(2)	2.78(3)
C(2)-O(1)	1.22(4)
C(2)-O(2)	1.27(4)
C(2)-C(3)	1.56(5)
C(3)-N	1.56(4)
C(3)-C(4)	1.52(4)
C(4)-C(5)	1.48(5)
C(5)-C(6)	1.46(5)
C(6)-C(7)	1.34(8)
C(7)-C(8)	1.47(5)
C(8)-C(9)	1.24(6)
C(9)-C(10)	1.46(7)
C(10)-C(11)	1.43(6)
C(11)-C(6)	1.48(6)

Table 2.2.8.

Bond angles (°) with standard deviations in parentheses for complex **(2)**.

C(1)-Hg-N	177(2)
C(1)-Hg-O(1)	114(2)
C(1)-Hg-O'(2)	109(2)
N-Hg-O(1)	68(1)
N-Hg-O'(2)	70(1)
O(1)-Hg-O'(2)	138(1)
Hg-N-C(3)	114(2)
Hg-O(1)-C(2)	99(2)
O(1)-C(2)-O(2)	124(3)
O(1)-C(2)-C(3)	127(3)
O(2)-C(2)-C(3)	108(3)
C(2)-C(3)-N	106(2)
C(2)-C(3)-C(4)	113(3)
N-C(3)-C(4)	108(3)
C(3)-C(4)-C(5)	112(3)
C(4)-C(5)-C(6)	110(3)
C(5)-C(6)-C(7)	128(5)
C(5)-C(6)-C(11)	117(3)
C(6)-C(7)-C(8)	127(79
C(7)-C(8)-C(9)	117(5)
C(8)-C(9)-C(10)	123(4)
C(9)-C(10)-C(11)	119(4)
C(10)-C(11)-C(6)	118(4)

Fig. 2.2.3.

Molecular Structure of (2)

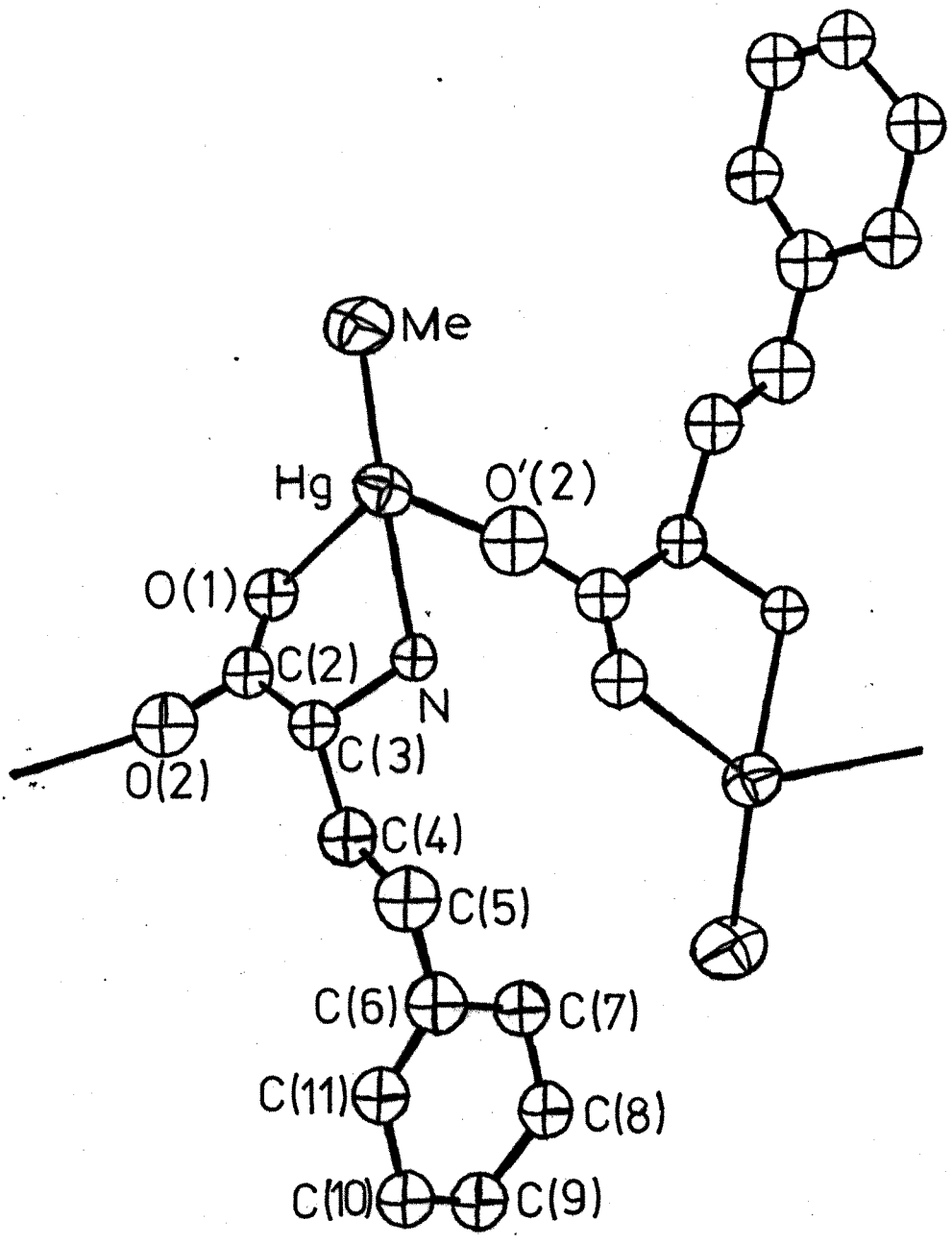

Table 2.2.9.

Hydrogen bond lengths (Å) and angles(°) for complex (2) with standard deviations in parentheses.

Bond lengths.

O(2)...N'	2.90(4)
O(2)...N''	2.89(4)
O(2)...HG'	2.78(3)

Bond angles.

N'..O(2)..N''	100(1)
Hg..O(2)..N'	44(1)
Hg..O(2)..N''	109(1)
C(3)..N..O(2)	135(2)
C(3)..N..O'(2)	101(2)

The molecule adopts an extended conformation in the crystal with no mercury-arene interaction. The mercury is principally co-ordinated through the amino group and has two further weaker interactions with one intermolecular and one intramolecular carboxylate oxygen. The Hg-N [2.15(3)Å] and Hg-C [2.12(3)Å] distances are both very similar to those observed in complex (1). The N-Hg-C(1) angle [177(2)°] is virtually linear unlike complex (1), perhaps due to O(1) and O'(2) bonding on opposite sides of the N-Hg-C(1) bond. The O(1)-Hg-O'(2) angle [138(1)°] is far from linear, and the mercury- oxygen bond lengths Hg-O(1) [2.72(2)Å] and Hg-O'(2)

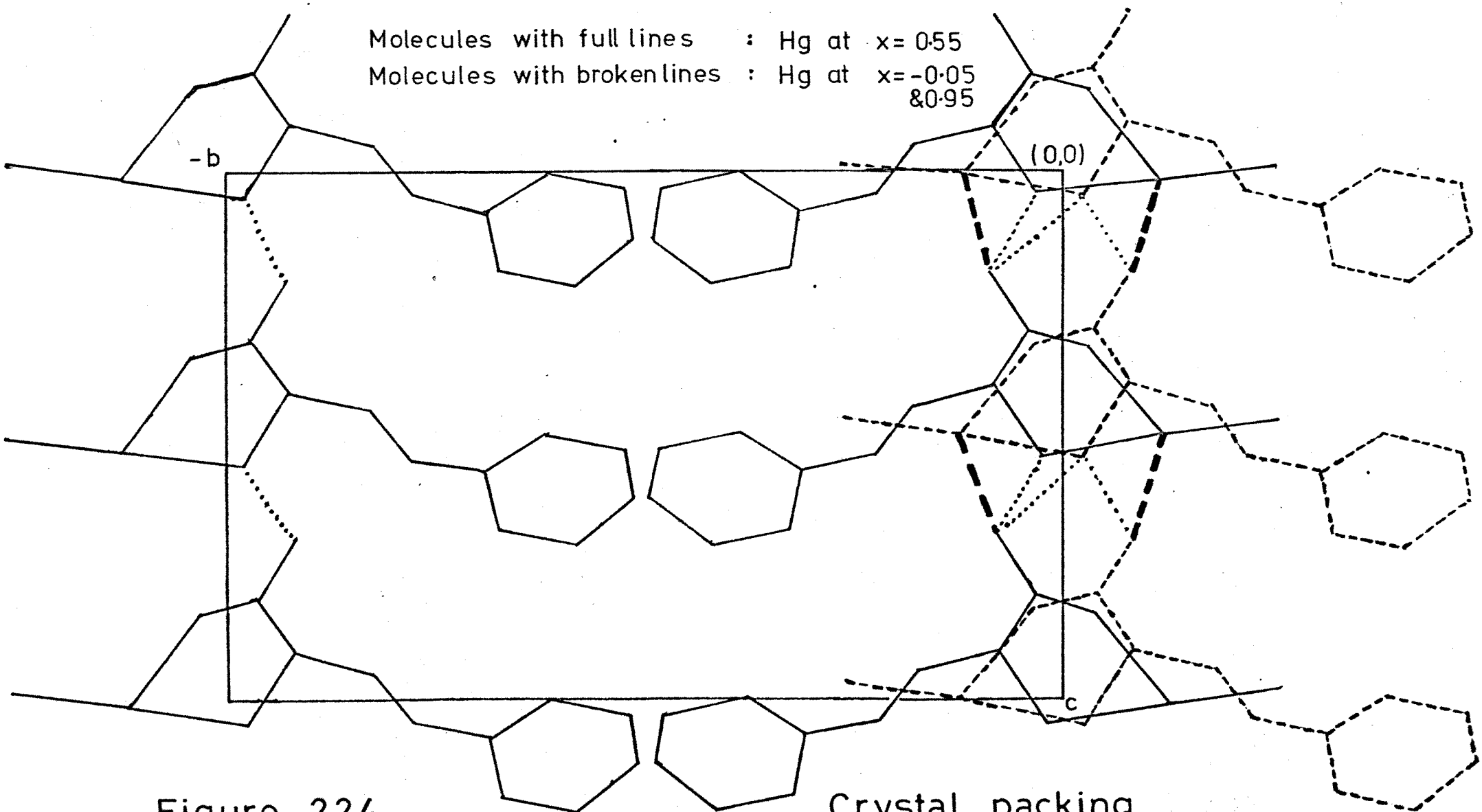

Figure 2.2.4 Crystal packing diagram for (2)

[2.78(3)Å] are notably longer than that found in (1) [2.62(2)Å] but still considerably shorter than the sum of the van der Waals radii.

A crystal packing diagram is shown in Figure 2.2.4.. Hydrogen bond lengths and angles are shown in Table 2.2.9.. There are two principal packing forces together with the stronger Hg-O'(2) interaction. There are N-O'(2) and N-O''(2) hydrogen bonds at the edge of the unit cell which with the Hg-O'(2) bond link the molecules into sheets. These sheets are held together by hydrophobic interactions between the phenyl rings in the middle of the cell.

2.3 Solution Studies.

The structure of (1) in solution and in the solid state has been compared by two methods. Using the crystal geometry of (1) the relationship between the centroid of the methyl protons (in their calculated positions) and the centroid of the phenyl ring can be examined. The methyl group centroid is 4.8Å above the plane of the ring and in the notation of Johnson and Bovey (see Appendix 1) the co-ordinates of this position are ρ=1.19 and Z=3.43. Using published tables (86) one can predict an upfield shift of 0.36ppm for the methyl resonance. The observed shifts (Table 2.3.1.) in the cases of tyrosine (shift=0.68ppm) and phenylalanine (where there are no ring substituents to perturb the ring current, shift=0.63ppm) are greater than the predicted shift.

However in view of the non-linear variation of the anisotropic shift parameter with ρ and Z (shown in Figure 7.1.1.) this agreement can be regarded as satisfactory and this indicates that the molecules are in similar conformations in both phases.

An alternative method of comparing the solution and crystal structures is to analyse the conformation of the amino acid backbone. The Karplus equation (see Appendix 1.) is used here to relate the ^3J vicinal coupling constants to the dihedral angles about the backbone C-C bond for amine bound complexes formed by L-tyrosine and L-phenylalanine. The three hydrogen atoms are treated as a ABX system due to the presence of the chiral centre in the molecule. The ^1H n.m.r. chemical shifts and coupling constants were iteratively fitted to the observed spectrum by the computer program ITRCAL (87). The calculated and observed coupling constants and dihedral angles are listed in Table 2.3.2..

Table 2.3.1.

MeHg ^{1}H n.m.r. shifts (δ/ppm relative to TMS) and $^2J(^{199}Hg-^1H)$ coupling constants in various MeHgL complexes ($L=C_6H_5(CH_2)_n X$ or $p\text{-}RC_6H_4(CH_2)_{n-1}CH(CO_2)NH_2$).

n	L	δ/ppm	^2J/Hz	Δ/ppm	Solvent
	X=S^-				
1	Benzyl mercaptan	0.57	156.6	0.21	$CDCl_3$
2	2-Phenylethylmercaptan	0.25	156.9	0.53	$CDCl_3$
3	3-Phenylpropylmercaptan	0.74	156.7	0	CD_3OD
	cf. $MeHgSC(Me)_3$ δ = 0.77 in $CDCl_3$				
	X=NH_2				
1	Benzylamine	0.62	211.7	0.28	D_2O
2	2-Phenylethylamine	0.43	210.0	0.47	D_2O
2	L-3-Phenylalanine	0.27	213.6	0.63	D_2O
2	L-Tyrosine	0.22	216.5	0.57	D_2O
3	3-Phenylpropylamine	0.77	208.8	0.13	CD_3OD
3	2-Amino-4-phenylbutanoic acid	0.78	216.0	0	CD_3OD/D_2O
	cf. $MeHg\overset{+}{N}H_2CH_2CO_2^-$ δ = 0.80 in D_2O				
	X=CO_2^-				
0	Benzoic acid	0.86	225.3	0	CD_3OD
1	Phenylacetic acid	0.83	231.5	0	CD_3OD
2	3-Phenylpropionic acid	0.83	231.2	0	CD_3OD
2	L-3-Phenylalanine	0.92	232.0	0	D_2O
2	L-Tyrosine	0.89	233.0	0	D_2O
3	2-Amino-4-phenylbutanoic acid	0.89	232.0	0	CD_3OD/D_2O
	cf. $MeHgO_2C(CH_2)_2NH_2$ δ = 0.85 in D_2O				

Δ = upfield shift in ppm = [δ(observed) - δ(typical complex with the same donor group but for a ligand without a phenyl ring)]

Table 2.3.2.

Coupling constants and estimated dihedral angles (in parentheses) of the ABX backbone protons in some NH_2 bound amino-acid Methylmercury(II) complexes.

Species	$^2J_{AB}$/Hz	$^3J_{AX}$/Hz	$^3J_{AX}$/Hz
Methyl(L-Phenylalanine) mercury(II)	-14.0	5.5 (50°)	4.1 (59°)
Methyl(L-Tyrosinato) mercury(II)	-14.6	5.6 (50°)	4.5 (57°)
Methyl(L-Tyrosinato) mercury(II)-solid state		(57°)	(62°)

The coupling constants calculated for the free ligand are close to those expected from a $CH-CH_2$ group with a freely rotating C-C bond (88). However in the NH_2bound amino acid complexes this is not the case and the coupling constants are used to estimate the dihedral angles between the hydrogen atoms. In these calculations the Karplus equation constants given by Shaw (89) were used. For comparison the dihedral angles in the solid state were calculated by assuming a tetrahedral environment at the carbon atoms and including the hydrogen atoms at their calculated positions. The dihedral angles in the solid state are included in Table 2.3.2. for comparison. The dihedral angles for the L-tyrosine and L-phenylalanine complexes are very similar and are both in good agreement with the estimated dihedral angles from the crystallographic study of (1).

Other factors which affect the mercury-arene interaction

are examined, again using ^1H n.m.r. as the experimental probe. The effect of donor atom (X) and carbon backbone chain length were studied in a series of ligands $C_6H_5(CH_2)_nX$ (C) ($X=NH_2$, S^-, n=1,2,3; $X=CO_2^-$, n=0,1,2) including the amino acids described previously. The chemical shifts and mercury-proton coupling constants are shown in Table 2.3.1.. The ^2J coupling constants are used as an indicator of the type of co-ordination involved (principally distinguishing between carboxylato and amino bound amino acid complexes). The amino acid complexes all show pH dependent equilibria between carboxylato and amino bound species, the latter being favoured at low pH when the amino group is protonated. An upfield shift of the methyl group resonance is used to detect the presence of a mercury-arene interaction. The "typical" complex in each case (Table 2.3.1.) was prepared from an analogous ligand with an aliphatic backbone.

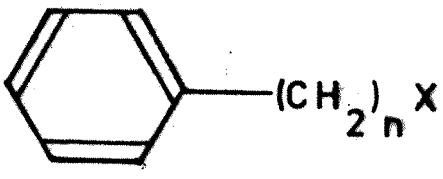

C

The complexes showing an upfield shift produce five and six membered "chelate" rings (for n=1 and 2 respectively) with similar upfield shifts from both the amino and mercapto complexes. When n=3 ($X=NH_2, S^-$) entropy considerations presumably overcome the relatively weak binding energy of the mercury-arene bond and the resultant 7-membered chelate ring is not formed.

None of the carboxylato complexes exhibit the upfield shift that might have been expected. This is probably because of the lower flexibility of the carboxylate moiety which would restrict the ease with which the rest of the molecule could bend to bring the phenyl ring into a co-ordinating position. The carboxylato complexes are the least stable of the complexes studied here (45) but as the complexes are all very labile the absence of an arene interaction in these cases cannot reasonably be attributed to a kinetic effect. The chemical shift of the methyl group does not exhibit any significant solvent dependence although there is the expected slight increase in the mercury-proton coupling constant in the presence of a donor solvent (see Table 2.3.2. $X=S^{-}, n=3$).

The most interesting facet of the solid state structure work concerns the mercury-arene interaction noted above. In this work we have completed the X-ray crystal structure of (1) and found the mercury atom to be bonding with the phenyl ring in a manner similar to that noted recently by other workers. This poses a point of considerable chemical interest in the sense that since it is a definite interaction there must be some picture of the bonding which can explain the properties of the interaction. The properties of the mercury-arene interaction can be described as follows:-

(1) It is observed in solution and in the solid state so cannot be attributed to crystal packing forces.

(2) It is observed in protic and both polar and non-polar

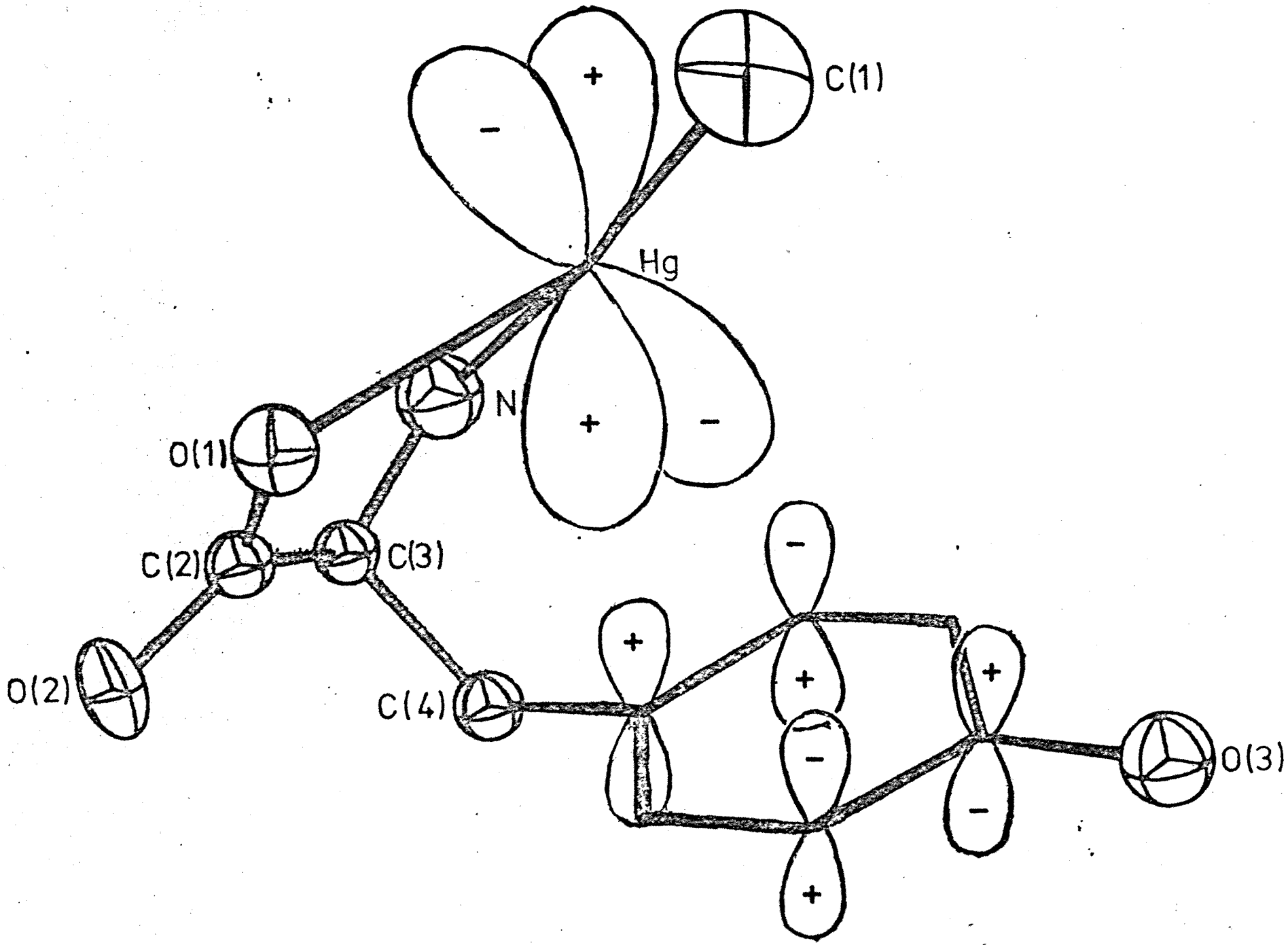
C(1)
Hg
N
O(1)
C(2)
C(3)
O(2)
C(4)
O(3)

aprotic solvents so it is not hydrophobic in nature.

(3) The presence of the interaction does not change the value of ^{2}J (^{199}Hg-^{1}H) which implies that rehybridisation at mercury does not occur.

(4) In the solid-state structure of (1) the bond lengths and angles of the phenyl ring are not significantly different from their values in non-interacting phenyl groups. Since aromatic ring current effects are observed, the ring cannot have undergone a major redistribution of electron density.

The spd_{z^2} hybridisation normally invoked to describe the bonding in methylmercury(II) has large diffuse d-orbitals orthogonal to the linear Me-Hg-Ligand bond. The lowest energy unocupied molecular orbitals of the phenyl ring are the π^* orbitals which are also quite diffuse. The binding energy to maintain the mercury-arene interaction arises from orbital overlap between the filled mercury d-orbitals and the unoccupied π^* orbitals of the ring (see overleaf). One slightly suprising fact is that the mercury atom, when projected onto the plane of the ring, is located outside the ring; it is also closer to C(5) than C(10). Being assymmetric with respect to the C(5)-C(10) bond the mercury cannot be located at a maximum orbital overlap position.

2.4 Summary.

The crystal structures of the 1:1 complexes formed by methylmercury(II) with L-tyrosine (1) and L-2-amino-4-phenylbutanoic acid (2) have been determined by X-ray diffraction studies. In both cases the ligand is bound principally via the the amino group with a weaker carboxylate bond. Complex (2) has an additional weak intermolecular bond with a neighbouring carboxylate group. Complex (1) shows further weak intramolecular contacts between mercury and the phenyl ring with Hg-C distances of 3.19(2) and 3.33(2)Å. In the case of (1) there is fairly good agreement between the crystal structure and that observed in solution as estimated from conformational analysis based on the backbone vicinal coupling constants and the ^1H n.m.r. anisotropic shift of the methyl group. Complexes of methylmercury(II) have been prepared with several homologous series of ligands which contain phenyl rings: $C_6H_5(CH_2)_nX$ ($X=NH_2, S^-, n=1,2,3$; and $X=CO_2^-, n=0,1,2$). The observation of a high field shift of the $[MeHg^+]$ ^1H n.m.r. resonance is interpreted as an anisotropic shielding effect due to an intramolecular interaction between the mercury(II) ion and the phenyl ring. Such an interaction is only observed when $X=NH_2$ or S^- and n=1 or 2.

2.5 Experimental

2.5.1 Methyl(L-tyrosinato)mercury(II) hydrate. (1)

Preparation.

Solutions of methylmercury(II)nitrate (0.55g,1.99mmol) (90) in water ($30cm^3$) and L-tyrosine (0.36g,1.99mmol) in water ($30cm^3$) were mixed and the pH adjusted to ca 7 with drops of HNO_3 and NaOH. The volume of the solution was reduced to $10cm^3$ on a rotary evaporator, and on standing white needles of the monohydrate precipitated.

Data collection. Intensity data from a crystal bounded by planes {001}, {100}, {101}, {011} and {111} and size 0.006 X 0.009 X 0.019mm was collected in the range $3<2\Theta<50°$ by the Θ-2Θ scan technique. In a preliminary data collection at room temperature the crystals were found to decompose fairly rapidly and therefore the temperature was maintained at 173K with a Syntex LT-1 attachment. Three check reflections were monitored after every 60 reflections and showed a 5% decay starting after ca 20h. These reflections were used to scale the data to a common level. A total of 1078 observed reflections ($I/\sigma(I)>3.0$) was measured and corrected for absorption giving transmission factors in the range 0.321-0.609. The crystal density was measured in chloroform/bromoform indicating two molecules per unit cell. The systematic extinction 0k0 for k=2n+1 was observed

indicating space groups $P2_1/m$ or $P2_1$. The latter was selected because the crystal contained resolved asymmetric molecules. For crystal data see Table 2.1 .

2.5.2 DL-2-amino-4-phenylbutanoic acid

This was prepared from diethylacetamidomalonate by an extension of the method of Goldsmith and Tishler (91).To t-butyl alcohol ($125cm^3$) was added sodium (0.57g,0.025mol) and the mixture was heated under reflux under dry nitrogen until the sodium was dissolved. Diethylacetamidomalonate (5.43g,0.025mol) was added to this warm stirred solution, followed by dropwise addition of (2-bromoethyl)benzene (4.62g,0.025mol). The mixture was heated under reflux for six hours and then evaporated to dryness under reduced pressure. The residue was extracted with ethanol ($250cm^3$) and the solution evaporated to dryness. Concentrated hydrochloric acid ($10cm^3$) and water ($40cm^3$) were added and the mixture heated under reflux for four hours. The resulting solution was neutralised with LiOH, filtered and then concentrated to $10cm^3$ on a rotary evaporator. The solution was left overnight in a refrigerator to form crystals which were filtered off and dried in air:

^1H n.m.r. in D_2O at δ7.14(m,5H,phenyl ring), δ3.06(m,1H,CH), 2.47(m,2H,CH_2) andδ1.68p.p.m. (m,2H,CH_2).

Analysis:calculated for $C_{10}H_{13}NO_2$; C,67.04; H,7.26; N,7.88%; found C,65.9; H,7.27; N,7.47%;

2.5.3 Methyl[2-amino-4phenylbutanato]mercury(II). (2)

Preparation.

Aqueous solutions of methylmercury(II) nitrate (0.147g,0.5mmol) and DL-2-amino-4-phenylbutanoic acid (0.089g,0.5mmol) were mixed and the pH adjusted to ca 7 with drops of HNO_3 and NaOH.The solvent was evaporated very slowly (over two weeks) and white needles of the title compound were produced.

Data collection.

A small crystal of dimensions 0.004 X 0.011 X 0.03mm bounded by planes $\{100\}$, $\{010\}$ and $\{101\}$ was selected and centered on the diffractometer. The observed systematic extinctions 0kl for l=2n+1 and h0l for h=2n+1 were consistant with orthorhombic space groups $Pca2_1$ and Pcam. A density measurement made in chloroform/ bromoform indicated four molecules per unit cell, consistent only with $Pca2_1$ in view of the lack of molecular symmetry, i.e. with the molecules having resolved upon crystallisation from a racemic mixture in solution. Intensity data were collected in the range $3<2\Theta<50°$ by the Θ-2Θ scan technique at 173K. Three check reflections were monitored after every 50 reflections and showed a gradual decay of ca 10%. These reflections were used to scale the data to a common level. A total of 674 observed reflections [$I/\sigma(I)>3.0$] were measured and corrected for absorption giving transmission factors in the range

0.265-0.608. For crystal data see table 2.1 .

2.5.4 Structure Solutions

The structures were solved using the heavy atom method involving a three dimensional Patterson synthesis to locate the position of each mercury atom. The remaining atoms were located in subsequent electron density maps and refined by minimising the function (Fo-Fc) . The final refinement of complex (1) with anisotropic temperature factors for Hg, O(1), O(2), N and C(1) gave an R factor of 0.044. The final refinement of complex (2) with anisotropic temperature factors for Hg and C(1') gave an R factor of 0.046. The handedness of the crystal was tested by carrying out a refinement with negative co-ordinates. The R value was unchanged but (Fo-Fc) was slightly lower with the original hand (corresponding to an L-amino acid). This configuration for the particular crystal examined is, therefore, preferred but from the available data cannot be regarded as conclusively proven.

2.5.5 2-Phenylethylmercaptan.

Thiourea (7.5g,0.1mol) was dissolved in water (30cm^3) and bromoethylbenzene (18.5g,0.1mol) added.The mixture was refluxed with vigorous stirring for 2h, sodium hydroxide (6.6g,0.15mol) added and the mixture refluxed for a further

2h. The aqueous (lower) layer was separated, acidified and then extracted several times with diethyl ether. The ether extracts were combined with the separated upper layer and dried over anhydrous magnesium sulphate. Ether was removed under reduced pressure and the resulting oil distilled **in vacuo** (b.p. 104°C,@17mm).

2.5.6 Methylmercury(II) mercaptide complexes.

These were prepared by mixing equimolar amounts of mercaptan, methylmercury(II) chloride and sodium hydroxide, all in methanol. The solvent was removed on a rotary evaporator, the solid extracted with diethyl ether and dried over anhydrous magnesium sulphate. Ether was removed to give products which were used without further purification.

2.5.7 Amine and carboxylate complexes of methylmercury(II).

These were prepared **in situ** by mixing equimolar amounts of methylmercury(II) nitrate and the appropriate ligand in either D_2O or CD_3OD. The pH of the amino acid complexes was adjusted by addition of HNO_3 or NaOH.

Chapter 3

Chelate methylmercury(II) complexes with dithiolate ligands.

3.1 Introduction.

Methylmercury(II) is known to form very few three co-ordinate complexes, and those that have been prepared with chelating ligands have consisted of a much weaker angled interaction with the second donor atom (36,62). 2,3-dimercapto-1- propanol (BAL), which has been used extensively in treating inorganic mercury poisoning, is potentially a chelating dithiolate ligand. However, it forms bis(methylmercury(II)) complexes that show no evidence of enhanced stability due to chelation (92,93). In an attempt to force three co-ordination on methylmercury(II), complexes with three potentially chelating dithiolate ligands have been studied. Thiolate ligands were chosen because they are known to form very strong bonds with methylmercury(II) and ligands (A), (B) and (C) in particular were chosen because of their rigid carbon backbone which was expected to enhance the stability of any chelate complexes they may form.

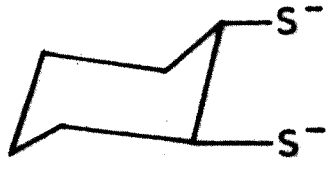

A

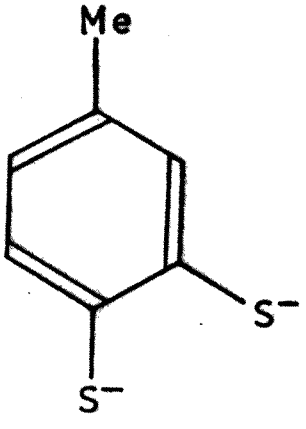

B

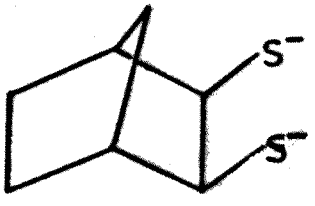

C

3.2 Results and Discussion.

The preparation of [$(MeHg)_2$,L],L=A trans-(1,2-dimercapto) cyclohexanebis(methylmercury(II))(3) and the solution of the crystallographic structure are described in Section 3.4.1.. Crystal data, atomic co-ordinates, bond lengths and bond angles are given in Tables 3.2.1., 3.2.2., 3.2.3. and 3.2.4. respectively. A perspective view of (3) is shown in Figure 3.2.1.. The atom Hg(1) is primarily co-ordinated through S(1) [Hg(1)-S(1) 2.367(4)Å] and has a further weak bond with S(2) [Hg(1)-S(2) 2.857(3)Å]. The S(1)-Hg(1)-C(1) angle is significantly distorted from 180°[167.8(5)°] being bent away from the Hg(1)-S(2) bond with S(1), S(2), Hg(1) and C(1) co-planar. The atom Hg(2) is bonded almost linearly [S(2)-Hg(2)-C(2) 177.1(5)°] to S(2) [Hg(2)-S(2) 2.363(4)Å] and the only further bonds to Hg(2) are due to long range packing interactions. The mercury-carbon bond length is increased from 2.08(2)Å [Hg(2)-C(2)] to 2.12(2)A [Hg(1)-C(1)] when chelation is present although the mercury-sulphur bond lengths are identical within experimental error. This increase in mercury-carbon bond length is similar to that which occurs in the methylmercury(II) pyridyl and bipyridyl complexes where the bond length increases from 2.04 to 2.07Å upon chelation (37,61). The cyclohexyl ring is in the chair conformation with all bond lengths and angles within the expected range.

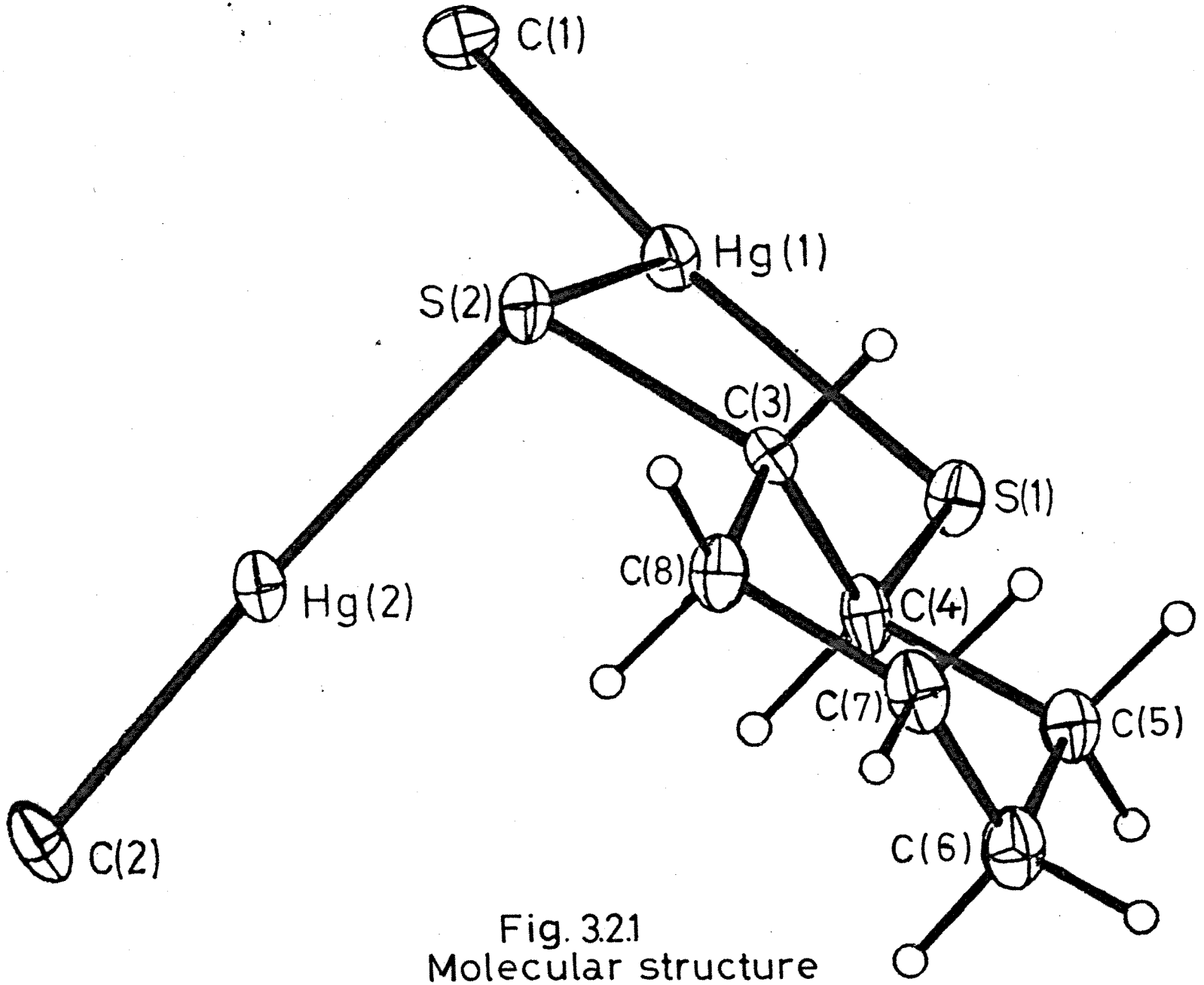

Fig. 3.2.1
Molecular structure
of (3)

Table 3.2.1.

Crystal data.

Colour	White
Habit	Hexagonal Block
Crystal System	Monoclinic
a/Å	9.609(3)
b/Å	13.428(3)
c/Å	10.268(3)
β/°	112.87(2)
U/Å^3	1220.6(6)
T/K	123
Space group	$P2_1/c$
μ/cm	260.1
M	576
D_{obs} /g cm	3.06 (295K)
D_{calc}/g cm	3.14 (123K)
Z	4
N(3σ)	1794
λ(Mo-K$_\alpha$)/Å	0.71069

Table 3.2.2.

Atomic co-ordinates ($X10^4$) with standard deviations in parentheses for complex (3).

Atom	X	Y	Z
Hg(1)	1854.8(6)	0194.9(4)	4513.4(6)
Hg(2)	-1478.0(6)	-1749.1(4)	2478.6(6)
S(1)	0032(4)	1485(3)	3843(4)
S(2)	0034(4)	-629(3)	1822(4)
C(1)	3751(17)	-744(14)	5455(20)
C(2)	-2875(19)	-2675(12)	3060(18)
C(3)	-1169(15)	0476(10)	1212(14)
C(4)	-1573(18)	1002(11)	2300(15)
C(5)	-2568(19)	1919(11)	1675(16)
C(6)	-4029(19)	1595(12)	0446(16)
C(7)	-3659(19)	1062(12)	-682(18)
C(8)	-2620(18)	0179(10)	-055(14)
H(31)	-594	934	892
H(41)	-2180	528	2602
H(51)	-2814	2256	2375
H(52)	-2037	2370	1312
H(61)	-4662	2166	0049
H(62)	-4594	1155	0802
H(71)	-3161	1512	-1094
H(72)	-4572	0839	-1445
H(81)	-2383	-128	-780
H(82)	-3188	-292	0252

Table 3.2.3.

Bond lengths (Å) with standard deviations in parentheses for complex **(3)**.

Hg(1)-S(1)	2.367(4)
Hg(1)-S(2)	2.857(3)
Hg(1)-C(1)	2.12(2)
Hg(2)-S(2)	2.363(4)
Hg(2)-C(2)	2.08(2)
S(1)-C(4)	1.85(1)
S(2)-C(3)	1.83(1)
C(3)-C(4)	1.50(2)
C(4)-C(5)	1.54(2)
C(5)-C(6)	1.54(2)
C(6)-C(7)	1.52(3)
C(7)-C(8)	1.52(2)
C(8)-C(3)	1.55(2)

Table 3.2.4.

Bond angles (°) with standard deviations in parentheses for complex **(3)**.

S(1)-Hg(1)-C(1)	167.8(5)
S(2)-Hg(1)-C(1)	107.8(5)
S(1)-Hg(1)-S(2)	84.0(1)
S(2)-Hg(2)-C(2)	177.1(5)
Hg(1)-S(1)-C(4)	105.6(5)
Hg(1)-S(2)-C(3)	94.8(4)
Hg(1)-S(2)-Hg(2)	100.6(1)
Hg(2)-S(2)-C(3)	103.7(5)
S(2)-C(3)-C(4)	108.7(9)
S(2)-C(3)-C(8)	116(1)
S(1)-C(4)-C(3)	116(1)
S(1)-C(4)-C(5)	105(1)
C(4)-C(5)-C(6)	110(1)
C(5)-C(6)-C(7)	110(1)
C(6)-C(7)-C(8)	110(1)
C(7)-C(8)-C(3)	113(1)
C(8)-C(3)-C(4)	110(1)
C(3)-C(4)-C(5)	112(1)

Table 3.2.5.

Hydrogen bond lengths (Å) and angles(°) for complex (3) with standard deviations in parentheses.

Bond lengths.

Hg(1)-S'(1)	3.689(4)
Hg(1)-Hg'(2)	3.859(1)
Hg(2)-S'(1)	3.499(4)
Hg(2)-S''(1)	3.295(4)

Bond angles.

S(1)-Hg(1)-S'(1)	98.1(1)
S(1)-Hg(1)-Hg'(2)	63.25(9)
S(2)-Hg(2)-S'(1)	102.3(1)
S(2)-Hg(2)-S''(1)	86.3(1)

The superscripts refer to the following co-ordinate transformations:

M' :-x, -y, 1-z

M'':-x, y-1/2, 1/2-z

A crystal packing diagram for (3) is shown in Figure 3.2.2.. Table 3.2.5. contains a list of the relevant contact distances and angles. Overall the packing forces produce a three-dimensional network in which each mercury is bonded to a total of three sulphur atoms and one mercury atom. Atom Hg(1) is within contact distance of S'(1) and Hg'(2) in

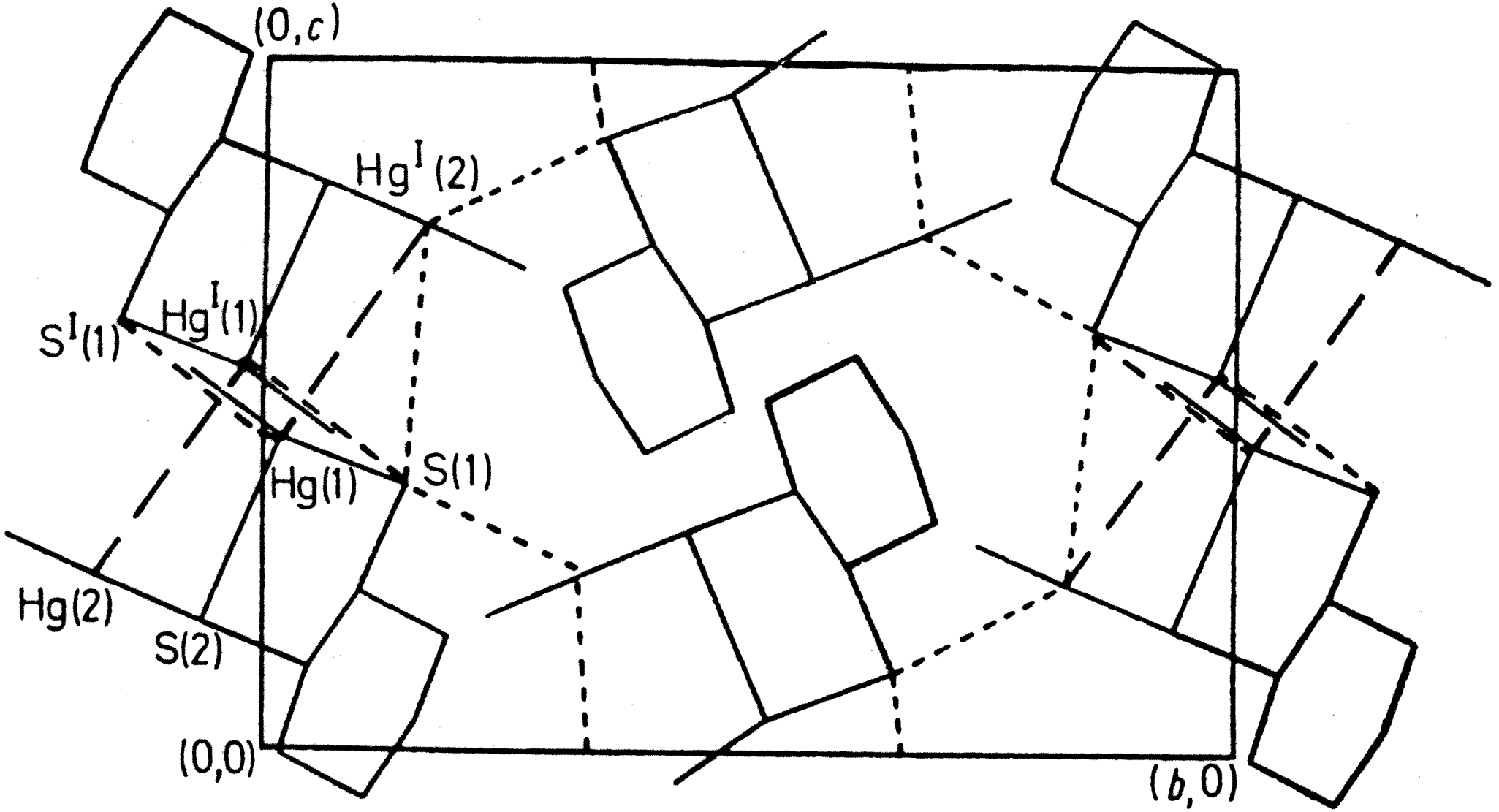

Packing diagram for (3)
Fig. 3.2.2

addition to two strong bonds with S(1) and S(2). Atom Hg(2) has two additional contacts with S'(1) and S''(1). As might be expected the contact distances of Hg(2) [3.499(4) and 3.295(4)Å] are considerably shorter than that of Hg(1) [3.689(4)Å] which has the additional primary bond to S(2).

Table 3.2.6.

^{1}H Shifts (p.p.m.) and coupling constants (Hz) of complexes [$(MeHg)_2$ L] (L=(A,B,C)) and [MeHgL] (L=a,b).

L	Solvent	δ(^{1}H)	^{2}J(H-Hg)	
A	d_5 pyridine	0.473	163.2	
A	d_6 dmso	0.61	166.6	
$C_6H_{11}S^-$(a)	d_5 pyridine		157.0	[ref 22]
B	d_8 toluene	0.72	170.2	
B	d_6 dmso	0.66	178.0	
$C_6H_5S^-$(b)	dichloromethane		161.5	[ref 25]
C	d_2 dichloromethane	0.82	163.0	
C	d_6 dmso	0.71	169.0	

(a)=cyclohexylmercaptan

(b)=thiophenol

There is good evidence of chelation in the ^{1}H n.m.r. spectra of (3) and the analogous complexes [$(MeHg)_2$ L] with L= B (4) and C (5), details of which are shown in Table 3.2.6.. The value of ^{2}J is expected to increase from that observed in an analogous complex with a unidentate ligand

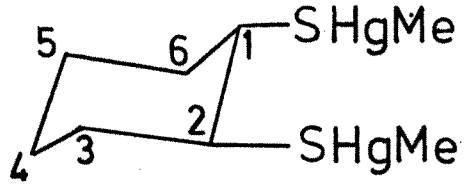

3

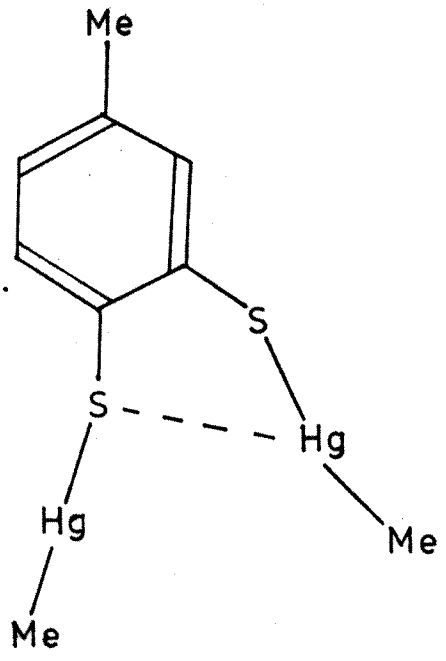

4

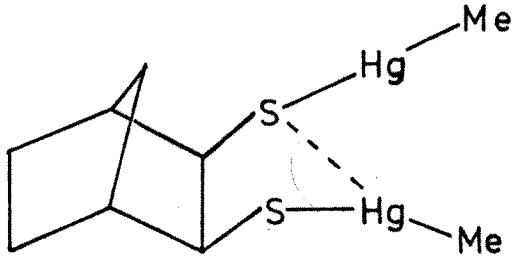

5

when chelation occurs. The values of ^2J for the bis(methylmercury(II) complexes (3-5) are larger than those for complexes formed with structurally similar unidentate thiolate ligands. For example ^2J=163.2 Hz for complex (3) in pyridine solution whereas ^2J=157.0 Hz for methyl(mercaptocyclohexane) mercury(II) in the same solvent. In the spectrum of (3) there is only one resonance (with mercury satellites) for the methyl group of methylmercury (II). This requires the metal atoms to be in fast exchange with the ligand as reported previously for methylmercury(II) mercaptides (25). The value of the coupling constant is a weighted average of the individual ^2J values for each of the mercury environments present. Assuming the solution structure of (3) is similar to that observed in the crystal, then only one of the mercury atoms is chelated, so ^2J for the non-chelated methylmercury(II) will be similar to that of methyl(mercaptocyclohexane)mercury(II). To produce the averaged value of ^2J which is observed, ^2J for the chelated methylmercury(II) would need to be about 169 Hz which is an increase in ^2J of 12Hz upon chelation. If the same reasoning is applied to (4) (which is compared with the methylmercury(II) complex of thiophenol) the value of ^2J increases from 162 Hz to 179 Hz upon chelation. This increase in ^2J upon chelation is similar to that in $MeHg(SCN)_3^{2-}$ and $[MeHg(bipy)]NO_3$ where the increases in ^2J were 14 and 9 Hz respectively (35-37).

Further evidence that one of the sulphur atoms is bonded

Figure 3.2.4

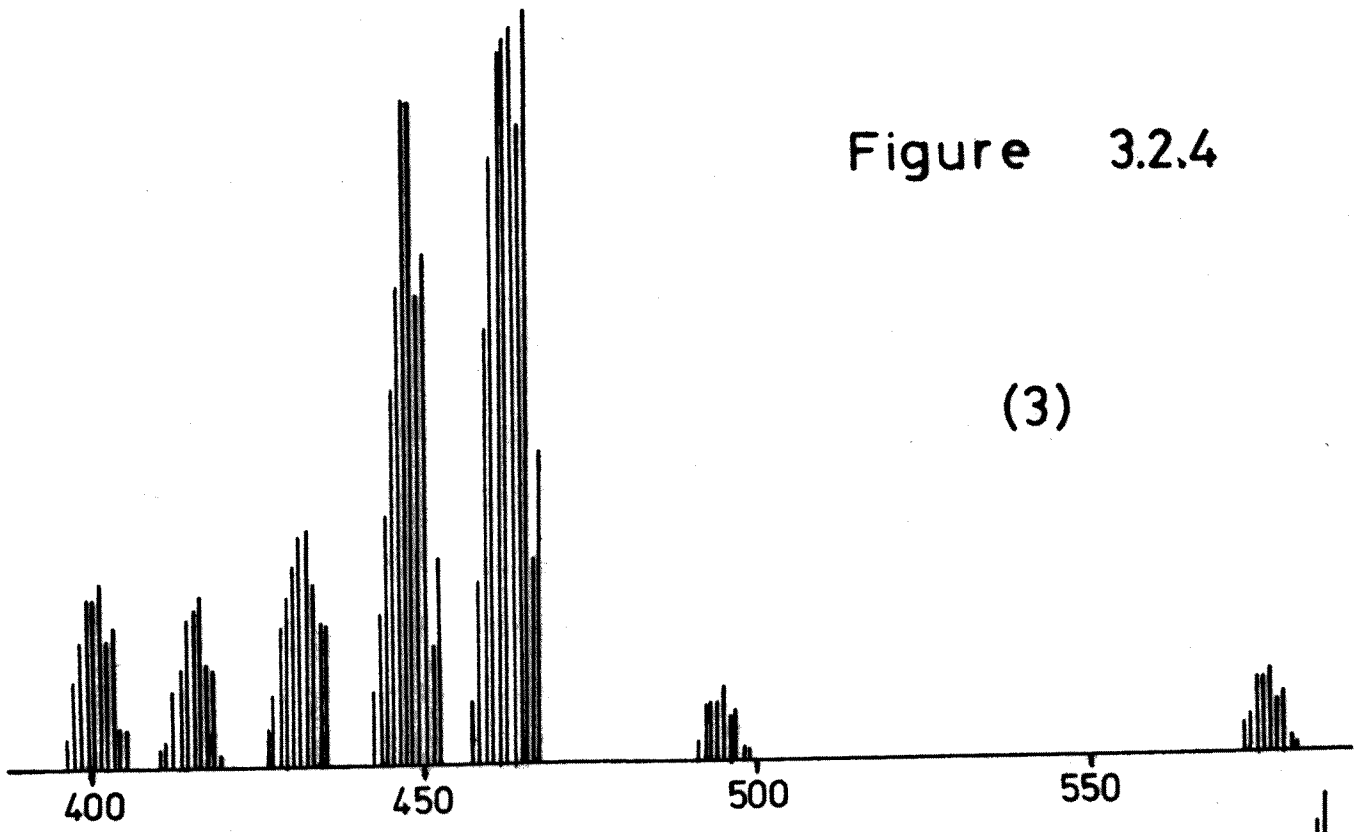

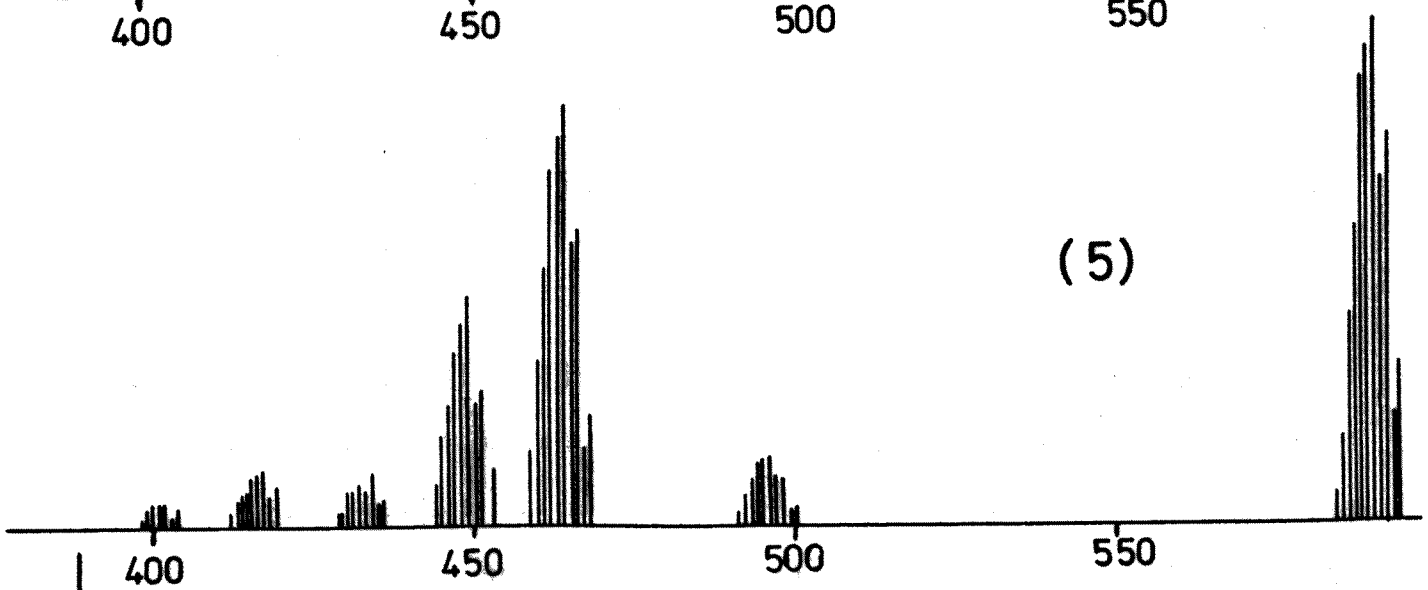

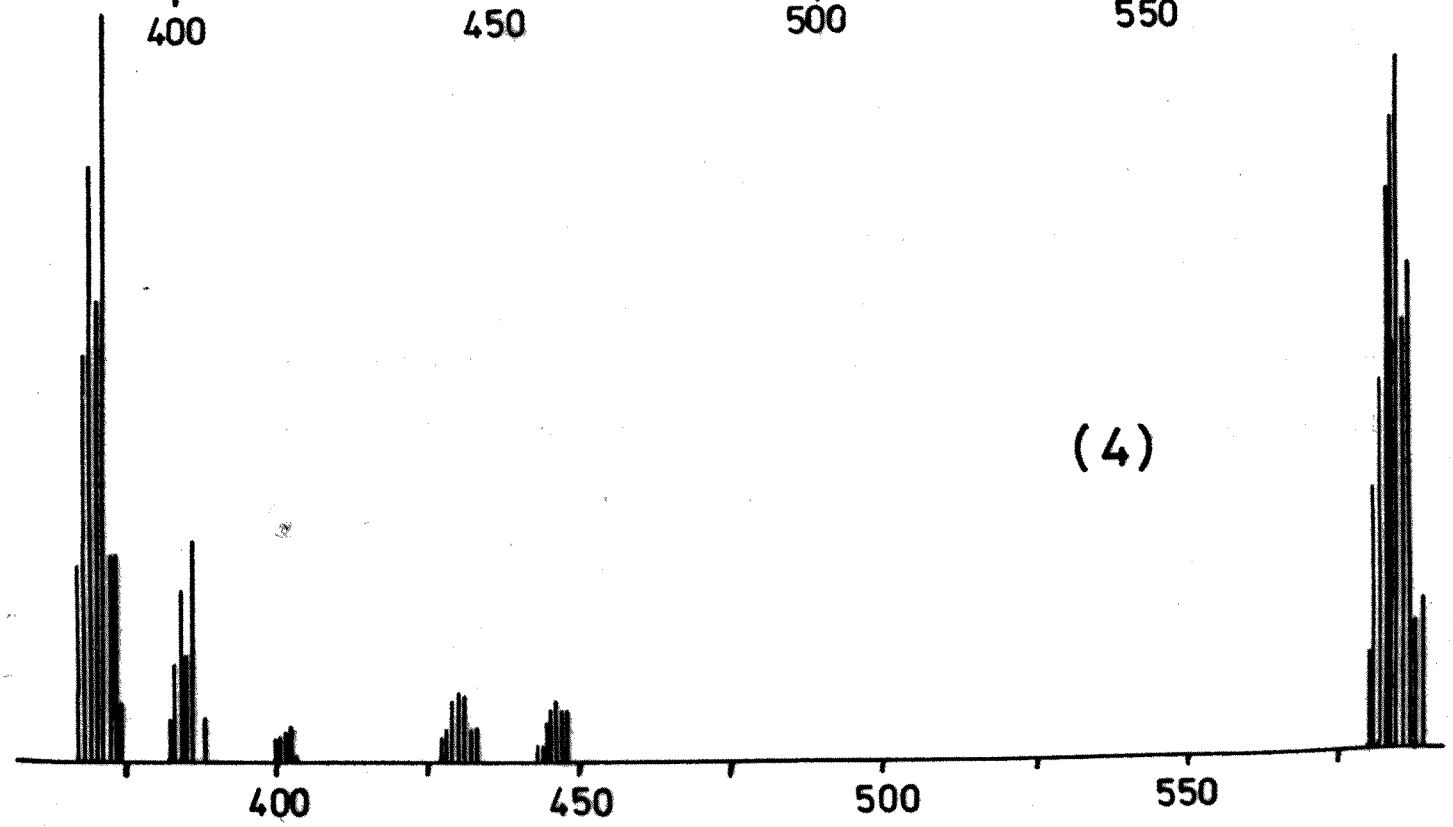

to both mercury atoms comes from the mass spectra of (3), (4) and (5). The spectra (Figure 3.2.4) contain peaks with a Hg_2 isotope pattern around m/e 436 ($^{202}Hg_2{}^{32}S$) which probably arises from chelation of the type found in the crystal structure although it is possible that this arises from an internal rearrangement upon fragmentation.

It is interesting that 1:1 and 2:1 [MeHg]:ligand ratios give only bis(methylmercury(II)) species which are observed in solution by both ^1H and ^{13}C n.m.r.. The ^{13}C n.m.r. spectrum of a solution containing equimolar amounts of (C) and methylmercury(II) chloride (ca 0.2 mol dm^{-3} in CD_2Cl_2) shows separate resonances for free and bound ligand species (at 255K) which undergo fast exchange at room temperature. This observation is consistent with the formation of the bis(methylmercury(II)) complex in solution as well as in the isolated solid.

For the bis(methylmercury(II)) complex to be formed in an equimolar mixture the formation of the second mercury-sulphur bond must occur in preference to the formation of another mono-methylmercury(II) complex. An increase in the basicity of the more weakly bonded sulphur seems to be the most likely reason for the formation of the bis(methylmercury(II)) species (3-5). This increase in basicity is presumably a result of the weak chelation of the second sulphur atom since strong chelation would be expected to have the opposite effect on the basicity of the second

sulphur and the bis(methylmercury(II)) complexes would not be formed in equimolar mixtures.

3.3 Summary.

Bis(methylmercury(II)) complexes have been prepared with three dithiolate ligands which each have a rigid carbon backbone structure holding the two sulphur stoms in a favourable position for chelation. The crystal structure of trans-(1,2-dimercapto)cyclohexanebis(methylmercury(II)) shows that one of the mercury atoms is bonded to a single sulphur (Hg(2)-S(2) 2.363(4)Å) while the other mercury atom has a weaker chelate bond (Hg(1)-S(2) 2.857(3)Å) in addition to the primary mercury-sulphur bond (Hg(1)-S(1) 2.367(4)Å). There is good evidence (from n.m.r. spectra) that a similar structure exists in solution for all three complexes. The J values are larger than would be expected for unidentate methylmercury(II) complexes and the increase is similar to that observed previously for methylmercury(II) chelate complexes.

3.4 Experimental

3.4.1 trans-(1,2-Dimercapto)cyclohexanebis[methylmercury(II)]

Preparation.

DL-trans-cyclohexane-1,2-dithiol was prepared from

cyclohexene and carbon disulphide by the method of Taguchi (94). Solutions of methylmercury(II) chloride (0.25g,1mmol) in methanol (50cm^3) and DL-trans-cyclohexane-1,2-dithiol (0.148g,1mmol) and NaOH (0.04g,1mmol) in methanol (30cm^3) were mixed and a white precipitate formed. The complex was filtered off and the solid washed with water (5X10 cm^3). The solid was then recrystalised from acetone, and crystals of the bis[methylmercury(II)] complex (3) suitable for crystallography were obtained by slow evaporation from aqueous acetone solution. The same compound was also prepared by mixing ligand and $[MeHg]^+$ in a 1:2 ratio.

Analysis: calculated for $C_6H_{10}Hg_2S_2$: C,16.65; H,2.75%; found: C,16.80; H,3.05%.

^{13}C n.m.r. shift data (p.p.m.) in $d_5$pyridine for

(A) 48.62 (C1,C2); 37.24 (C3,C6); 26.91 (C4,C5);

(3) 54.06(C1,C2);42.43(C3,C6);27.87(C4,C5) 10.06 (MeHg); $^1J(^{199}Hg-^{13}C)$=1276.6Hz; For numbering see Fig. 3.2.3.

Infra-red absorptions: 1312(w), 1272(w), 1210(w), 1175(m), 1100(w), 1040(w), 985(m), 843(w), 817(w), 763(s), 740(w), 720(m), 530(m), 517(sh), 482(m), 410(w) cm^{-1}.

Crystallographic Data Collection.

A small crystal of size 0.017 X 0.032 X 0.012 mm bounded by planes [001], [010] and [111] was selected and centered on the Syntex diffractometer. X-Ray intensity data was collected in the range $3<2\theta<50°$ by the θ-2θ scan technique. In an attempt to reduce crystal decomposition, the

temperature was kept at 123K with the Syntex LT-1 attachment. Five check reflections were monitored after every 50 reflections, and showed a gradual decay of ca 5%. These reflections were used to scale the data to a common level. A total of 1794 observed reflections [$I/\sigma(I)>3.0$] were measured and corrected for absorption, giving transmission factors in the range 0.0967-0.0215. The systematic extinctions h01, l=2n and 0k0, k=2n were observed, indicating space group $P2_1/c$. The crystal density, measured by floatation in an aqueous cadmium tungstoborate solution, indicated four molecules per unit cell. The unit-cell dimensions were obtained by a least-squares fit to 15 strong reflections.

Structure Solution

The structure was solved using the heavy atom method involving a three-dimensional Patterson synthesis to locate the positions of the mercury atoms. The remaining carbon and sulphur atoms were located in subsequent density maps and refined by minimising the function $\Sigma W(F_{obs}-F_{calc})^2$. The contribution from the hydrogen atoms in calculated positions was included before the final refinement with anisotropic temperature factors for the mercury, sulphur and carbon atoms which gave a final R factor of 0.037. Weights of the form W=X*Y were used, where X=1.0 or $[(\sin\Theta)/\lambda]/0.35$ for $(\sin\Theta)/\lambda<0.35$, Y=1.0 or 100/F for F>100 or F/40 for F<40.

3.4.2 3,4-Dimercaptotoluenebis[methylmercury(II)] (4)

Methylmercury(II) nitrate (0.54g,2mmol) in methanol ($40cm^3$) was added to 3,4-dimercaptotoluene (B.D.H.,0.16g, 1mmol) and NaOH (0.08g,2mmol) in methanol ($30cm^3$). After stirring for 30 minutes the solvent was removed on a rotary evaporator and water ($30cm^3$) added to the solid. The suspension was then extracted with toluene (5X20 cm^3) and after separation the toluene was removed on a rotary evaporator. The crude product was recrystallised from toluene to give white crystals of (4). The bis[methyl mercury(II)] complex was also isolated from the equimolar reaction mixture.

Analysis: calculated for $C_9H_{12}Hg_2S_2$, C,18.45; H,2.05%; found, C,18.83; H,2.13%.

^{13}C n.m.r. shift data for:

(a) (B) 137.08, 131.94, 126.74 (C1,C3,C4); 131.68, 131.36, 127.65 (C2,C5,C6); 20.80 (Ph<u>Me</u>); in $CDCl_3$.

(b) (4) 140.56, 136.22, 133.88 (C1,C3,C4), 134.22, 133.75, 125.47 (C2,C5,C6); 20.15 (Ph<u>Me</u>), 10.82, ^1J=1332.0Hz (<u>Me</u>Hg); in $d_6$dmso.

Infra-red absorptions: 1252(w), 1175(w), 1167(w), 1100(s), 1030(m), 877(w), 860(w), 810(sh), 803(m), 770(m,b), 720(w), 680(w), 550(w), 530(m) cm^{-1}.

3.4.3 The bis[methylmercury(II)] complex of endo,cis-2,3-dimercaptobicyclo[2.2.1]heptane.(5)

The ligand was prepared from norbornene and sulphur by the method of Shields and Kurtz and the purity checked by ^{13}C n.m.r. (95). Methylmercury(II) nitrate (0.50g,2mmol) in methanol (30cm^3) was added to the ligand (0.16g,1mmol) and NaOH (0.08g,2mmol) in methanol (30cm^3). After stirring for 30 minutes the methanol was removed with a rotary evaporator and water (50cm^3) added. The aqueous suspension was extracted with toluene (5X20 cm^3) and after separation the toluene was removed with a rotary evaporator. The solid was then recrystallised from toluene to give white crystals of (5). The bis[methylmercury(II)] complex was also crystallised from an equimolar reaction mixture.

Analysis: calculated for $C_9H_{16}Hg_2S_2$, C,18.37; H,2.72%; found, C,18.75; H,2.85%.

^{13}C n.m.r. chemical shift data (p.p.m.) in CD_2Cl_2 for

(a) (5) :53.27 (C1,C4); 49.83 (C2,C3); 33.91 (C7); 29.36 (C5,C6); 10.05 (MeHg); ^1J=1216.3Hz.

(b) (C) :48.03 (C1,C4); 47.58 (C2,C3); 32.63 (C7); 28.79 (C5,C6);

Infra-red absorptions: 1310(w), 1292(w), 1230(w), 1175(m), 1140(m), 830(w), 765(b), 720(m), 515(sh), 511(m), 478(m) cm^{-1}

cis,cis-1,3,5-tristhiacyclohexane

The title compound was prepared by the method described in reference (150) in which the compound was reacted further and not isolated in a pure state. The oil was distilled under vacuum (115°C, 0.1mm) to produce a clear, maloderous oil. The ^{13}C n.m.r. spectrum of the oil (in $CDCl_3$) consisted of two resonances at δ 59.73 and 51.28. The ligand was reacted with both methylmercury(II) and mercury(II) under a wide range of reaction conditions and in all cases produced a white polymeric solid which would not subsequently redissolve. Methylmercury(II) chloride, bromide and nitrate and mercury(II) nitrate, chloride and perchlorate all gave an insoluble product even when prepared under high dilution. Several different solvents were used to mix the reactants but in each case a precipitate was formed which failed to dissolve in numerous mixtures of the following solvents : dmso, pyridine, methanol, toluene, THF, chloroform, dichloromethane, acetone, diethyl ether, nitromethane and acetonitrile. Elemental analysis of the precipitates did not give results consistant with stochiometric species. The ligand is potentially a tri-dentate donor but in the cases described above if is obviously cross-linking with other complexes in a very efficient manner. Because of the solubility problems it has not been possible to discover if methylmercury(II) was chelated by all three thiol groups or if it was simply a monodedentate complex with disulphide bridges forming the cross-linking.

Chapter 4

Metal ion induced re-arrangement of 2-methyl-2-(2-pyridyl)thiazolidine.

4.1 Introduction.

Thiols such as 1,2-dimercaptopropan-1-ol (BAL), which are commonly used for treating heavy metal poisoning, suffer from the disadvantage that their shelf life is poor due to oxidation to disulphide-bridged species of no therapeutic value. Ligand (A) has been prepared and studied because the thiazolidine ring is potentially a method of protecting thiol groups from oxidation in a form which can regenerate a thiol moeity in the presence of metal ions to give (B).

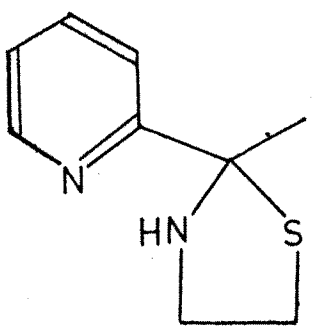

(A)

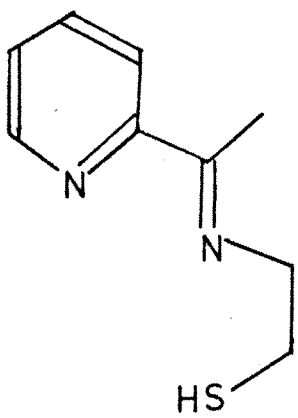

(B)

Ligands of type (A) are readily prepared by base catalysed condensation of B-aminothiols with ketones and aldehydes. There have been several reports of metal induced rearrangements with structurally similar ligands to give their corresponding Shiff bases (96-99).

The ligands prepared from aldehydes are very prone to oxidation which produces an imine bond in the thiazolidine ring such that metal ions can no longer promote ring opening (100). There are two probable mechanisms which can result in

a complex containing a ring opened ligand:

(a) If an equilibrium exists for the ligand between the thiazolidine ring and the Schiff base, the metal complex would form with the latter.

(b) The metal ion can react directly with the thiazolidine ring inducing a rearrangment to produce a ring opened ligand in the complex.

4.2 2-methyl-2-(2-pyridyl)thiazolidine

As stated above the ligand could exist in either of the two forms **(A)** or **(B)**. At 400MHz the CH_2 region of the ^1H n.m.r. spectrum (in CCl_4) consists of separate multiplets for each of the four methylene protons and this is shown in Figure 4.2.1. (the simulated spectrum was calculated using the computer program PANIC (101)). Only the structure shown in **(A)** will cause the protons to be magnetically inequivalent and there can be no significant exchange between forms **(A)** and **(B)**. The magnetic inequivalence of the methylene protons is caused by both the presence of a chiral centre in the ring and the fact that the ring is non-planar.

Further confirmation that the ligand exists in solution in the form of **(A)** is the presence of a resonance at $\delta = 80$ in the ^{13}C n.m.r. spectrum. This is within the expected range for the quaternary carbon atom in **(A)** and there is no resonance at $\delta = 170$ which would be expected for the imine carbon resonance in **(B)**.

Figure 4.2.1 Methylene region of the 400 MHz ^1H n.m.r. spectrum of (A)

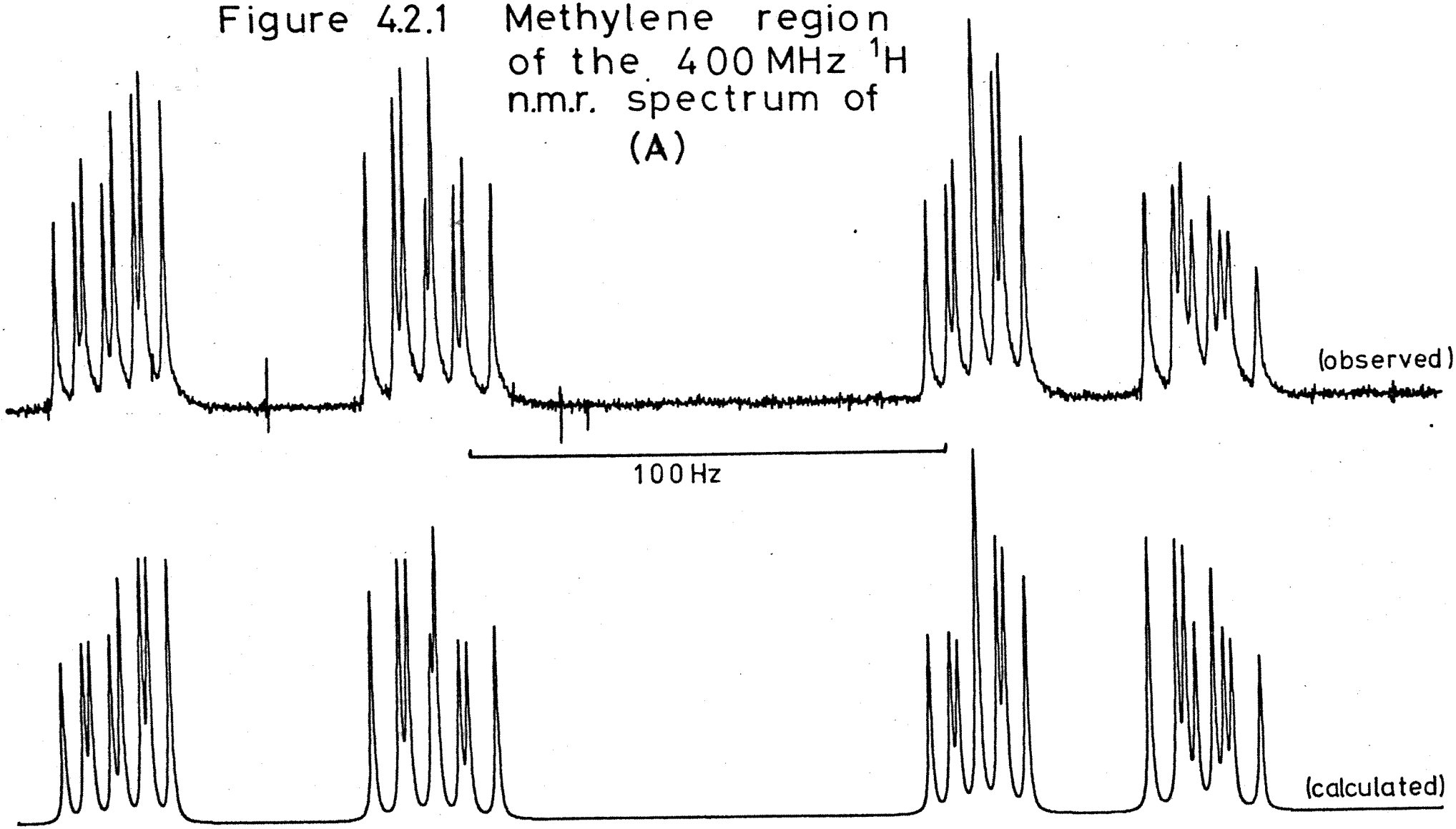

The ligand appears to be protonated easily by addition of perchloric or sulphuric acid, producing a change in the ultra-violet spectrum shifting λ_{max} from 263nm (ϵ=3600-100) to 258nm (ϵ=4600-100) with shoulders at 253 and 263nm. Addition of base has no effect on the ultra-violet spectrum. The ^{13}C n.m.r. resonances of the ligand are shifted upon addition of acid in a manner consistent with protonation of the basic sites of the ligand i.e. at pyridine and the thiazolidine amine.

4.3 The reaction of methylmercury(II) with 2-methyl-2-(2-pyridyl)thiazolidine.

An equimolar mixture of methylmercury(II) chloride and **(A)** reacts to produce two different species which are readily detected in the ^{1}H and ^{13}C n.m.r. spectra of the resultant solution. In the ^{13}C spectrum the methyl resonance of MeHg is a singlet (with ^{199}Hg satellites) while there are two sets of resonances (in a 2:1 ratio) attributable to the ligand. When a two fold excess of methylmercury(II) chloride is added the ligand resonances all revert to those of the major species present in the equimolar mixture. The methylmercury(II) resonance remains a singlet with the value of ^{1}J (^{199}Hg-^{13}C) (1500Hz) increasing towards that of methylmercury(II) chloride (1670Hz) (17). The major species in the equimolar mixture has a resonance attributable to an imine carbon while the minor species has a resonance attributable to the 2-carbon of the thiazolidine ring.

Therefore the major species present contains a thiol group which will preferentially bind methylmercury(II) while in the minor species bonding will occur at the pyridine rather than the thio-ether group when the amine is protonated.

In the ^1H n.m.r. spectrum of an equimolar solution of methylmercury(II) chloride and (A) the value of $^2J(^{199}Hg-^1H)$ is 182Hz. This averaged value is greater than that expected for completely thiol bound methylmercury(II) (normally 160Hz) and is consistent with a 2:1 ratio of thiol and pyridine bound methylmercury(II) and would require the minor species to have ^2J of about 225Hz (cf [MeHg(pyridine)]NO_3, ^2J=230Hz) (37).

The incomplete ring opening of the ligand when equimolar with methylmercury(II) chloride must be a pH effect in that the proton released by thiol co-ordination to methylmercury (II) protonates the thiazolidine amine, so preventing complete ring opening for all the ligand present. Methylmercury (II) acetate was tried so as to buffer the solution and had the desired effect of causing complete formation of a thiol co-ordinated ring opened complex (with ^2J=163Hz).

4.4 The reaction of $Hg(ClO_4)_2$ with 2-methyl-2-(2-pyridyl)thiazolidine.

A mixture of ligand (A) and $Hg(ClO_4)_2$ in methanol

produces a complex which has a much more intense absorption in the ultra-violet spectrum and λ_{max} is shifted from 262nm (ε=3600) to 277nm (ε=9200). The nature of the complex formed was investigated by changing the relative amounts of metal to ligand and it was found to be a 1:1 complex when the metal was in excess. In solutions containing excess ligand there was evidence of other species (probably including $Hg(A)_2$) but these were not investigated further.

Since complex formation will result in the loss of a proton from the ligand the effect of acid and base on the complex has been investigated. Addition of either acid or base produces spectral changes but neither causes significant decomposition of the complex. Addition of an excess of $HClO_4$ causes a non-stoichiometric change in the spectrum: the intensity of the absorbance at 277nm is decreased and a new absorbance appears at 258nm which is probably due to protonation of the complexed ligand. Addition of KOH to the complex produced a change in both the position and the intensity of the absorbance (λ_{max} 267, ε=7500).

The ^{13}C n.m.r. spectrum of the complex showed that the ligand was in a ring opened configuration when it was complexed to mercury(II). At ligand to metal ratios of 1:1 and 1:3 the presence of a resonance assignable to an imine carbon and the corresponding absence of one for a quaternary carbon indicated that the ligand was only present in a co-ordinated ring-opened form. This is in contrast to the complex $Hg(C)_2$

(C = 2-(2-pyridyl) benzothiazoline) where in the isolated complex, the ligand is reported to be in a ring closed conformation although in solution the ligand is possibly in a ring opened form (98).

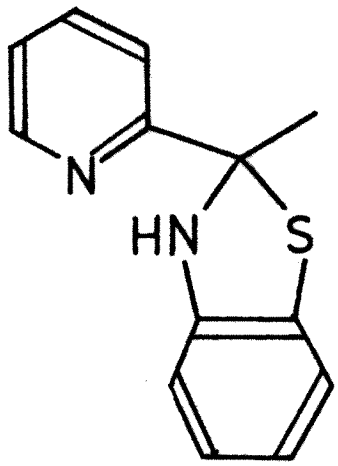

(C)

The kinetics of complex formation between (A) and $Hg(ClO_4)_2$ were briefly studied in methanol. Single wavelength stopped-flow spectrophotometry was used to study this extremely fast reaction. Only the end of the reaction could be detected at 3.5°C and even this did not yield very reliable data. At 280nm a large increase in absorbance would be expected but only a small change was detectable since most of the reaction was completed before the solutions reached the observation chamber (see Appendix 3 for an explanation of this technique).

Pseudo first-order rate constants of 170, 400 and 200s^{-1}(all ±20%) were determined with reactant concentrations of (metal:ligand) $1.0X10^{-4}$:$1.1X10^{-5}$, $2.0X10^{-4}$:$1.0X10^{-5}$ and $5.0X10^{-5}$:$5X10^{-6}$ respectively. A first order dependence on the

concentration of mercury is apparent despite the quality of the data.

The solvent exchange rate of mercury in methanol has not been determined but the water exchange rate should be comparable and can be calculated as follows.

$$MS_6 + L \underset{k_d}{\overset{k_f}{\rightleftharpoons}} MS_5L + S$$

where k_f and k_d are the formation and dissociation rate constants and K is the stability constant.

$$K = k_f/k_d$$

$$k_f = k_dK = 10^{1.4} \times 10^{9.6} = 10^{11} \quad \text{(from ref (102))}$$

With an exchange rate of the order of 10^{11} it is obvious that the reaction detected by the stopped-flow experiment was not initial complexation but rather a subsequent re-arrangement, possibly of the type:

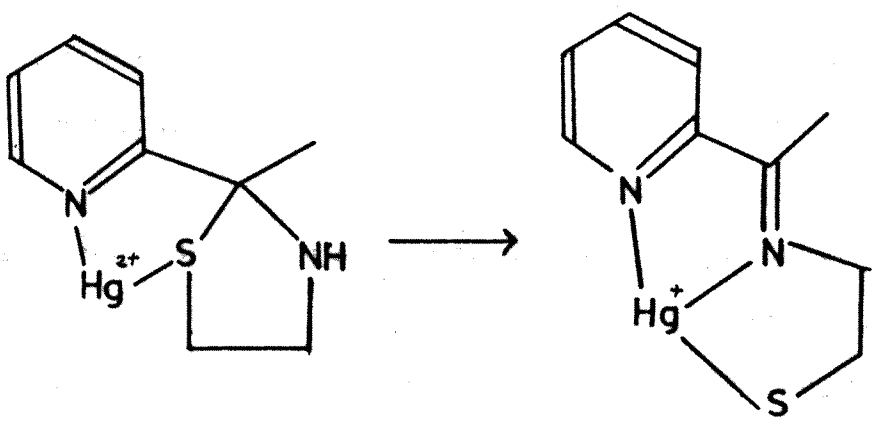

Since the reaction was really too fast for a meaningful kinetic study a metal with a slower solvent exchange rate was sought and zinc (with a methanol exchange rate of $1.74 \times 10^6 s^{-1}$ at 298K) proved suitable for this more detailed study (103).

4.5 The reaction of zinc(II) with 2-methyl-2-(2-pyridyl)thiazolidine

$Zn(ClO_4)_2$ was found to be strongly complexed by ligand (B) giving a peak in the ultra-violet spectrum at 277nm (ε=7000±400) with shoulders at 268 and 284nm in methanol. Addition of perchloric or sulphuric acid caused decomposition of the complex with the ultra-violet spectrum corresponding to protonated ligand (as described above).

A two stage process was observed in a stopped-flow experiment for the reaction of $Zn(ClO_4)_2$ with (B) in methanol. Rapid Scanning Spectrophotometry (RSS) showed a fast stage ($t_{\frac{1}{2}}$ ca 20ms at 4°C) followed by a much slower stage ($t_{\frac{1}{2}}$ ca 2s at 4°C). An isosbestic point for the second stage seen at 260nm was subsequently used for single wavelength studies of the first stage. Sample RSS traces are shown in Figure 4.5.1. .

The reactions were carried out under pseudo first order conditions with the metal in at least a ten-fold excess. The reaction was found to have a first order dependence on the ligand concentration. The dependence on zinc concentration was significantly first order although there was also a small zero order term. Pseudo first order rate constants are listed in Table 4.5.1 and shown diagramatically in Figure 4.5.2. A linear least squares fit of k(obs) vs [Zn] yields an equation

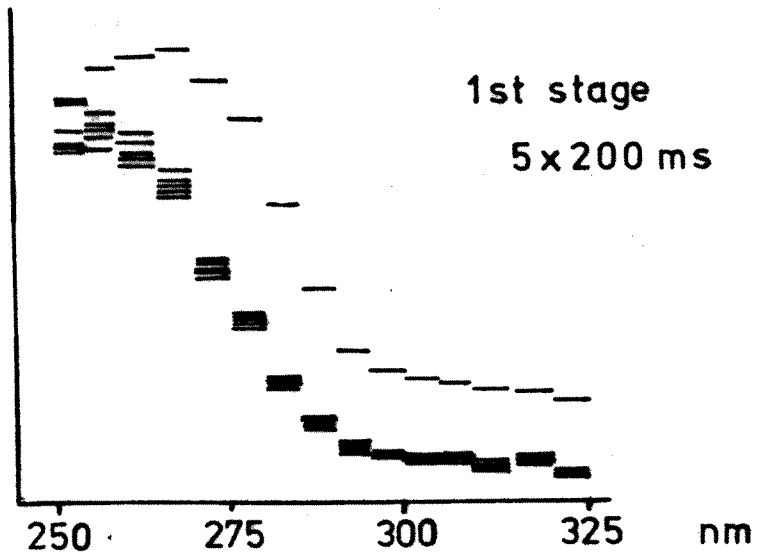

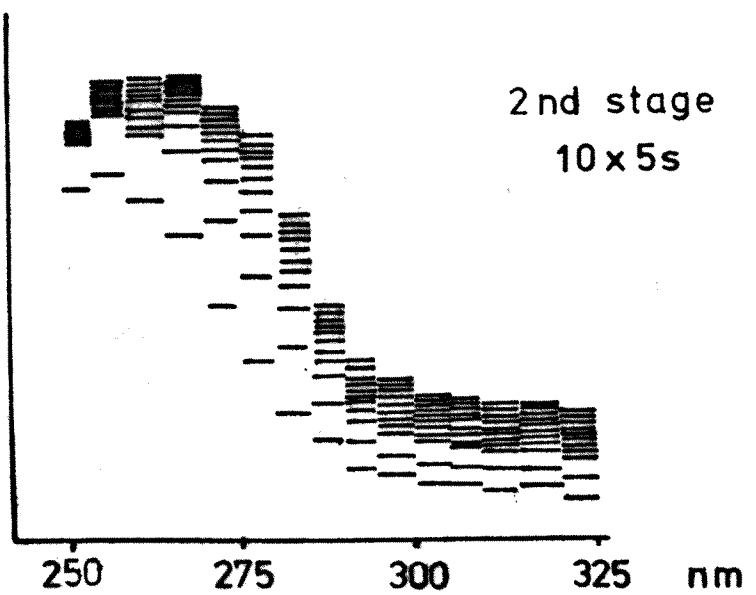

Figure 4.5.1

RSS traces of $Zn(ClO_4)_2$ + (A)

Figure 4.5.2

$Zn(ClO_4)_2$ + (A)

$\lambda = 280nm$ $T = 4.5°C$

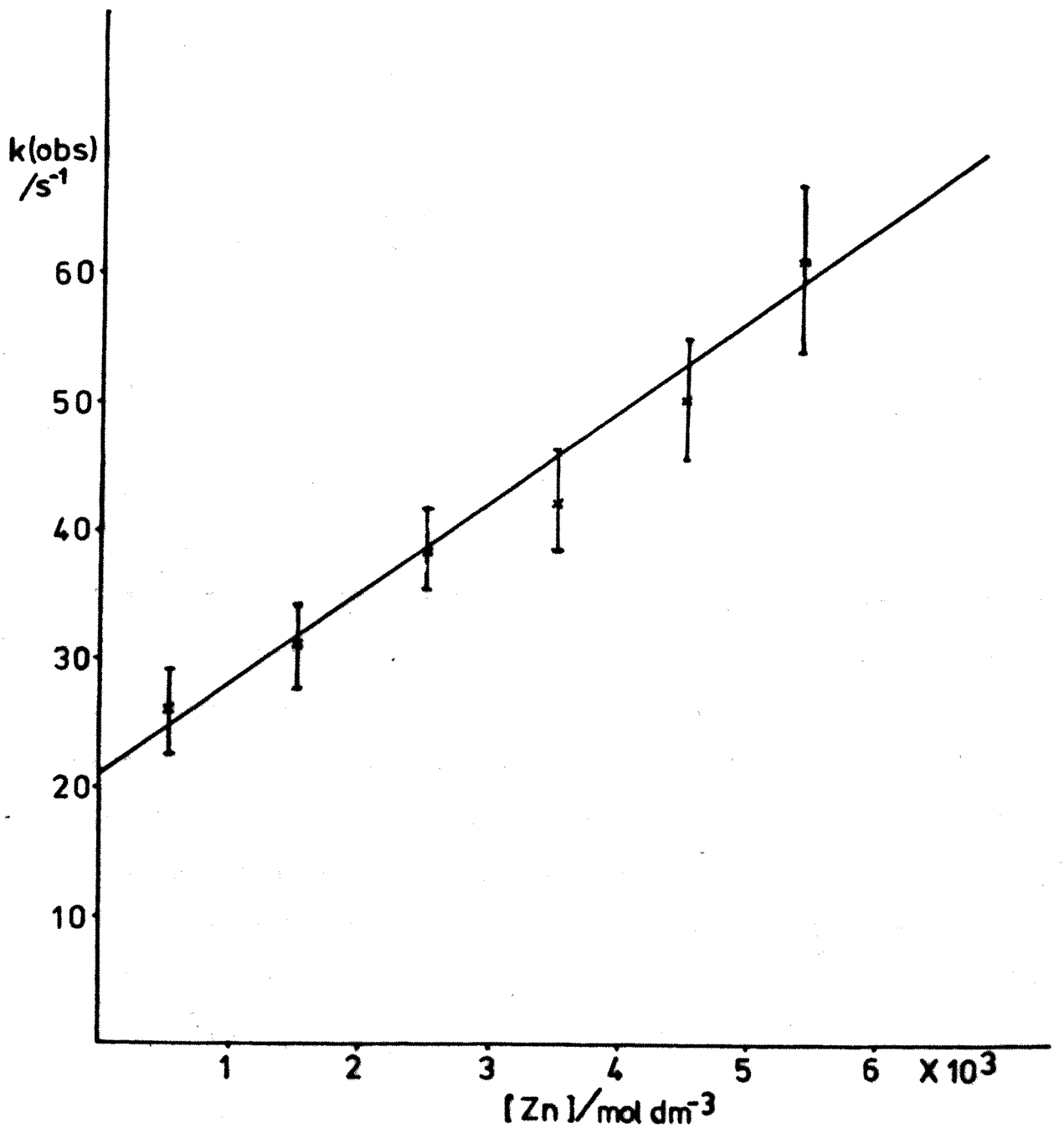

for the fitted line of:

$k(obs) = 21(\pm2) + 7000(\pm600)[Zn]$

The zero-order term arises from decomposition of the initial complex although it cannot reliably be used to quantify this term.

Table 4.5.1.

The first stage of the reaction of $Zn(ClO_4)_2$ with **(A)** in methanol. T=4.5±0.5°C λ=260nm

$10^3[Zn]/M$	$10^5[L]/M$	k_{obs}/s^{-1}
0.54	3.3	26±3
1.5	3.3	31±3
2.5	3.3	38±4
3.5	3.3	42±4
4.5	3.3	50±5
5.0	3.3	61±6

$k_{obs}=k_o+k_1[Zn]$

$k_o=21\pm2\ s^{-1}$

$k_1=7.0\pm0.6\ X10\ M^{-1}s^{-1}$

The slower second stage was followed at 280nm where there was only a small change in absorbance for the first stage. This stage was not first order with respect to ligand (the reaction being progressively slowed from that expected for a first order reaction) so only initial rate constants could be measured. The initial rate constants (shown in Table 4.5.2) showed an inverse dependence on the concentration on zinc(II).

Table 4.5.2.

The second stage of the reaction of $Zn(ClO_4)_2$ with (A) in methanol. T=4.5±0.5°C λ=280nm

10^3[Zn]/M	10^5[L]/M	$10^3 k_{INIT}$/OD s^{-1}	$10^7 k_{INIT}$/M s
0.54	3.3	5.9	8.9
1.5	3.3	4.0	6.1
2.5	3.3	3.3	5.0
3.5	3.3	3.0	4.5
4.5	3.3	2.4	3.6
10.0	3.3	1.4	2.1

using ϵ=6600 for Zn(**A**) complex

These observations can be explained by the mechanism shown in Figure 4.5.3. . In the second stage of the reaction a proton is expelled from the complex as the thiazolidine ring opens. The non-first order dependence on the ligand concentration is due to zinc suffering from increasing competition from protons for the ligand binding sites. The inverse dependence upon the zinc concentration is probably also explained by an acid effect, in that the zinc(II) perchlorate may contain traces of perchloric acid which become increasingly significant with the large excess of zinc present in these reactions. Addition of KOH in methanol accelerates the second stage of the reaction in a manner consistent with the mechanism described above.

The use of zinc(II) acetate instead of the perchlorate salt

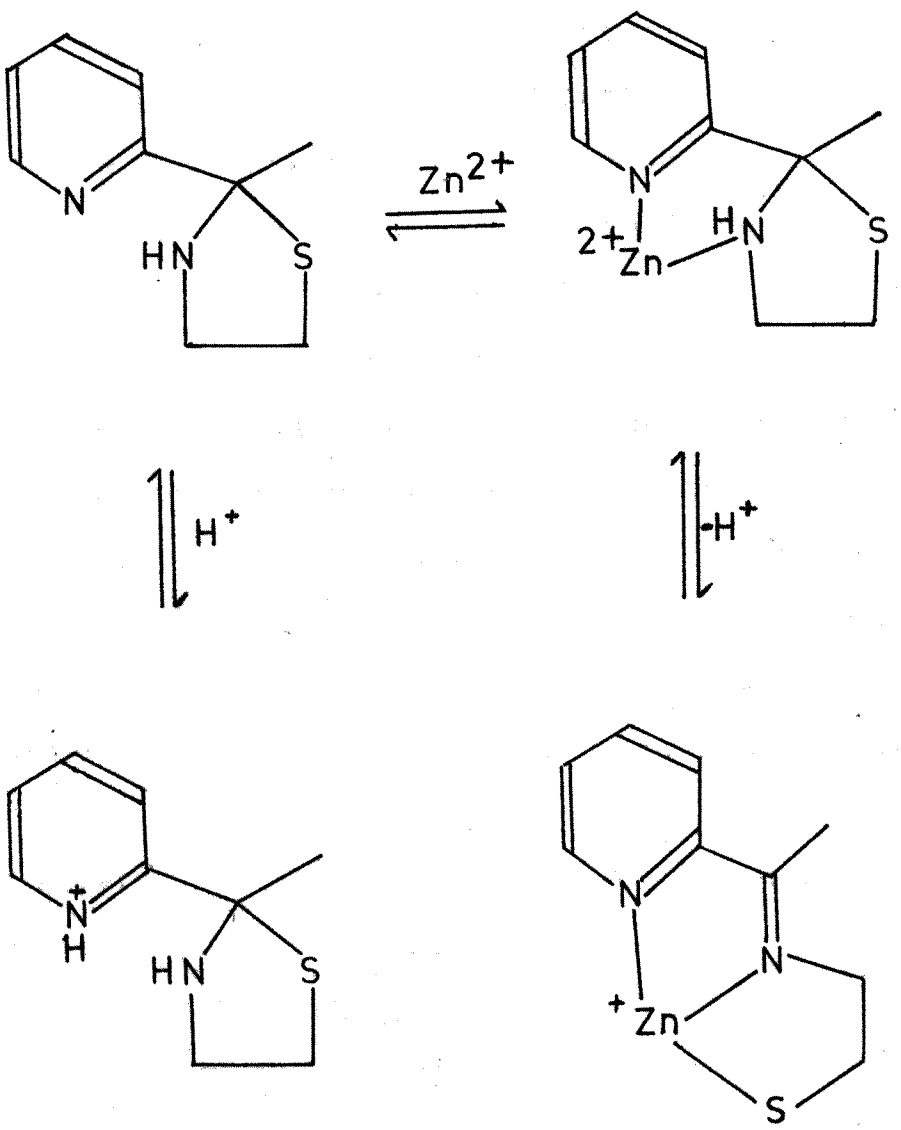

Figure 4.5.3

was tried in an attempt to avoid the non-first order dependence of the rate on ligand concentration and the inverse dependence of the rate upon the zinc concentration. The acetate anion would be a good scavenger for protons released in the course of the reaction. The use of zinc(II) acetate however, has the disadvantage of increasing the solvent exchange rate on the metal to such an extent that the initial binding stage is too fast to detect by stopped-flow spectrophotometry. However the use of zinc(II) acetate had the desired effect on the second stage of the reaction which became first order with respect to ligand concentration and independent of zinc concentration (at greater than 100 fold excess) - see table 4.5.3.. At lower zinc concentration however there appeared to be a slight slowing of the reaction, so further measurements of the reaction rate were carried out with zinc in an excess of between 10 and 100.

The slowing of the rate can be attributed to a rapid pre-equilibrium of the form:

$$Zn^{2+} + LH \overset{K}{\rightleftharpoons} ZnLH \xrightarrow{k_1} ZnL + H$$

where $k_{obs} = (k_1 K[M])/(1+K[M])$

A least squares fit of the data in Table 4.5.4 to the equation above is shown in Figure 4.5.4. and gave values of:

$$k_1 = 0.52(\pm 0.07)\ s^{-1}$$

and $$K = 1.90(\pm 0.14)\ X10^{4}$$

The magnitude of the equilibrium constant, K, is similar to that for the reaction:

Figure 4.5.4

$Zn(OAc)_2$ + (A)

T = 10·3°C λ = 280 nm

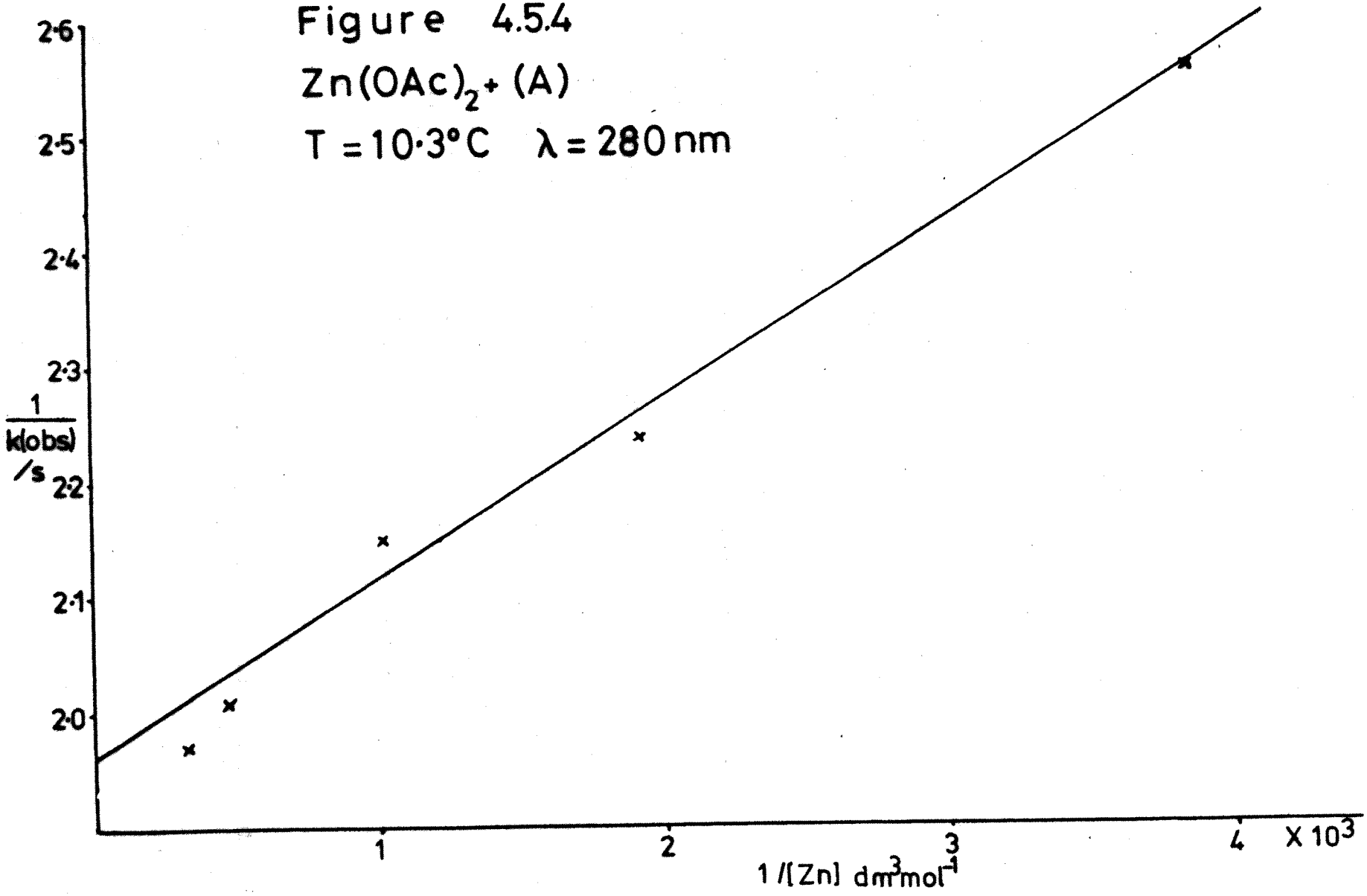

Zn^{2+} + pyridine + NH_3 ⟶ Zn(pyridine)$(NH_3)^{2+}$

The donor set of one pyridine and one amine group is the same for both reactions, the later having a log(Kf) value of 4.07 at 20°C (104).

Table 4.5.3.

The reaction of $Zn(OAc)_2$ with (A) in methanol. T=4.8°C λ=280nm

10^3[Zn]/M	10^5[L]/M	k_{obs}/s^{-1}
1.3	3.3	0.219±0.003
3.3	3.3	0.237±0.003
6.6	3.3	0.254±0.003
13.0	3.3	0.257±0.003
20.0	3.3	0.267±0.003
26.0	3.3	0.262±0.003
33.0	3.3	0.268±0.003

Table 4.5.4.

The reaction of $Zn(OAc)_2$ with (A) in methanol. T=10.3°C λ=280nm

10^3[Zn]/M	10^5[L]/M	k_{obs}/s^{-1}
0.26	3.3	0.391±0.004
0.52	3.3	0.447±0.004
1.0	3.3	0.465±0.004
2.1	3.3	0.498±0.004
3.1	3.3	0.507±0.004

The activation parameters for the second stage of the

reaction were determined from a series of experiments at different temperatures. These results are shown in Table 4.5.5 and a least squares fit to the Eyring equation for the data is shown in Figure4.5.5. .The results obtained were:

$\Delta H^{\ddagger}$ = 69.6 ± 1.3 kJ/mole $\Delta S^{\ddagger}$ = -4.3 ± 4.6 J/K/mole

Table 4.5.5.

Variation of the reaction rate with temperature for the reaction of $Zn(OAc)_2$ and (A) in methanol. λ =280nm, [Zn]=0.038M, [A]=$3.7X10^{-5}$M.

T/K	k/s^{-1}
281.7	0.44±0.01
282.8	0.53±0.01
284.5	0.60±0.01
287.0	0.76±0.01
291.5	1.21±0.05
297.1	2.36±0.05
300.2	3.09±0.09
304.4	4.62±0.1
309.3	6.46±0.2

These activation parameters are consistent with the proposal that the second stage of the reaction is a re-arrangement of the co-ordinated ligand to produce a binding thiol group, in that the large positive value of $\Delta H^{\ddagger}$ would be expected for the breaking of the carbon-sulphur bond.

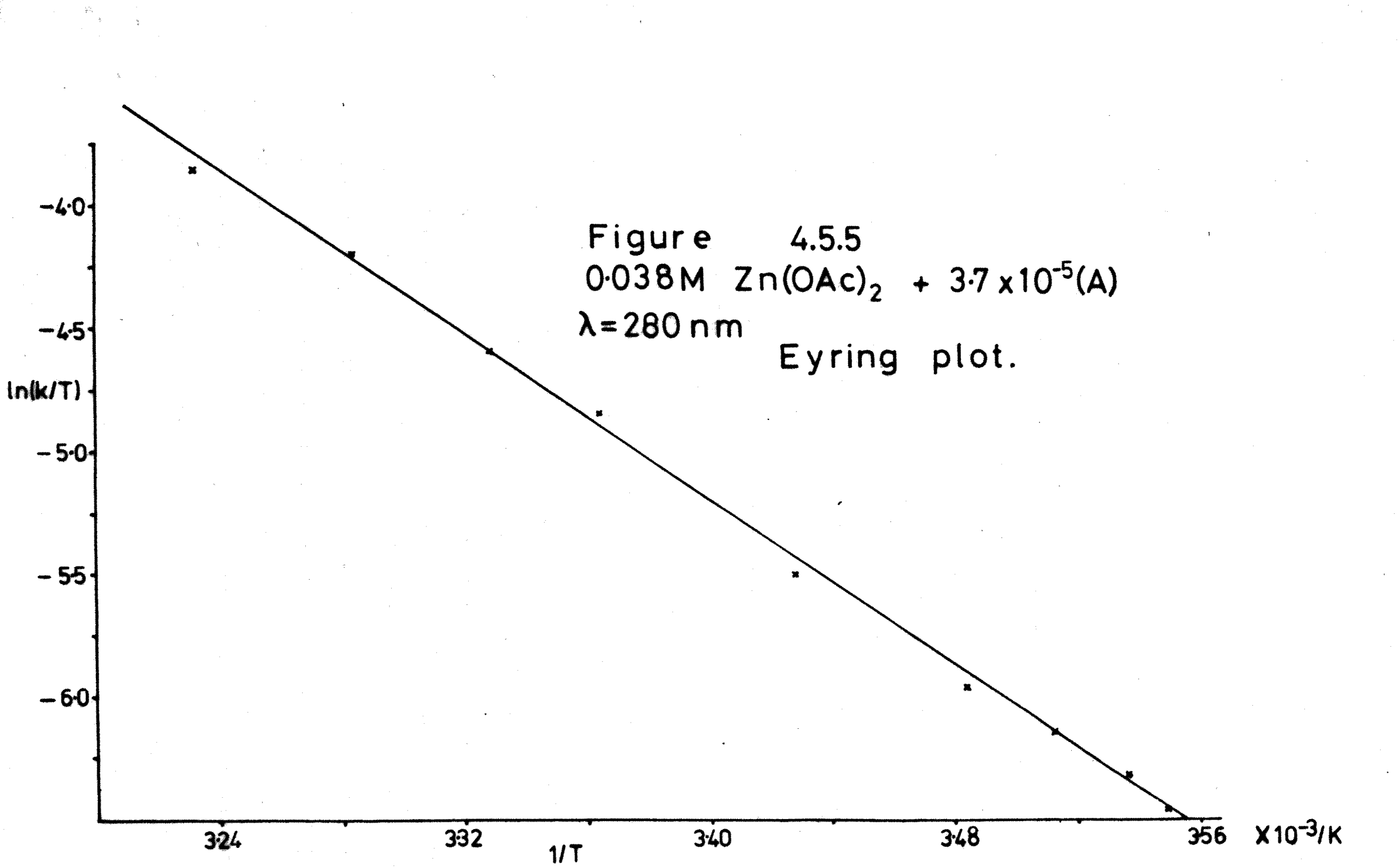
Figure 4.5.5
0·038M Zn(OAc)2 + 3·7 x10-5(A)
λ=280 nm
Eyring plot.
-4·0
-4·5
ln(k/T)
-5·0
-5·5
-6·0
3·24
3·32
3·40
3·48
3·56
X10-3/K
1/T

4.6 Summary

The reaction of 2-methyl-2-(2-pyridyl)thiazolidine (A) has been studied with methylmercury(II), mercury(II) and zinc(II). The thiazolidine ring of the ligand was opened to form the corresponding Shiff base in the presence of the metal ions. In an unbuffered solution the reaction of methylmercury(II) with (A) produces two species, only one of which is ring opened and co-ordinated through the thiol. When the reaction is buffered by using methylmercury(II) acetate there is complete formation of the thiol bound, ring opened complex. In the reaction of mercury(II) with (A) there was a very fast rearrangment of the coordinated ligand. The product Hg(A)ClO_4 was characterised by ^{13}C n.m.r. as containing the ligand in a ring opened form. The reaction of zinc(II) perchlorate with (A) was seen to have two distinct stages. The initial binding of the ligand was found to be first order in both (A) and Zn(II) although there was also a small zero order term. The second stage was not first order in ligand due to competition between zinc and protons (released in the course of the reaction) for the ligand binding sites. Zinc(II) acetate which was tried in an attempt to solve this problem caused the initial binding rate to increase beyond detection but it did cause the second stage to become first order with respect to ligand. The activation parameters for the second stage (i.e. co-ordinated ligand rearrangment) are reported together with characterisation of the complex by ^{13}C n.m.r. .

4.7 Experimental

4.7.1 2-methyl-2-(2-pyridyl)thiazolidine

Preparation.

2-aminoethanethiol hydrochloride (11.3g,0.1mol) was dissolved in 20% aqueous methanol (100cm^3) and KOH (1.2g,0.2mol) added carefully with stirring. 2-acetylpyridine (12.1g,0.1mol) was then added and the mixture stirred overnight under a nitrogen atmosphere. The solvent was removed with a rotary evaporator, water (30cm^3) added and the aqueous suspension extracted with dichloromethane (5X30cm^3). The solvent was then removed under reduced pressure and the product distilled at 105°C (0.05mm Hg).

Characterisation.

^{13}C n.m.r. shifts (ppm relative to TMS) in $CDCl_3$: 163.60 (ring C2); 148.46(ring C6); 136.44 (ring C3); 121.68,118.69 (ring C4/C5); 80.61 (quaternary carbon); 51.88,38.03 (methylene); 30.75 (methyl);

^{1}H n.m.r. shifts (in ppm relative to TMS) in 1:3 CD_3NO_2 :CCl_4 :8.36 (m,1,ring); 7.56 (m,1,ring); 7.39 (m,1,ring); 7.04 (m,1,ring); 3.36 (ddd,1,CH_2); 3.25 (ddd,1,CH_2); 2.95 (ddd,1,CH_2); 2.84 (ddd,1,CH_2); 1.80 (s,3,methyl). Couplings in the methylene ring system (numbered 1-4 as listed) $^1J(1,2)$ 12.39; $^2J(1,3)$ -4.36; $^2J(1,4)$ -5.87; $^2J(2,3)$ -5.89; $^2J(2,4)$ -7.61; $^1J(3,4)$ 9.81.Hz.

Electronic spectrum in methanol: λ_{max} 263nm, ε = 3600±100

$dm^3 mol^{-1} cm^{-1}$

Elemental analysis calculated for $C_9H_{12}N_2S$: C, 60.00; H, 6.67; N, 15.56; S, 17.78%; found: C, 59.79; H, 6.75; N, 15.62; S, 17.84%.

Mass spectrum:

m/e	formed by loss of	relative intensity
180		1.1
165	15 (CH_3)	0.5
147	33 (SH)	2.0
138	42 (C_2H_4N)	0.7
133	47 (SCH_3)	1.9
121	59 (SC_2H_3)	1.0
106	74 (SC_2H_4N)	1.5
102	78 (C_5H_4N)	1.4
79	101 (SC_4H_7N)	1.4
78	102 (SC_4H_8N)	1.1

4.7.2 Standardisation of metal solutions.

The hydrated perchlorate salts of mercury(II) (Ventron) and zinc(II) (Pfaltz and Bauer) were used as supplied, containing an unknown quantity of water. Stock solutions (approximately 0.01M) of both salts were prepared and the exact metal ion concentration determined as follows. $10cm^3$ of a standard 0.01M aqueous solution of EDTA, $5cm^3$ of the stock solution, 5 drops of concentrated ammonia solution and Solochrome Black indicator were placed in a flask. The free EDTA which remained uncomplexed by the metal was titrated with a standard aqueous solution of zinc(II) sulphate.

4.7.3 n.m.r spectral data for metal complexes

^{13}C shift data for Hg(**A**)(ClO_4) in 9:1 d_6 dmso/CD_3NO_2 (shifts in ppm relative to TMS).
198.52 (imine), 150.22, 149.31, 141.58, 129.62, 125.07 (pyridine), 43.24, 27.90 (methylene), 26.54 (methyl).

^{13}C shift data for Zn(**A**)(OAc) in CD_3OD (shifts in ppm relative to TMS). 179.73, 179.20 (carboxylate and imine), 166.80, 148.45, 140.98, 127.85, 124.28 (pyridine), 51.17, 27.21, 26.91 (methylenes and methyl) 22.58(acetate methyl).

^{13}C shift data for Zn(**A**)(ClO_4) in 3:1 d_6 dmso/CD_3NO_2 (shifts in ppm relative to TMS). 163.29, 148.01, 142.75, 126.18, 125.66 (pyridine), 79.51 (C-2 in thiazolidine), 54.61, 36.09 (methylene), 33.23 (methyl).

^{13}C shift data for d_6 dmso solution containing 3:1 MeHgCl/(**A**) (shifts in ppm relative to TMS).
9.10 (MeHg, ^1J=1506Hz), 25.18, 26.07 (methyl and methylene), 43.46 (methylene), 120.80, 127.67, 137.21, 148.97, 152.74 (pyridine), 198.89 (imine).

^1H n.m.r. spectral data for an equimolar solution (in $d_6$dmso) of MeHgCl and (**A**) (shifts in ppm relative to TMS).
0.45 (s,3,MeHg, ^2J=182.6Hz), 2.00 (s,3,Me), 3.07 (t,2,CH_2) 3.40 (t,2,CH_2), 7.20 (m,1,ring), 7.55 (m,1,ring), 7.65 (m,1,ring), 8.45 (m,1,ring).

^1H n.m.r. spectral data for an equimolar solution (in CD_3OD) of methylmercury(II) acetate and **(A)** (shifts in ppm relative to TMS). 0.55 (s,3,MeHg,^2J=163.0Hz), 1.95 (s,3,acetate), 2.65 (s,3,methyl), 3.15 (t,2,CH_2), 3.25 (t,2,CH_2), 7.60 (m,1,ring), 7.95 (m,1,ring), 8.05 (m,1,ring), 8.55 8m,1,ring).

Chapter 5

Some reactions involving the mercury-carbon bond.

5.1 The reaction of methylmercury(II) with some tetra-aza macrocyclic ligands.

5.1.1 Introduction.

Methylmercury(II) shows a very pronounced tendency to form linear Me-Hg-L bonds and in searching for better chelators of methylmercury(II) it has been of interest to study the effect of binding to multidentate macrocyclic ligands (A)-(D).

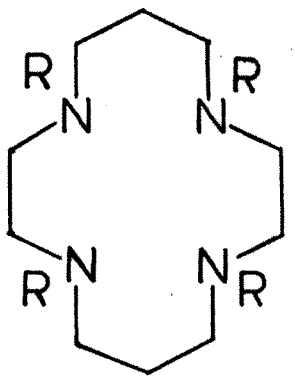

A : R=H

B : R=Me

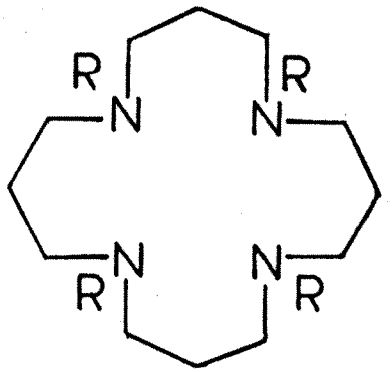

C : R=H

D : R=Me

The ligands are formally named:

(A) 1,4,8,11 tetra-azacyclotetradecane

(B) 1,4,8,11 tetramethyl 1,4,8,11 tetra-azacyclotetradecane

(C) 1,5,9,13 tetra-azacyclohexadecane

(D) 1,5,9,13 tetramethyl 1,5,9,11 tetra-azacyclohexadecane

For preparative details see reference (112) and references cited therein.

These macrocycles are known to form stable metal ion complexes with a wide range of ligand geometries (104-112). Without exception, they all contain an endo-quadradentate conformation of the ligand although the actual geometries present are dependant on several factors.

The major factor which determines the ligand geometry is the suitability of the metal ion for the macrocycle "hole size". Ideal metal-nitrogen distances have been determined from strain-energy calculations for square-planar co-ordination of the ligand (113). The 14 and 16 membered macrocycles studied here have ideal metal-nitrogen distances of 2.07 and 2.38Å respectively, which are within the normal range of mercury-nitrogen bond lengths. Mercury(II) forms an extremely stable complex with **(A)** (log(K)=23.0), confirming that the ligands are well suited for the large Hg(II) ion (114). The ligand geometries are readily changed by the use of different anions or a solvent with different donor properties. The ligands **(A)-(D)** are particularly suitable for study by n.m.r. methods because the high symmetry of the ligands greatly simplifies the problem of spectral interpretation.

5.1.2 Results and discussion.

Upon mixing equimolar quantities of methylmercury(II) nitrate and **(A)** there was a rapid decomposition to produce a black precipitate in each of the solvents tried (ie. water,

methanol dmso, pyridine, nitromethane, chloroform and dichloromethane). ^1H n.m.r. spectra of the soluble reaction products have been observed in different solvents and in each case there is a small quantity (less than 10%) of dimethylmercury together with a major product containing co-ordinated methylmercury(II). Peak integration for the spectrum of the major species left in solution shows a 1:1 stoichiometry and that there is no free ligand remaining. Therefore the precipitate must contain (A) in some co-ordinated form. The values of $^2J(Hg-H)$ in methanol and dmso (223 and 224Hz respectively) are slightly higher than those normally seen for amine bound methylmercury(II) species as would be expected if chelation is present. The value of ^2J in water is anomolously low (208Hz) and is probably the result of a rapid exchange between amine bound methylmercury(II) and methylmercury(II) hydroxide which may be formed due to the presence of the very basic amine groups. The high pH present in these solutions also facilitates reduction of methylmercury(II) to a mercury(I) species which may in turn disproportionate to Hg° and Hg^{2+}.

The reaction of methylmercury(II) nitrate with (C) (equimolar in methanol) also produces a black precipitate but the soluble products contain equimolar dimethylmercury and complexed methylmercury(II). Identical reaction products result from the reaction of equimolar (C) and methylmercury (II) acetate with, ^2J=219Hz for the complex formed in methanolic solution.

The reaction of methylmercury(II) with the tetramethylated ligand **(B)** did not cause decomposition of the type described above, but did produce three different types of mercury(II) namely dimethylmercury(II), complexed methylmercury(II) and complexed mercury(II).

The ^1H n.m.r. spectra of equimolar solutions of methylmercury(II) nitrate and **(B)** clearly show two different types of methylmercury(II), one of which is dimethylmercury(II) (δ=ca.0.1ppm, ^2J=ca.105Hz) while the other is assignable to complexed methylmercury(II) (δ=ca.0.6ppm, ^2J=212-237Hz). The ligand resonances in the ^1H n.m.r. spectrum are too broad to resolve the different types of ligand present but the distinct ^{13}C n.m.r. resonances are readily resolved. In CD_3NO_2 solution there are two sets of ligand resonances in a 1:4 ratio. The minor species has shifts (at 303K) identical to those of [Hg(B)Cl] at high temperature (112). The decomposition products in this reaction are therefore, free dimethylmercury(II) and mercury(II) complexed to the macrocycle. In the reaction of methylmercury(II) nitrate with **(D)** there is production of dimethylmercury(II), presumably in a reaction analogous to that with **(B)**.

The value of ^2J in complexes with **(B)** and **(D)** is significantly larger than that with **(A)** and **(C)** since the tertiary amines are more basic than secondary amines and ^2J is inversely proportional to the donor group basicity.

The decomposition can be explained by electrophilic attack of any free methylmercury(II) present at the complexed methylmercury(II) to produce free dimethylmercury(II) - see Figure 5.1.1. . This proposed mechanism is analogous to that proposed for the cleavage of the cobalt-carbon bond in methylcobalt(III) chelate species by electrophilic attack by Hg^{2+} (115). If the amount of free methylmercury(II) is reduced by using a large excess of ligand, there is no detectable formation of dimethylmercury(II), as would be expected if the electrophilic attack described above is the actual mechanism.

It has been suggested that the position of the equilibrium in:

$$2MeHgCl \rightleftharpoons HgMe_2 + HgCl_2$$

should be driven to the right if $HgCl_2$ is effectively removed from the equilibrium situation by complexation (116). This proposition is consistent with the results reported here since mercury(II) chloride is known to form very stable complexes with ligands **(A)-(C)** (112,117).

Attempts to react methylmercury(II) nitrate with an anologous sulphur macrocycle TTP (1,4,8,11-tetrathiacyclotetradecane) (148) were unsuccessful in methanol, dichloromethane, chloroform, nitromethane, dmso, toluene and pyridine. Thio-ethers co-ordinate methylmercury(II) quite poorly but would normally be expected to complex in the absence of better donor groups (46). This result is slightly suprising since the ligand is very flexible and is known to

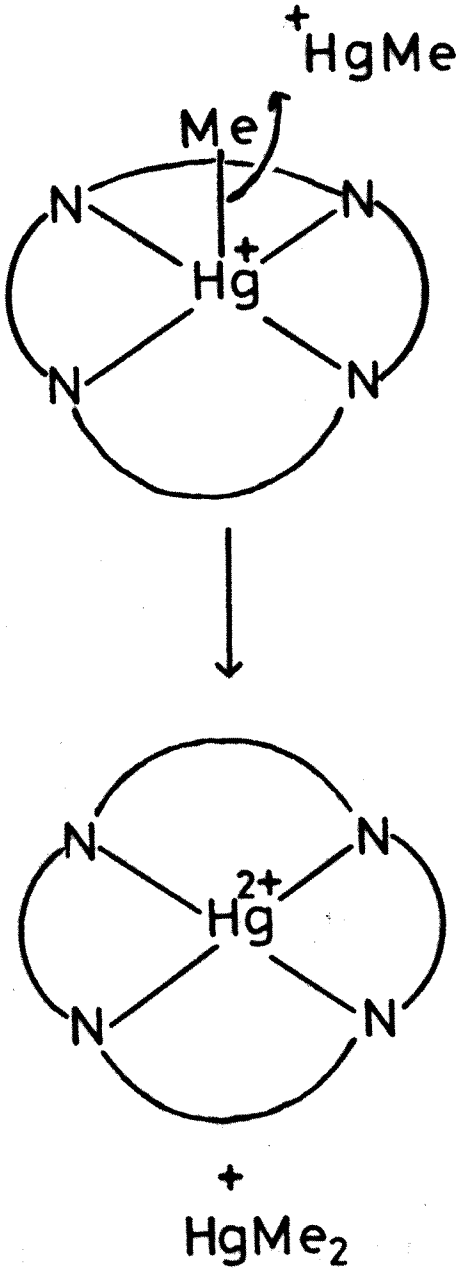

Figure 5.1.1

form an endo S. complex with $Hg(ClO_4)_2$ as well as an exo-complex of the type $(L(HgCl_2)_2)$ with $HgCl_2$, where each mercury atom is chelated by two sulphur atoms with chlorines occupying the two remaining co-ordination sites (118).

5.1.3 Spectral Data.

^1H n.m.r. data for an equimolar mixture of $MeHgNO_3$ and (A).

Ligand shifts(rel. to TMS):

2.95 (t,8,N-CH_2), 2.90(s,8,N-CH_2), 1.85 (m,4,central methylene).

Methylmercury(II) shifts:

δ/ppm	^2J/Hz	solvent
0.83	208	solvent
0.49	224	d_6 dmso
0.67	223	CD_3OD

^{13}C n.m.r. data for equimolar solution (in CD_3NO_2) of MeHgNO and (B).

Major species 8(80)% : 22.24 (central methylene), 43.15 (N-Me), 55.31 56.22 (N-CH_2).

Minor species (20%) : 23.29 (central methylene), 44.70 (N-Me), 57.26 63.21 (N-CH_2).

^1H n.m.r. data for an equimolar mixture of $MeHgNO_3$ and (B).

Ligand resonances:

2.54 (t,J=5.3Hz,8,N-CH_2), 2.42 (s,8,N-CH_2), 2.09 (s,12,N-Me), 1.54 (m,4,central methylene).

Methylmercury(II) species:

	$HgMe_2$		MeHg(B)		
Solvent	δ/ppm	^2J/Hz	δ/ppm	^2J/Hz	ratio
D_2O	0.05	106.2	0.66	211.8	1:20
CD_3OD	0.10	103.6	0.54	231.2	1:13
C_5D_5N	0.16	103.8	0.61	231.8	1:9
CD_3NO_3	0.11	105.7	0.60	237.1	1:1

^{1}H data for an equimolar solution (in CD_3OD) of $MeHgNO_3$ and **(C)**. 2.93 (m,8,CH_2), 1.81 (t,16,N-CH_2), 5:4 (MeHg**(C)**:Me_2Hg) (0.80,^2J=219Hz):(0.24,^2J=105Hz).

^{1}H data for an equimolar solution (in CD_3OD) of MeHgOAc and **(C)**. 2.91 (m,8,CH_2), 1.91 (t,16,N-CH_2), 5:4 (MeHg**(C)**:Me_2Hg) (0.86,^2J=219Hz):(0.25,^2J=105Hz).

^{1}H data for an equimolar solution (in CD_3OD) of MeHgOAc and **(D)**. 2.35 (t,16,N-CH_2), 2.17 (s,12,N-CH_3), 1.92 (s,3,OAc), 1.54 (m,8,CH_2), 0.85 (s,3,MeHg,^2J=204.1Hz).

5.1.4 Summary.

The reaction of methylmercury(II) with four tetra-aza macrocyclic ligands was investigated by n.m.r. spectroscopy. The reaction with the secondary amine ligands **(A)** and **(C)**

caused partial decomposition of methylmercury(II) to produce varying quantities of Hg°, and Me_2Hg. In the reactions with the tetramethylated ligands (B) and (D) decomposition of the methylmercury(II) complex produces Hg^{2+} and $HgMe_2$. Electrophilic attack by free methylmercury(II) at complexed methylmercury(II) is proposed to account for the observed decomposition.

5.2 The demethylation of methylmercury(II) under mild conditions.

5.2.1 Introduction.

There are several reports in the literature concerning cleavage of the mercury-carbon bond in methylmercury(II) species. Recently several species of bacteria and yeasts have been reported capable of demethylating methylmercury(II) under mild conditions (119-122). Yields of up to 58% have been reported in the decomposition of methylmercury(II) to Hg. (123). The enzyme **Pseudamonas** K-62 catalyses the decomposition of methylmercury(II) in the presence of sulphydryl compounds to produce Hg^{o} and CH_4 (124). The demethylation of methylmercury(II) by "symmetrisation" is a well known reaction which produces Hg^{2+} and $HgMe_2$ and has been reported in the reaction of methylmercuy(II) with amines (this work) and with phosphines (125,126). Dialkylmercury(II) compounds, RHgR', are reported to undergo cleavage of the mercury-carbon bond in acetic acid to produce R'HgOAc and RH (127).

5.2.2 Discussion.

It was during the course of the work described in Chapter 2 of this thesis that demethylation of methylmercury(II) by thiolate ligands was first observed. When equimolar quantities of methylmercury(II) chloride and 2-phenylethyl-

mercaptan were mixed in methanol a precipitate formed which when collected and dissolved in chloroform was found not to contain methylmercury(II). The isolatable products were in fact mercury(II) chloride and bis-(phenylethylmercapto) mercury(II). However when one equivalent of base was added to the thiol solution prior to addition of methylmercury(II) chloride the only isolated mercury containing compound was methyl(2-phenylethylmercapto) mercury(II). Some literature preparations (22,25) of methylmercury(II) thiolate complexes involve addition of one equivalent of base to absorb the acidic proton, while omission of the base can still give the expected methylmercury(II) complexes in favourable cases(93).

The absence of a MeHg resonance in the ^{1}H n.m.r. spectrum was the first evidence that demethylation had taken place. This was confirmed by the ^{13}C n.m.r. spectrum which showed just eight ligand resonances which were shifted from those of the free ligand. The mass spectrum gave conclusive evidence that the products were $Hg(RS)_2$ and $HgCl_2$. The fate of the methyl group was not known so an **in situ** preparation of the complex was carried out in d_4 methanol. The ^{1}H n.m.r. spectrum of the soluble species in the reaction showed no sign of methylmercury(II) species but there was a small singlet in the methyl region which seemed to be due to a small quantity of dissolved methane. In an attempt to confirm the production of methane a gas-liquid chromatographic experiment was carried out as described in Section 5.2.4. .

The methane yields of the reaction were highly irreproducible - ranging from 12% to less than 1% yield under apparantly identical conditions (with the use of recrystallised methylmercury(II) chloride and freshly distilled solvent and ligand). It seemed possible that the methane produced in the reaction was saturating the solvent before any was released into the gas phase. In an attempt to check this possibility the volume of gas produced in the course of the reaction was determined by compressing the gas into a known volume with a Toepler pump and then measuring the pressure of that vessel (128,129). An all glass reaction vessel was constructed and attached to a vacuum line with a Toepler pump. The solutions of reactants were degassed several times by the freeze-thaw method, allowed to melt and then mixed. The reactant solution was stirred vigorously for two hours and then frozen again in liquid nitrogen. The methane produced was then pumped into the calibrated volume by the Toepler pump, the solution frozen and the cycle repeated until there was no further change in the pressure. This pressure was noted and the volume of methane produced at STP was readily calculated from the volume of the vessel. The yields determined by this method were also irreproducible - ranging from 10 to 45%.

The fact that this demethylation reaction only occurs when methylmercury(II) is co-ordinated to a thiol group would seem to indicate that only the very strong mercury-sulphur bond weakens the mercury-carbon bond sufficiently to permit the

reaction to take place. The observation of demethylation of dialkymercury(II) compounds by acetic acid would seem to support the idea that the mercury-carbon bond strength is important in this reaction since the values of ^2J in dimethylmercury(II) (cal05Hz) and methylmercury(II) thiolate complexes (cal60Hz) are the lowest for methylmercury(II) species.

The reaction could not be followed by n.m.r. since the precipitation was too great so a ligand was sought which would allow the $Hg(SR)_2$ species to remain in solution. 4-amino-thiophenol was reacted with methylmercury(II) chloride but it only produced the methylmercury(II) complex (with ^2J=178Hz) and no methane could be detected by g/c possibly because protonation of the ligand amine absorbed the released proton.

In order to test the theory that demethylation was caused by the acidic thiol proton which is displaced by complexation the addition of acid to thiolato-methylmercury(II) complexes was studied. The complexes were prepared with an equivalent of base present and after purification redissolved and an excess of hydrochloric acid added. A g/c analysis of the gas in the reaction vessel showed that methane was indeed produced although the yields were typically around 1%. This is not too suprising since a high concentration of acid would tend to produce decomposition of the complex to give MeHgX and RSH.

5.2.3 The determination of methane concentration .

The calibration of the gas chromatograph equipment was carried out as follows. Equal volumes of methane and ethane were introduced into an Argon filled Schlenk tube at a concentration similar to that expected in the demethylation experiment. 100μl aliquots of the gas mixture were introduced into a Perkin-Elmer F11 gas chromatagraph with a gas-tight syringe. A phenylisocyanate column operated at room temperature was found to produce a satisfactory seperation of the gases with methane and ethane separated by 15 seconds.

The response (R) of the flame ionisation detector was measured as the product of the peak height and the retention time. The ratio of the response to methane and ethane was:

$$R(Me)/R(Et) = 0.58$$

This was used subsequently to determine the volume of methane produced relative to an internal standard of ethane contained in the sample.

Typically 0.5 mmol of reactants were mixed in a 300cm^3 Schlenk tube under an atomosphere of Argon. Methylmercury(II) chloride was dissolved in 30cm^3 of methanol and the solution then degassed by the freeze-thaw method. Argon was subsequently introduced since an "air" peak in the g/c trace was too close to the CH_4 peak for reliable data to be obtained.

5.2.4 Spectral Data.

^{13}C n.m.r. shift data for bis(2-phenylethylmercapto)-mercury(II) in $CDCl_3$. 141.09 (C4), 129.39 129.20 (C3/C2), 127.06 (C4) 40.80 29.88 (methylene).

^{1}H n.m.r. shift data for bis(2-phenylethylmercapto)-mercury(II) in d_6 dmso. 7.23 (m,5,ring), 3.03 (t,2,CH_2), 2.86 (t,2,CH_2).

Mass spectral data for bis(2-phenylethylmercapto)-mercury(II) (^{202}Hg masses quoted) 476 (M^+,0.6%), 374 ($HgS_2C_8H_{12}^+$,1.0%), 234 (HgS^+,0.3%) 202 (Hg^+,5.5%), 135 ($C_8H_7S^+$,2.9%), 105 (C_8H_9,7.0%) 104 (C_8H_8,8.2%), 91 (C_7H_7,20.3%), 77 (C_6H_5,100%).

5.2.5 Summary.

The demethylation of methylmercury(II) under mild conditions in its reaction with thiolate ligands is reported. Equimolar quantities of mercaptan and methylmercury(II) produced varying quantities of $Hg(SR)_2$, $HgCl_2$ and CH_4 as additional reaction products to the methylmercury(II) thiolate complex. The thiolate proton which is released upon complexation is proposed to cause the demethylation reaction.

6. Conclusions and extensions of this work.

The results reported in this thesis have lead to the following conclusions and possible extensions of the work.

(1) Methylmercury(II) can form a weak bond with the phenyl ring of a ligating molecule providing the donor atom and the phenyl ring are separated by not more than two atoms and there are not any other geometric restrictions. This additional interaction of methylmercury(II) could be utilised in drug design as a means of increasing the stability of the drug-methylmercury(II) complex.

(2) In the reaction of methylmercury(II) with those dithiolate ligands which contain a rigid carbon backbone linking the sulphur atoms, bis(methylmercury(II)) complexes are formed rather than the expected mono-methylmercury(II) complexes. Both chelate and monodentate methylmercury(II) moieties are present in the molecules which form under equimolar conditions. These molecules represent an improvement upon the thiolate molecules currently used to treat methylmercury(II) poisoning since they form stronger complexes due to chelation. They should be biologically evaluated to determine if their **in vivo** activity would make them suitable for drug use and to establish whether or not they are a real improvement upon the drugs currently used.

(3) Chemically protected thiol groups which can be re-activated by metal ions (such as the compound discussed in

Chapter 4) have not yet been used in the treatment of heavy metal poisoning. The incorporation of this type of thiol protection into a drug which possesses other desirable properties might be one direction that further research could take.

(4) The tetra-aza macrocycles studied in Chapter 5 could not be used to treat methylmercury(II) poisoning since they cause decomposition and produce the much more toxic species dimethylmercury(II). However chemical modifications of the macrocycle could overcome this problem and also make them more selective towards the toxic heavy metals present in the body. A possible extension of this work would involve the study of macrocycles with a fifth donor atom present on a "dangling arm" (Figure 6.1) . In the case of methylmercury-(II) complexation, a ligand of this type might well overcome the drawbacks of the ligands discussed in Chapter 5.

(5) The demethylation of methylmercury(II) described in Chapter 5 provides an alternative method of detoxifying methylmercury(II) since the product, mercury(II), has a much shorter biological half-life and would therefore be removed from the body much more quickly. It is difficult to see how the reproducibility of the reaction could be improved, although a systematic study of this reaction using a wide range of thiolate ligands may throw some light on this problem.

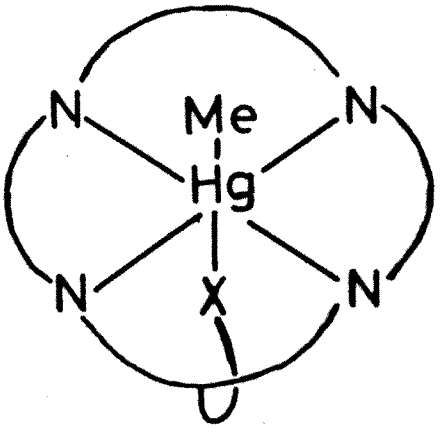

X = NH_2 or S^-

Figure 6.1

Appendices.

Appendix 1 - N.M.R. Spectroscopy.

Since the theoretical aspects of n.m.r. spectroscopy have been adequately covered in numerous standard texts(130-133), only some pertinent considerations will be discussed further.

(1) ^{1}H n.m.r.

Spectra were normally obtained using 0.5 cm^3 of solution in a 5 mm spinning sample tube on a Bruker WH90 (90MHz) and Perkin Elmer R34 (220MHz) spectrometers. The sample solutions were normally at least 0.05 mol dm^{-3} in a deuterated solvent which was used as a field lock on the Bruker WH90. The internal shift reference was normally dioxan (δ 3.55.) since TMS often obscured the mercury satellites of the methylmercury(II) resonance.

The extra shielding of the methyl group by a neighbouring phenyl group (discussed in Chapter 2.3) is due to the electrons of the phenyl ring perturbing the effective magnetic field. The small magnetic field of the phenyl ring, arising from the circulating ring current induced by the applied field, assists the applied field in the neighbourhood of the ring hydrogen atoms and decreases the applied field

over the phenyl ring. This has the effect of deshielding the aromatic protons and further shielding the protons (such as those in the methyl group of (1)) above the aromatic ring. Both Z (the distance above the ring plane) and ρ (the distance from the ring centroid) are measured in units of 1.28A - the average C-C bond length (see Figure 7.1.1 for the spatial dependence of the ring current shift).

(2) ^{13}C n.m.r.

The low sensitivity of this nucleus ($1.6X10^{-2}$ relative to ^{1}H) together with long spin-lattice relaxation times (T_1) mean that ^{13}C spectra normally take several hours to accumulate. Since the observation of $^{1}J(^{199}Hg-^{13}C)$ is often desirable and these satellites are each only 10% of the central peak height, high concentrations (ca 1 mol dm^{-3}) and long accumulation times (often 80,000 transients) are usually needed even for a solution in a 1cm tube.

A further problem arises in observing the methylmercury(II) resonance since its T_1 value (a measure of the time taken to reach thermal equilibrium) is often greater than those of the other carbon atoms in the molecule and it therefore becomes saturated more quickly. The saturation arises when the ^{13}C nuclei do not have sufficient time to relax to their lower energy level before the arrival of the next excitation pulse. The value of the T_1 depends on the relative efficiencies of energy exchange by any relaxation processes which are present

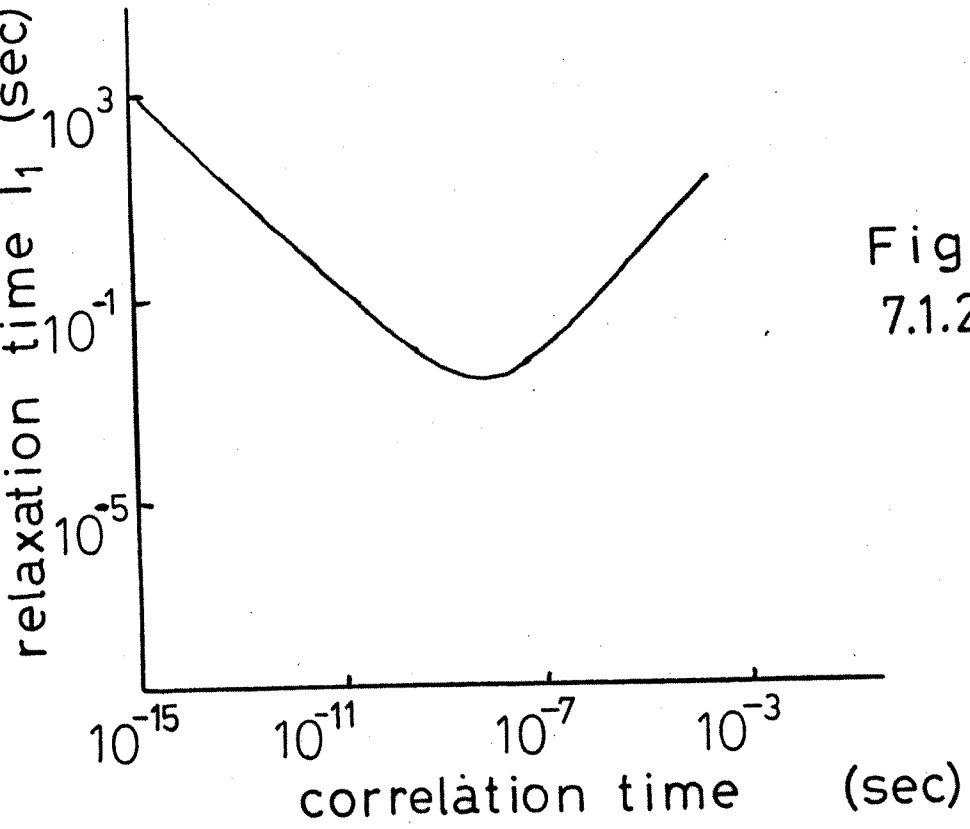

Figure 7.1.2

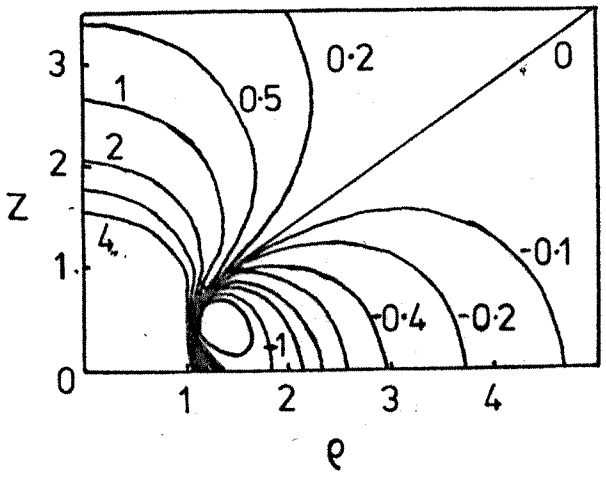

Figure 7.1.1

and is related to the correlation time, τ_c, for each carbon atom. The reason for the long T_1 value is that the methyl moeity is spinning rapidly and hence has a short correlation time whereas the molecule as a whole is tumbling relatively slowly in the bulk solvent and so has a much longer correlation time. It can be seen from Figure 7.1.2 that with decreasing correlation time - say from 10^{-12} to 10^{-14} - the T_1 value increases significantly.

A significant gain in signal intensity is obtained in a ^1H decoupled experiment each carbon resonance appears as a singlet and those attached to protons gain intensity due to Nuclear Overhauser Enhancement (NOE). This signal enhencement arises from population perturbation caused by the dipole-dipole relaxation of the C-H system. The theoretical maximum for the NOE is 2.98 and since this is not always achieved the peak heights in ^{13}C spectra cannot be used as a reliable measure of the concentration of each carbon atom.

The Karplus equation is used to relate vicinal coupling constants (^3J) to the dihedral angle between planes containing the two C-H bonds. The equation may be written in the form :

$$J = A + B \cos(\Theta) + C \cos(2\Theta)$$

where Θ is the dihedral angle between planes containing the two C-H bonds. The constants A, B and C are determined empirically and in this work the values A=7, B=-1 and C=5 were used (149).

Appendix 2 - X-ray Crystallography.

The course of a single crystal structure determination may be divided into (a) the collection of the X-ray diffraction data and (b) the structure solution.

(a) Data Collection.

The equipment used for these diffraction studies was a Syntex P2, four circle diffractometer. In this instrument the X-ray beam direction is fixed and the detector can move in the 2θ circle, which is in the equatorial plane of the beam and the crystal. The crystal can be moved in the other three circles ie. rotated on the goniometer head (θ circle), moved within the χ circle or the χ circle itself moved within the ω circle.

A crystal suitable for diffraction studies would typically have each dimension about 0.1mm, so obviously handling of the crystals must be carried out with the aid of a microscope. Crystals with well defined edges and with no obvious defects are mounted on a quartz fibre using an epoxy resin glue. The crystallinity is checked under a microscope by rotating the crystal with respect to a polarised light source and noting a

sharp cut-off of the light.

The quartz fibre is mounted on a copper rod which is in turn mounted on a goniometer which permits centring of the crystal in the X-ray beam by small movements in three orthogonal directions. Once the crystal has been satisfactorily centred on the diffractometer a rotation photograph is taken around an arbitrary axis of the crystal. Co-ordinates of up to 15 diffraction spots from this photograph are entered into the computer. They are then accurately centred on and their refined diffraction angles are used to generate a series of possible axes. Selection of suitable axes is based upon their length and inter-axial angles. Axial photographs are used to confirm the axis length and the presence of any required symmetry about the axis (though only 2-fold or mirror symmetry can be observed at this stage).

A rapid data collection of around 200 reflections is then carried out to find 15 strong reflections, which are centred, producing a further refinement of the axial vectors and the orientation matrix. The orientation matrix is later used to relate the chosen axes of the crystal to the axes of the diffractometer.

Once the above refinement has been carried out satisfactorily the full data collection can proceed. The data sets for the structures described in this thesis were

collected by the ω-2θ method in which the counter (2θ circle) and the crystal (ω circle) are rotated at relative angular rates $2\dot{\theta} = 2\Delta\dot{\omega}$

Each diffraction peak is scanned over a pre-determined range on either side of its centre at a scan speed which depends upon the intensity of the peak. The background for each reflection is measured at both sides of the peak for one quarter of the time taken for the full peak scan. A coincidence correction is automatically applied to intense reflections (greater than 12,000 cps) which begin to saturate the detection equipment while very intense reflections are ignored.

Several standard reflections are measured at regular intervals to check for variations in intensity due to crystal movement or decomposition. The diffractometer intensity data are stored on magnetic tape prior to transfer to the computer where the structure refinement is carried out.

The computer program SYNDAT (134) converts the intensity data into structure factors using the relationship

$F(hkl) = K*I(hkl)/L*p$

where the Lorentz factor, $L = 1/\sin(2\theta)$. The polarisation factor has the general form $p=(1+\cos^2 2\theta)/2$ although this has to be modified slightly to allow for the crystal monochrometer. The Lorentz factor arises because the time taken for a given reciprocal lattice point to travel through

its diffraction position is not constant but rather is a function of the data collection geometry (135-137).

When crystal decomposition has been detected by a change in the intensities of the standard reflections, SYNDAT is used to apply a correction to the structure factor using the scaling equation

$F(\text{corrected}) = F(\text{observed})*(1+\alpha(t))(1+\beta*t*\sin(\Theta/\lambda))$

where α and β are determined from a plot of the decay of the standards.

As the X-ray beam passes through a crystal, it is attenuated due to absorption according to the equation

$I = I_o e(-\mu\tau)$

where I is the measured intensity, I_o is the incident beam intensity, μ is the linear absorption and τ is the beam path length through the crystal. The magnitude of u depends on the number and type of atoms in the unit cell and on the wavelength of the radiation. The pathlength of each reflection through the crystal requires a full knowledge of the crystal dimensions in relation to the diffractometer axes. A published method for measuring the crystal and the analytical correction program ABSCOR were used in this work (138-140). The calculation method is to divide the crystal into Howell's polyhedra so that the rays enter and leave by one face only. The contribution of each polyhedron to the total diffracted intensity, A(t), is calculated and the transmission is then given by A(t)/V, where V is the crystal

volume.

(b) Structure solution.

A crystal consists of a unit cell (defined by a, b, c and their interaxial angles) which is periodically repeated in all three dimensions. The X-ray beam is diffracted by each of the planes present in the crystal to satisfy Bragg's law:

$$n\lambda = 2d^{*}\sin\Theta$$

where n is an integer, λ is the radiation wavelength, d is the spacing between planes and Θ is the angle of incidence. The diffracted beam in each direction is a composite of the individual waves (including their phase) that are diffracted in that direction. The measured intensity data only contains information about the amplitude of the diffracted beam and has no phase information. In order to obtain a measure of the electron distribution (it is the electrons in the atoms which diffract the X-rays) it is necessary to perform a three-dimensional Fourier summation. Fourier series are used because they can be applied to the periodic distribution of scattering matter which is found in crystals. the electron density (p) at any point is given by the equation

$$p(XYZ) = 1/V \sum_{h}\sum_{k}\sum_{l} F(hkl)\exp(-2\pi i(hZ+kY+lZ))$$

where F includes both the phase and the amplitude of the diffracted beam. Since the phase is not known, another method must be used to generate the required phase information.

The heavy atom method was used in this work to derive

approximate phase angles since the heavy atoms present dominate the X-ray scattering (141-143). In this method phases calculated from the positions of the heavy atom are used to generate approximate electron density maps from which further portions of the molecule can hopefully be recognised. The position of the heavy atom was found from a Patterson (or F^2) map which does not require phase information. The Patterson map is made up from a summation of a Fourier series that has structure factor amplitudes as coefficients. The maxima in the map represent the end points of all the interatomic vectors referenced to the origin. The height of a Patterson peak is approximately the product of the atomic numbers for the atoms concerned so vectors between heavy atoms tend to dominate the Patterson map and readily yield the atomic co-ordinates required.

Once the first atomic co-ordinates are found their positions are improved by the method of least-squares refinement (144). This is a method of fitting the variables of an equation to a set of observations in such a way that the sum of squares of the deviations of the observed quantities from those calculated is minimised. After a cycle of refinement an electron density map is calculated and any more atoms that can be found are included in the next cycle of refinement. At each stage of the refinement a measure of the accuracy of the current structural model is given by

reliability index= $R = (|\Sigma|F(obs)| - |F(calc)|\,|)/\Sigma|F(obs)|$

As R decreases and the model becomes accurate it is necessary to

use a better description of the "shape" of each atom. The scattering of an atom is reduced because of atomic vibration (or static disorder) so the temperature factor is used in calculations to quantify this smearing of electron density and is of the form $\exp(-B(iso)\sin^2\Theta/\lambda^2)$ where B(iso) is the isotropic temperature factor representing a spherical vibration. More accurate anisotropic temperature factors may be used which describe a triaxial, ellipsoidal vibration and are of the form

$$\exp-(b_{11}h^2 + b_{22}k^2 + b_{33}l^2 + b_{12}hk + b_{23}hl + b_{31}kl)$$

When the structure is well refined, a careful statistical analysis of R values over the range of F and $\sin(\Theta)$ may show small systematic errors in F(obs) and if so appropriate weights are applied to the the F values before the final least-squares refinement. For one structure in this work non-unit weights were necessary and the scheme used had the effect of downweighting reflections at the extremes of F(obs) and $\sin(\Theta)$. The XRAY76 suite of computer programs (including some local modifications) were used through this work (145).

Appendix 3 - Rapid Scanning Spectrophotometry.

Single wavelength stopped-flow spectrophotometry is an established technique for monitoring chemical reactions with $t_{\frac{1}{2}}$>1ms (146,147). Very reliable kinetic information about transient species can be obtained by this technique but to obtain full electronic spectra of transients, numerous experiments must be performed at different wavelengths. This point by point construction of an electronic spectrum can be acceptable in some cases but when overlapping spectra of successive intermediates are present the separate spectra are highly prone to error.

Rapid Scanning Spectrophotometry is a development which allows successive electronic spectra to be collected and transient spectra readily determined. This technique is particularly useful in finding isosbestic points at which single wavelength kinetic measurements can be made. The apparatus used for the work described in Chapter 4 was a Model 601 Multiplex Spectrophotometer as supplied by Applied Photophysics, London. A schematic diagram of the apparatus is shown in Figure 7.3.1. .

The stopped-flow equipment used had an all glass inlet system (to reduce metal ion contamination of the solutions) which was enclosed in a thermostated water jacket. Light from a power stabilised 150W xenon-arc lamp was directed along an optical fibre onto the entrance slit of a modified F/4 Czerny-Turner grating monochrometer which produces a spectrum in the plane of 30 groups of quartz fibres. The grating used in this work enabled a range of 150nm to be observed at a resolution of 5nm per channel. Each group of fibres is in turn connected to separate photomultipliers which are coupled to individual precision amplifiers. The outputs from the amplifiers are then multiplexed on to a single output channel in a manner suitable for display on a Tektronix 5115 storage oscilloscope. Each channel has an individual gain control to correct for wavelength dependences of both the photomultiplier gain and the lamp output. Up to 900 seperate spectra may be recorded with delays from 0.5ms to 5s between successive scans although in practice any more than 15 scans becomes too difficult to interpret.

Appendix 4 - Final Temperature and Structure Factor Tables.

Final temperature and structure factor tables for (1) and (2) are available as Supplementary Publication No. 22309 and those for (3) are available as Supplementary Publication No. SUP 22773.

References.

1. R.C. Harris, D.B. White and R.B. Macfarlane, Science, 1970, 170, 736.

2. L. Friberg and J. Vostal, Mercury in the Environment, The Chemical Rubber Co., 1972.

3. C.A. McAuliffe, The Chemistry of Mercury, The Macmillan Press Ltd., 1977.

4. R. Hartung and B.D. Dinman, Environmental Mercury Contamination, Ann Arbour Science Publisher Inc., 1972.

5. T. Tsubaki and K. Irukayama, Minimata Disease, Elsevier Scientific Publishing Co., 1977.

6. W.E. Smith and A.M. Smith, Minimata, Chatto and Windus Ltd., 1975.

7. M. Uchida, K. Hirakawa and T. Inoue, Kumamoto Med. J., 1961, 14, 181.

8. M. Uchida and T.Inoue, Kumamoto Med. J., 1962, 15, 149.

9. K. Irukayama, T. Kondo, F. Kai and M. Fujiki, Kumamoto Med. J., 1961, 143, 157.

10. S. Jensen and A. Jernevov, Nature, 1969, 223, 753.

11. J.M. Wood, F.S. Kennedy and C.G. Rosen, Nature, 1968, 220, 173.

12. N. Imura, E. Sukegana, S.K. Pan, K. Nagao, J.Y. Kim, T. Kwan and T. Ukita, Science, 1971, 172, 1248.

13. F. Baker, S.F. Damluji, L. Amin-zaki, M. Murtadha, A. Khalidi, N. Al-Rawi, S. Tikriti, H.I. Chahir, T.W. Ckarkson, J.C. Smith and R.A. Doherty, Science, 1973, 181, 230.

14. F.A.C. Anet and J.L. Sudmeier, J. Magn. Reson., 1969, 1, 124.

15. H.F. Henneike, J. Am. Chem. Soc., 1972, 94, 5945.

16. J.V. Hatton, W.G. Schneider and W. Siebrand, J. Chem. Phys., 1963, 39, 1330.

17. A.J. Brown, O.W. Howarth and P. Moore, J.C.S. Dalton, 1976, 1589.

18. S. Libich and D.L. Rabenstein, Anal. Chem., 1973, 45, 118.

19. D.L. Rabenstein, R. Ozubko, S. Libich, C.A. Evans, M.T. Fairhurst and C. Suvanprakorn, J. Coord. Chem., 1974, 3, 263.

20. D.F. Evans, P.M. Ridout and I. Wharf, J. Chem. Soc. A, 1968, 2127.

21. A.J.Canty, P. Barrow and P.C. Healy, J. Organomet. Chem., 1979, 179, 447.

22. L.F. Systma and R.J. Kleine, J. Organomet. Chem., 1973, 54, 15.

23. R. Scheffold, Helv. Chim. Acta, 1967, 50, 1419.

24. R. Scheffold, Helv. Chim. Acta, 1969, 52, 56.

25. R.D. Bach and A.T. Weibel, J. Am. Chem. Soc., 1976, 98, 6241.

26. M.T. Fairhurst, Ph.D. Thesis, University of Alberta, 1975.

27. G. Schwarzenbach and M. Schellenberg, Helv. Chim. Acta, 1965, 48, 28.

28. J.H. Clarke and L.A. Woodward, Trans. Faraday Soc.,

1968, 64, 1041.

29. J.H. Clarke and L.A. Woodward, Trans. Faraday Soc., 1966, 62, 3022.

30. P.L. Goggin and L.A. Woodward, Trans. Faraday Soc., 1960, 56, 1591.

31. P.L. Goggin and L.A. Woodward, Trans. Faraday Soc., 1962, 58, 1495.

32. D.L Rabenstein, C.A. Evans, M.C. Tourangeau and M.T. Fairhurst, Anal. Chem., 1975, 47, 338.

33. D.L. Rabenstein, M.C. Tourangeau and C.A. Evans, Can. J. Chem., 1976, 54, 2517.

34. P.L. Goggin and R.J. Goodfellow, J.C.S. Dalton, 1978, 561.

35. J. Relf, P. Cooney and H.F. Henneike, J. Organomet. Chem., 1972, 39, 75.

36. A.J. Canty, A Marker and B.M. Gatehouse, J. Organomet. Chem., 1975, 88, C31.

37. A.J. Canty and A. Marker, Inorg. Chem., 1976, 15, 425.

38. A.J. Canty, A. Marker, P. Barron and P.C. Healy, J. Organomet. Chem., 1978, 144, 371.

39. R.G. Pearson, J. Chem. Educ., 1968, 45, 581.

40. R.G. Pearson, J. Chem. Educ., 1968, 45, 581.

41. R.B. Simpson, J. Am. Chem. Soc., 1961, 83, 4711.

42. D.L Rabenstein and M.T. Fairhurst, J. Am. Chem. Soc., 1975, 97, 2086.

43. D.L. Rabenstein, J. Am. Chem. Soc., 1973, 95, 2797.

44. S.R. Reid, M. Sc. Thesis, University of Warwick, 1976.

45. D.L.Rabenstein, Acc. Chem. Res., 1978, 11, 100.

46. D.L. Rabenstein and M.T. Fairhurst, Inorg. Chem,, 1975, 14, 1413.

47. C.A. Evans, D.L. Rabenstein, G. Geier and I. Erni, J. Am. Chem. Soc. , 1977, 99, 8106.

48. D.W. Gruenwedel and N. Davidson, J. Mol. Biol., 1966, 21, 129.

49. S. Mansy, T.E. Wood J.C. Sprowles and R.S. Tobias, J. Am. Chem. Soc. , 1974, 96, 1762.

50. S. Mansy and R.S. Tobias, J. Am. Chem. Soc., 1974, 96, 6874.

51. S. Mansy and R.S. Tobias, Biochemistry, 1975, 14, 2952.

52. A.J. Canty and R.S. Tobias, Inorg. Chem., 1979, 18, 413.

53. H.J. Segall and J.M. Wood, Nature, 1974, 248, 456.

54. J.C. Mills, H.S. Preston and C.H.L. Kennard, J. Organomet. Chem., 1968, 14, 33.

55. M. Bruno, D. Grdenic, B. Kamenar and S.Pocev, Izv. Jugosl. Cent. Kristalografijv, Ser-A, 1976, 11, 24.

56. U. Muller, Z. Naturforsch., B, 1973, 28, 426.

57. N.G. Bokii, Zh. Strukt. Khim., 1978, 19, 380.

58. A.J. Carty, S.F. Malone and N.J. Taylor, J. Organomet. Chem., 1979, 172, 201.

59. A.J. Canty and B.M Gatehouse, J.C.S. Dalton, 1976, 2018.

60. A.J. Canty, N. Chaichit, B.M. Gatehouse and A. Marker,

Acta Crystallogr. (B), 1978, 34, 3229.

61. R.T.C. Brownlee, A.J.Canty and M.F. Mackay, Aust. J. Chem., 1978, 31, 1933.

62. C. Chieh and L.P.C. Leung, Can. J. Chem., 1976, 54, 3077.

63. C. Chieh, Can. J. Chem., 1978, 56, 560.

64. Y.S. Wong, A.J.Carty and P.C. Chieh, Can. J. Chem., 1973, 51, 2597.

65. Y.S. Wong, A.J.Carty and P.C. Chieh, J.C.S. Chem. Commun., 1973, 741.

66. Y.S. Wong, A.J.Carty and P.C. Chieh, J.C.S. Dalton, 1977, 1801.

67. Y.S. Wong, A.J.Carty and P.C. Chieh, J.C.S. Dalton, 1977, 1157.

68. Y.S. Wong, N.J. Taylor, P.C. Chieh and A.J. Carty, J.C.S. Chem. Commun., 1974, 625.

69. Y.S. Wong, N.J. Taylor, P.C. Chieh and A.J. Carty, J.C.S. Dalton, 1975, 438.

70. L. Prizant, M.J. Oliver, R.Rivest and A.L. Beauchamp J. Am. Chem. Soc., 1979, 101, 2765.

71. D.L. Rabenstein, J. Chem. Educ., 1978, 55, 292.

72. D.L. Rabenstein and C.A. Evans, Bioinorg. Chem., 1978, 8, 107.

73. A. Rothstein, in "Mercury, Mercurials and Mercaptans", C.C. Thomas, 1973, p73.

74. T.W. Clarkson, Ann. Rev. Pharmacology, 1972, 12, 375.

75. T.W. Clarkson, CRC Critical Rev. in Toxicology, 1971-2, 1, 203.

76. M. Berlin, L.G. Jerksell and G. Nordberg, Acta Pharmacol. et Toxicol. , 1965, 23, 312.

77. L.Magos, Br. J. Pharmacol., 1976, 56, 479.

78. J. Aaseth, Acta Pharmacol. et Toxicol., 1976, 39, 289.

79. R. Gronbaek and J.D. Dunitz, Helv. Chim. Acta, 1964, 47, 1889.

80. E.F. Kiefer, W.L. Waters and D.A. Carlson, J. Am. Chem. Soc., 1968, 90, 5127.

81. R.D. Bach, A.T. Wiebel, W. Schmonsees and M.D. Glick, J.C.S. Chem. Commun., 1974, 961.

82. A.J. Brown, M.Sc. Thesis, University of Warwick, 1975.

83. M.C. Bull and A.H. Nornury, "Physical Data for Inorganic Chemists." Longman, 1974.

84. A.J. Canty, N. Chaichit and B.M. Gatehouse, Acta Crystallogr (B), 1980, B36, 786.

85. A. Medici, G. Rosini, E.F. Serantoni and L.R. Sanseverino, J.C.S. Perkin I, 1978, 1110.

86. J.W. Emsley, J Feeney and C.H. Sutcliffe, "High Resolution Nuclear Magnetic Resonance Spectroscopy.", Pergamon Press, Oxford, 1965.

87. Nicolet 1080 Series (1973) "ITRCAL", Published by the Nicolet Instrument Corporation.

88. A.A. Bothner-by, Adv. in Mag. Res., 1975, 1, 195.

89. D. Shaw, "Fourier Transform N.M.R. Spectroscopy.", Elsevier, Amsterdam, 1976, p221.

90. I.B. Johns, W.D. Paterson and R.M. Hixon, J. Am. Chem. Soc., 1930, 52, 2820.

91. O.Goldsmith and M. Tishler, J. Am. Chem. Soc., 1946, 68, 144.

92. A.J. Canty and R. Kishimoto, Nature, 1975, 253, 123.

93. A.J. Canty and R. Kishimoto, Inorg. Chim. Acta, 1977, 24, 109.

94. T. Taguchi, Y. Kiyoshima, O. Komori and M. Mori, Tetrahedron. Lett., 1969, 41, 3631.

95. T.C. Shields and A.N. Kurtz, J. Am. Chem. Soc., 1969, 91, 5416.

96. L.F. Lindoy and S.E. Livingstone, Inorg. Chem., 1968, 7, 1149.

97. D.C. Liles, M. McPartlin and P.A. Tasker, J. Am. Chem. Soc., 1977, 99, 7705.

98. L.F. Lindoy and S.E. Livingstone, Inorg. Chim. Acta, 1967, 1, 365.

99. L.F. Lindoy and S.E. Livingstone, Inorg. Chim. Acta, 1968, 2, 119.

100. PANIC, (a program for the Aspect 2000 computer), Bruker Spectrospin, 1979.

101. R.H. Holyer, C.D. Hubbard, S.F.A. Kettle and R.G. Wilkins, Inorg. Chem., 1965, 4, 929.

102. W.Q. Gilmour, Ph.D. Thesis, University of Warwick, 1980.

103. "Stability Constants Supplement no.1", 1971, The Chemical Society, London, p362.

104. M. Kadoma and E.Kimura, J.C.S. Dalton, 1977, 2269.

105. E.K. Barefield and M.T. Mocella, Inorg. Chem., 1973, 12, 2829.

106. P.K. Chan and C.K. Poon, J.C.S. Dalton, 1976, 858.

107. C.K. Poon and M.L. Tobe, J.C.S. A, 1968, 1549.

108. E.K. Barefield and F. Wagner, Inorg. Chem., 1973, 12, 2435.

109. N.W. Alcock, N. Herron and P. Moore, J.C.S. Dalton, 1978, 1282.

110. N.W. Alcock, N. Herron and P. Moore, Inorg. Chim. Acta, 1979, 32, L25.

111. N. Herron and P. Moore, Inorg. Chim. Acta, 1979, 36, 89.

112. N. Herron, Ph.D. Thesis, University of Warwick, 1978.

113. D.H. Busch, L.Y. Martin, L.J. Dehayes and L.J. Zompa, J. Am. Chem. Soc., 1974, 96, 4046.

114. M. Kodama and E. Kimura, J.C.S. Dalton, 1976, 2335.

115. J.H. Espenson, W.R. Bushey and M.E. Chmielewski, Inorg. Chem, 1975, 14, 1302.

116. K. Stanley, J. Martin, J. Schnittker, R. Smith and M.C. Baird, Inorg. Chim. Acta, 1978, 27, L111.

117. N.W. Alcock, E.H. Curzon, N. Herron and P. Moore, J.C.S. Dalton, 1979, 1987.

118. N.W. Alcock, N. Herron and P. Moore, J.C.S. Dalton, 1978, 394.

119. W.J. Spangler, J.L. Spigarelli, J.M. Rose, R.S. Flippin and H.H. Miller, Appl. Micro., 1973, 26, 488.

120. W.J. Spangler, J.L. Spigarelli, J.M. Rose and H.H.

Miller, Science, 1973, 180, 192.

121. R.L. Brunker and T.L. Bott, Appl. Micro., 1974, 27, 870.

122. M. Shariat, A.C. Anderson and J.W. Mason, Bull. Environ. Contam. Toxicol., 1979, 21,255.

123. J.W. Mason, A.C. Anderson and M. Shariat, Bull. Environ. Contam. Toxicol., 1979, 21,262.

124. T. Tezuka and K. Tonomura, J. Biochem., 1976, 80, 79.

125. G.E. Coates and A. Lauder, J. Chem. Soc., 1965, 1857.

126. D.P. Graddon and J. Mondal, J. Organomet. Chem., 1977, 132, 1.

127. W.A. Nugent and J.K. Kochi, J. Amer. Chem. Soc., 1976, 98, 5979.

128. D.F. Shriver, "The manipulation of air sensitive compounds", McGraw-Hill, 1969.

129. A. Stock, "Hydrides of Boron and Silicon", Cornhill University Press, 1973.

130. J.W. Emsley, J. Feeney and L.H. Sutcliffe, "High Resolution Nuclear Magnetic Resonance Spectroscopy", 1966, Pergamon Press, Oxford.

131. G.C. Levy and G.L. Nelson, "Carbon-13 Nuclear Magnetic Resonance for Organic Chemists.", 1972, Wiley, New York.

132. J.B. Stothers, "Carbon-13 NMR Spectroscopy.", 1972, Academic Press, New York.

133. K. Mullen and P.S. Pregosin, "Fourier Transform N.M.R. Tecniques: A Practical Approach.", 1976, Academic Press, New York.

134. SYNDAT - a data reduction program for a Syntex P2. diffractometer, N.W. Alcock, University of Warwick, 1974.

135. M.J. Buerger, "X-ray Crystallography", Wiley, London, 1960.

136. M.J. Buerger, "Crystal Structure Analysis", Wiley, London, 1960.

137. G.H. Stout and L.H. Jensen, "X-ray Structure Determination", Macmillan, London, 1968.

138. N.W. Alcock, Acta Cryst., 1970, A26, 437.

139. N.W. Alcock, G.S. Pawley, C.P. Rourke and M.R. Levine, Acta Cryst., 1972, A28, 440.

140. N.W. Alcock in "Crystallographic Computing", ed F. Ahmed, Munksgaard, Copenhagen, 1970, p271.

141. A.L. Patterson, Phys. Rev., 1934, 46, 372.

142. A.L. Patterson, Z. Krist.(A), 1935, 90, 517.

143. H. Lipson and W. Cochran, "The determination of Crystal Structure", G. Bell and Sons., London, p207.

144. J.S. Rollett, "Computing Methods in Crystallography", Pergamon, 1965.

145. J.M. Stewart, University of Maryland, TR-446, March 1976.

146. E.F. Caldin, "Fast Reactions in Solution.", 1964, Blackwell, Oxford.

147. K. Kustin, "Fast Reactions.", 1969, Academic Press, London.

148. K. Travis and D.H. Busch, Inorg. Chem., 1974, 13, 2591.

149. D. Shaw, "F.T.N.M.R. Spectroscopy.", 1976, Elsevier, Amsterdam.

150. A.R Amundsen, J. Whelan and B. Bosnich, J. Amer. Chem.